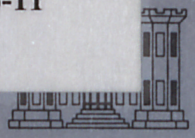

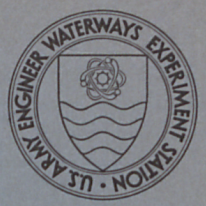

TECHNICAL REPORT S-75-11

PAVEMENT RESPONSE TO AIRCRAFT DYNAMIC LOADS

Volume III

COMPENDIUM

by

Richard H. Ledbetter

Soils and Pavements Laboratory
U. S. Army Engineer Waterways Experiment Station
P. O. Box 631, Vicksburg, Miss. 39180

June 1976

Final Report

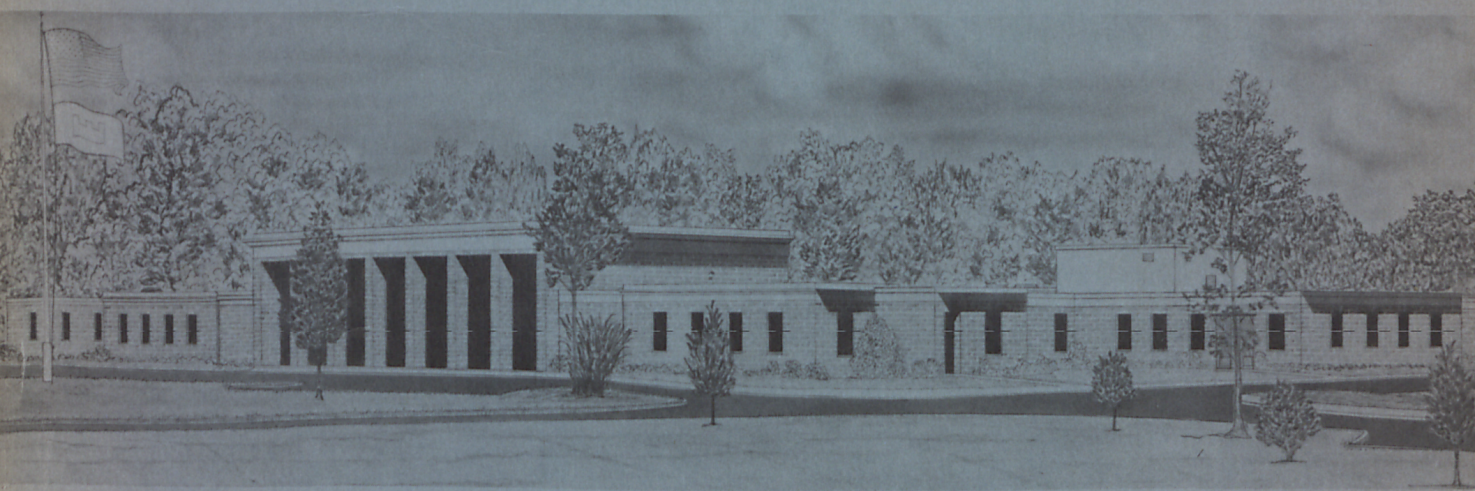

Prepared for U. S. Department of Transportation
Federal Aviation Administration
Systems Research and Development Service
Washington, D. C. 20591

Under Inter-Agency Agreement No. DOT FA71WAI-218

Unclassified

SECURITY CLASSIFICATION OF THIS PAGE (When Data Entered)

REPORT DOCUMENTATION PAGE

READ INSTRUCTIONS BEFORE COMPLETING FORM

1. REPORT NUMBER: Technical Report S-75-11, Vol III
2. GOVT ACCESSION NO.:
3. RECIPIENT'S CATALOG NUMBER:

4. TITLE (and Subtitle): PAVEMENT RESPONSE TO AIRCRAFT DYNAMIC LOADS; VOLUME III: COMPENDIUM

5. TYPE OF REPORT & PERIOD COVERED: Final report

6. PERFORMING ORG. REPORT NUMBER:

7. AUTHOR(s): Richard H. Ledbetter

8. CONTRACT OR GRANT NUMBER(s): Inter-Agency Agreement No. DOT FA71WAI-218

9. PERFORMING ORGANIZATION NAME AND ADDRESS: U. S. Army Engineer Waterways Experiment Station, Soils and Pavements Laboratory, P. O. Box 631, Vicksburg, Miss. 39180

10. PROGRAM ELEMENT, PROJECT, TASK AREA & WORK UNIT NUMBERS:

11. CONTROLLING OFFICE NAME AND ADDRESS: U. S. Department of Transportation, Federal Aviation Administration, Systems Research and Development Service, Washington, D. C. 20591

12. REPORT DATE: June 1976

13. NUMBER OF PAGES: 92

14. MONITORING AGENCY NAME & ADDRESS (if different from Controlling Office):

15. SECURITY CLASS. (of this report): Unclassified

15a. DECLASSIFICATION/DOWNGRADING SCHEDULE:

16. DISTRIBUTION STATEMENT (of this Report): Approved for public release; distribution unlimited.

17. DISTRIBUTION STATEMENT (of the abstract entered in Block 20, if different from Report):

18. SUPPLEMENTARY NOTES: Also published as FAA Report No. FAA-RD-74-39-III.

19. KEY WORDS (Continue on reverse side if necessary and identify by block number):
Aircraft dynamic loads
Elastic behavior
Flexible pavement response
Inelastic behavior
Rigid pavement response

20. ABSTRACT (Continue on reverse side if necessary and identify by block number):

Instrumented aircraft were used to apply static and dynamic loads to instrumented pavement structures (both flexible and rigid) at the National Aviation Facilities Experimental Center (NAFEC), Atlantic City, N. J. Volume I of this report describes the testing program and instrumentation systems. Volume II with Appendixes A and B presents the reduction and analysis of data and the test results. This volume contains a compendium of the entire study.

(Continued)

DD FORM 1 JAN 73 1473 EDITION OF 1 NOV 65 IS OBSOLETE

Unclassified

SECURITY CLASSIFICATION OF THIS PAGE (When Data Entered)

20. ABSTRACT (Continued).

Measurements of displacement, velocity, pressure, and temperature were made in the two pavement structures. Two phases of material behavior, elastic and inelastic, in both flexible and rigid pavement structures were identified. Each phase had to be treated independently for a full analysis of the static and dynamic load test results.

The tests at NAFEC showed that no basic aircraft ground operating mode induced pavement responses (elastic plus inelastic) greater than those occurring for static load conditions. However, extrapolations of the test results indicate that for stiff pavement structures (such as the rigid pavement, and the flexible pavement during cold weather) unusual conditions (pavement conditions rougher than those during testing at NAFEC) of dynamic loading could cause responses larger than what would occur under static loading. This behavior is possible because of the inelastic behavior being of low magnitude for stiff pavements. The test results also indicate that a reduction in the thickness of pavement structures could be allowed in the interior of runways except at exits where aircraft side thrust is high.

PREFACE

This project was conducted by the Soils and Pavements Laboratory (S&PL), U. S. Army Engineer Waterways Experiment Station (WES), for the Federal Aviation Administration under Inter-Agency Agreement DOT FA71WAI-218 during the period May 1971-January 1975.

The project was conducted under the general supervision of Mr. James P. Sale, Chief of S&PL. Results of the study are included in the following volumes of the report entitled "Pavement Response to Aircraft Dynamic Loads":

a. Volume I. "Instrumentation Systems and Testing Program."

b. Volume II and Appendixes A and B. "Presentation and Analysis of Data."

c. Volume III. "Compendium."

This volume (Volume III) of the report was prepared by Mr. Richard H. Ledbetter.

Because of the uniqueness of this study, WES requested and received assistance in the design of the experiment from the following consultants: Prof. R. E. Fadum, North Carolina State University; Prof. W. R. Hudson, University of Texas; Dr. Willard J. Turnbull, Consultant, Vicksburg, Miss.; Prof. C. L. Monismith, University of California, Berkeley; Prof. M. E. Harr, Purdue University; Prof. W. H. Goetz, Purdue University; Prof. A. S. Vesic, Duke University; Prof. R. K. Watkins, University of Utah; and Prof. K. B. Woods, Purdue University.

A concept for reduction and analysis of instrumentation data somewhat different from that normally used for pavement response analysis was used for this project. Because of this, WES requested that Volume II of the report, which describes the method of analysis in detail, be thoroughly reviewed by Professors Fadum, Hudson, Vesic, and Monismith. The consensus of the review was that the method of analysis was not only valid but essential to meet the stated objectives. It was the opinion of the reviewing consultants that the study has resulted in a major contribution to the understanding and knowledge of pavement response under static and dynamic loading.

Directors of WES during the conduct of the study were BG E. D. Peixotto, CE, and COL G. H. Hilt, CE. Technical Director was Mr. F. R. Brown.

TABLE OF CONTENTS

FIGURES

FIGURES (Continued)

TABLES

TABLES (Continued)

METRIC CONVERSION FACTORS

Approximate Conversions to Metric Measures

Symbol	When You Know	Multiply by	To Find	Symbol
	LENGTH			
in	inches	*2.5	centimeters	cm
ft	feet	30	centimeters	cm
yd	yards	0.9	meters	m
mi	miles	1.6	kilometers	km
	AREA			
in^2	square inches	6.5	square centimeters	cm^2
ft^2	square feet	0.09	square meters	m^2
yd^2	square yards	0.8	square meters	m^2
mi^2	square miles	2.6	square kilometers	km^2
	acres	0.4	hectares	ha
	MASS (weight)			
oz	ounces	28	grams	g
lb	pounds	0.45	kilograms	kg
	short tons (2000 lb)	0.9	tonnes	t
	VOLUME			
tsp	teaspoons	5	milliliters	ml
Tbsp	tablespoons	15	milliliters	ml
fl oz	fluid ounces	30	milliliters	ml
c	cups	0.24	liters	l
pt	pints	0.47	liters	l
qt	quarts	0.95	liters	l
gal	gallons	3.8	liters	l
ft^3	cubic feet	0.03	cubic meters	m^3
yd^3	cubic yards	0.76	cubic meters	m^3
	TEMPERATURE (exact)			
°F	Fahrenheit temperature	5/9 (after subtracting 32)	Celsius temperature	°C

*1 in = 2.54 (exactly). For other exact conversions and more detailed tables, see NBS Misc. Publ. 286, Units of Weights and Measures, Price $2.25, SD Catalog No. C13.10:286.

Approximate Conversions from Metric Measures

Symbol	When You Know	Multiply by	To Find	Symbol
	LENGTH			
mm	millimeters	0.04	inches	in
cm	centimeters	0.4	inches	in
m	meters	3.3	feet	ft
m	meters	1.1	yards	yd
km	kilometers	0.6	miles	mi
	AREA			
cm^2	square centimeters	0.16	square inches	in^2
m^2	square meters	1.2	square yards	yd^2
km^2	square kilometers	0.4	square miles	mi^2
ha	hectares (10,000 m^2)	2.5	acres	
	MASS (weight)			
g	grams	0.035	ounces	oz
kg	kilograms	2.2	pounds	lb
t	tonnes (1000 kg)	1.1	short tons	
	VOLUME			
ml	milliliters	0.03	fluid ounces	fl oz
l	liters	2.1	pints	pt
l	liters	1.06	quarts	qt
l	liters	0.26	gallons	gal
m^3	cubic meters	35	cubic feet	ft^3
m^3	cubic meters	1.3	cubic yards	yd^3
	TEMPERATURE (exact)			
°C	Celsius temperature	9/5 (then add 32)	Fahrenheit temperature	°F

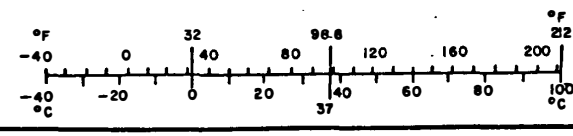

INTRODUCTION

BACKGROUND

Reports of pavement distress associated with current commercial aircraft loads and growing concerns over the possibility of detrimental aircraft dynamic load effects on airport pavements persuaded the Federal Aviation Administration (FAA) to sponsor a study described in Report No. FAA-RD-70-19, "Aircraft Dynamic Wheel Load Effects on Airport Pavements," dated May 1970.[1] This study consisted of a literature review, computer analyses to determine aircraft loads and pavement responses, scaled pavement tests, and correlations between experimental and analytical data. In general, the study concluded that aircraft dynamic loads have a significant effect on portions of airport pavements. Specifically, the study showed that the primary effects that influence pavement response to dynamic loads are:

a. The increased magnitudes of aircraft wheel loads resulting from aircraft modes of operation, pavement uneveness, and aircraft structural characteristics during moving ground operations.

b. The dynamic load phenomena associated with the materials used in the construction of both rigid and flexible pavements.

For a given aircraft and level of pavement unevenness, the loads imposed upon a runway can be accurately defined for various ground operations. On the other hand, there is presently a serious void in information necessary to obtain an accurate description of pavement response to dynamic loads.

PURPOSE

This study was undertaken in an effort to provide experimental pavement response data so that the effects of dynamic loads on airport pavements could be evaluated. Specifically, the basic purpose of the study was to determine the relationship between responses of typical flexible and rigid runway pavements to static and dynamic loads. The requirements to determine the magnitudes of the dynamic loads, to determine the depths of pavement structures affected by static and

dynamic loads, and to investigate the relationship between aircraft ground speeds and aircraft dynamic loads were essential elements of this study.

SCOPE

The investigation was accomplished by conducting tests using instrumented aircraft on instrumented sections of existing flexible and rigid pavement runways. One series of tests was conducted during a cold period of the year (1972) when the average temperature of the pavement surface layer was in the range of 35 to 55°F,* while the other series was conducted on the instrumented flexible pavement test section during the hot period of the year (1974) when the average temperature of the pavement surface layer was in the range of 84 to 116°F. An instrumentation system was installed aboard the aircraft to measure and record the three components of force of each of the main gear assemblies of the aircraft used. Instrumentation systems were installed within the flexible and rigid pavement structures to measure the pavement responses to aircraft loads in the form of relative displacements and pressures at various depths. A key element in this experimental approach was the recording of a common time base for both the aircraft load measurements and the pavement response measurements. This control provided a means of correlating the aircraft dynamic wheel loads and the response measurements of the two pavement structures to within 1 msec. The locations of the two instrumented pavement test sites were selected so that 10 modes of aircraft ground operation, ranging from static to high-speed taxi and takeoff, could be investigated during the course of the experimental study.

The scope of the subject matter was too broad to be presented in a single report. Therefore, Volume I of the report[2] describes the instrumentation systems and their installation and operation to collect aircraft loading and pavement response data; the history and chronology of the investigation; and the complete details of the testing program.

---

* A table of factors for converting units of measurement is presented on page 7.

Volume II of the report[3] describes the reduction, interpretation, and analysis of instrumentation data collected during the tests. Appendix A of Volume II describes the automatic data processing (digital) system and techniques, and Appendix B of Volume II presents the data in reduced form. This report, Volume III, contains a compendium of the entire study.

Instrumentation was installed in the pavement structures of runways 04-22 and 13-31 at the National Aviation Facilities Experimental Center (NAFEC) Airport, Atlantic City, N. J., at the two sites indicated in Figure 1. Instrumented aircraft were used to conduct the most common

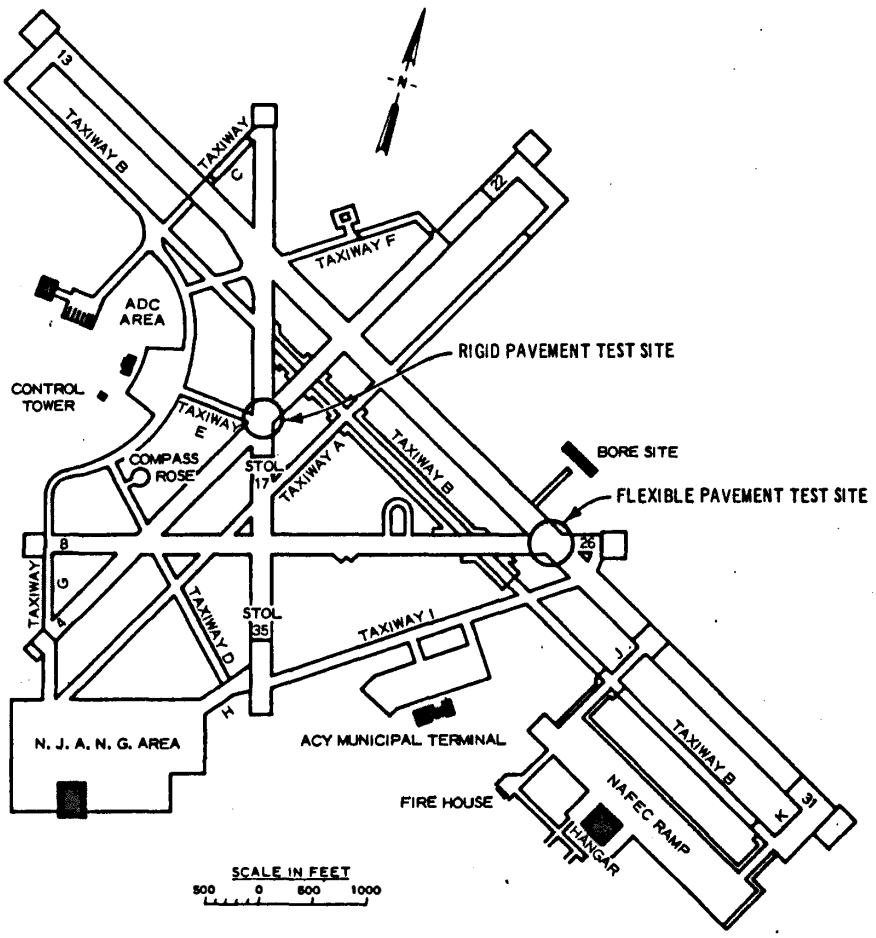

Figure 1. Locations of test sites at NAFEC Airport

aircraft ground operations for these test sites.

An 80-ft-long segment of runway 13-31 located at its intersection with runway 8-26 was selected as the flexible pavement test site. This test site was chosen to enable the collection of typical response measurements during landing and at the point of rotation for takeoff as well as during low- and high-speed taxiing, braking, and turning

operations. This particular site was in a portion of the runway being reconstructed, and this factor was of great benefit during the installation of instrumentation. After reconstruction, the flexible pavement structure in this area consisted of 3 in. of bituminous surface course, 6 in. of bituminous base course, 9 in. of base course constructed from the original pavement surface and base courses, and 12 in. of subbase course constructed from the original subbase course over the compacted subgrade. Table 1 summarizes the material properties determined for the flexible pavement test site during and after reconstruction. The bituminous base course conformed to Division 3, Section 2A, of the New Jersey State Highway Department "Standard Specifications for Road and Bridge Construction."[4] Aggregate was crushed stone conforming to the following gradation:

Sieve Size	Total Percent Dry Weight Passing
1-1/2 in.	100
3/4 in.	55 to 90
No. 4	25 to 60
No. 10	20 to 50
No. 40	15 to 30
No. 200	5 to 12

The mix design for the bituminous base course material conformed to mix No. 1 for hot-mixed bituminous concrete in Article 3.10.2 of the New Jersey specifications. The New Jersey and FAA specifications differ in requirements for gradation, asphalt content, stability, etc.

The bituminous surface course conformed to Item P-401 of FAA Advisory Circular AC 150/5370-1A[5] for aircraft weighing 30,000 lb or more. Gradation of the aggregate conformed to gradation B. The asphalt cement used was an 85-100 penetration grade.

A typical layout of the flexible pavement instrumentation system is shown in Figure 2. Three gage rows approximately 12 ft in length containing Bison coils, SE soil pressure cells, WES deflection gages, WES soil pressure cells, inductive probes, and velocity gages for a total of 162 instruments were installed in the pavement structure during the reconstruction of runway 13-31. Each gage row contained 12 SE soil pressure cells, 1 WES soil pressure cell, 1 WES deflection gage, and

Table 1

Summary of Material Properties for the Flexible Pavement Test Site

Station No.	Depth Below Surface in.	Pavement Structure Element	Measurements During Construction					Measurements After Construction†			Soil Classification	
			CBR*		Water Content*	Water Content**	Dry Density**	CBR		Water Content		
			0.1 in.	0.2 in.	percent	percent	pcf	0.1 in.	0.2 in.	percent	Unified	FAA
65+20	18	Subbase course	97.0	--	4.1	8.7	130.9				SP	E-1
	30	Compacted subgrade	39.0	40.5	6.7	12.2	121.4				SP	E-1
	42	Compacted subgrade	43.5	57.0	7.0						SP	E-1
	54	Compacted subgrade	16.0	21.0	7.0						SP	E-1
65+34	11	Base course						37.0	43.0	4.1		
	20	Subbase course						25.0	26.0	5.8	SP	E-1
	32	Compacted subgrade						27.0	30.0	7.5	SP	E-1
	44	Compacted subgrade						41.0	54.0	9.1	SP	E-1
65+35	10.5	Base course						42.0	41.0	4.2		
	19.5	Subbase course						24.0	26.0	5.2	SP	E-1
	31.5	Compacted subgrade						25.0	31.0	7.6	SP	E-1
	43.5	Compacted subgrade						37.0	45.0	8.4	SP	E-1
65+50	18	Subbase course	58.5	67.5	5.5	8.6	131.1				SP	E-1
	30	Compacted subgrade	48.0	56.5	6.3	12.0	119.3				SP	E-1
	42	Compacted subgrade	34.5	44.5	7.1						SP	E-1
	54	Compacted subgrade	17.5	20.5	6.8						SP	E-1
65+80	11	Base course						33.0	35.0	6.6		
	20	Subbase course						26.0	29.0	5.1	SP	E-1
	32	Compacted subgrade						24.0	30.0	5.8	SP	E-1
	44	Compacted subgrade						44.0	44.0	6.5	SP	E-1
65+81	11.5	Base course						55.0	54.0	6.9		
	20.5	Subbase course						33.0	39.0	5.3	SP	E-1
	32.5	Compacted subgrade						40.0	46.0	5.7	SP	E-1
	44.5	Compacted subgrade						64.0	--	7.8	SP	E-1
66+00	18	Subbase course	65.0	67.0	7.5	9.3	124.2				SP	E-1
	30	Compacted subgrade	34.0	41.5	6.5	10.8	124.7				SP	E-1
	42	Compacted subgrade	32.0	42.5	6.9						SP	E-1
	54	Compacted subgrade	27.5	33.0	7.0						SP	E-1

* Average values determined from measurements in two test pits.
** Average values determined from two measurements with nuclear density device.
† Determined from small aperture testing.

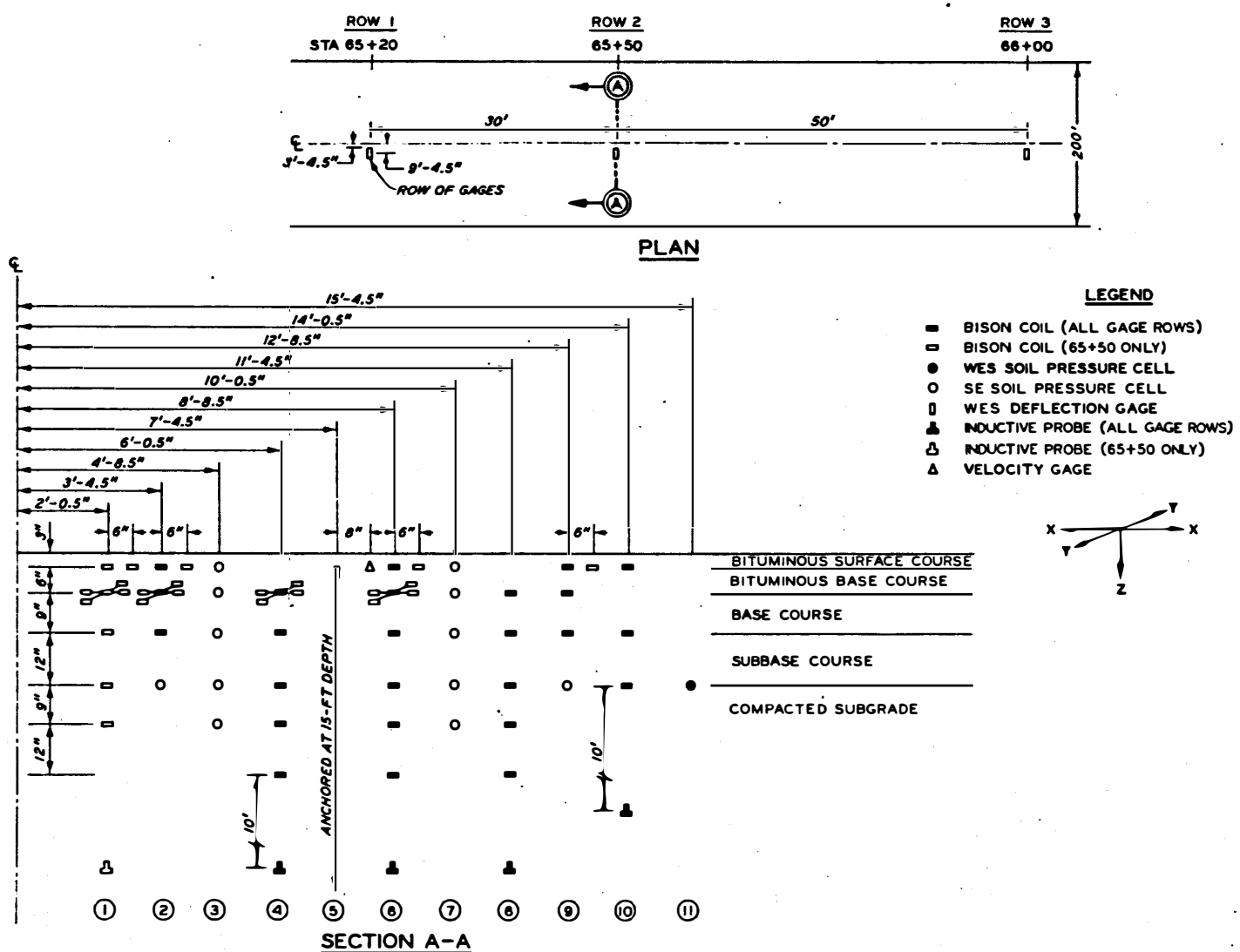

Figure 2. Typical layout of flexible pavement instrumentation

1 velocity gage. The middle gage row contained 50 Bison coils and 5 inductive probes, and the outer two rows contained 25 Bison coils and 4 inductive probes. In addition, a thermistor was installed on the surface and at depths of 3, 6, and 9 in. within the pavement structure.

A 72-ft-long segment of runway 04-22 was instrumented at its intersection with runway 17-35 to form the rigid pavement test site. The pavement structure in this area consisted of 7 in. of portland cement concrete (PCC) pavement and 8 in. of subbase course over the compacted subgrade. As was the case for the flexible pavement site, this site was chosen to enable the collection of typical measurements during normal aircraft ground operations. A 12-1/2- by 25-ft slab was removed from the runway at the location of each of the gage rows, and gages were installed in holes cored into the underlying material. Following installation of the instrumentation, high early (HE) strength concrete (type III) was used to replace the rigid pavement slabs. Tables 2 and 3 summarize the material properties determined for the rigid pavement test site.

Figure 3 shows a typical layout of the rigid pavement instrumentation system. A total of 153 gages consisting of 104 Bison coils, 13 inductive probes, 3 WES deflection gages, 9 Valore strain gages, 18 SE soil pressure cells, 3 WES soil pressure cells, and 3 velocity gages were installed in three gage rows at various depths and offsets within the pavement structure. Thermistors were installed on the surface of, at the bottom of, and at a depth of 3.5 in. within two slabs.

A system of laser light beam sources and detectors was installed along the edges of the runways such that a light beam was projected directly above and parallel to each gage row. An electrical impulse was generated when the wheels of the instrumented aircraft passed between the source and detector, thereby signaling the instant at which the wheels were directly over the gage row. The lateral position of the aircraft was determined by visual inspection of a stripe of flour and water solution painted on the surface of the runways adjacent and parallel to each gage row.

A synchronized common time signal was recorded on both aircraft

Table 2

Summary of Material Properties for the Rigid Pavement Test Site

Station No.	Depth Below Surface in.	Pavement Structure Element	CBR 0.1 in.	CBR 0.2 in.	Water Content percent	Water Content* percent	Dry Density* pcf	Soil Classification Unified	Soil Classification FAA
26+55	8	Subbase course	9	10	9.2	13.05	114.8	SP	E-1
	16	Compacted subgrade	10	10	8.2			SM	E-1
	28	Compacted subgrade	8	9	7.4			SM	E-1
	40	Compacted subgrade	13	11	6.1			SM	E-1
26+55	8	Subbase course	10	9	9.5	13.05	114.8	SP	E-1
	16	Compacted subgrade	20	20	6.9			SM	E-1
	28	Compacted subgrade	12	12	8.1			SM	E-1
	40	Compacted subgrade	13	12	6.8			SM	E-1
26+90	8	Subbase course	10	10	13.1	13.5	122.5	SP	E-1
	16	Compacted subgrade	23	24	6.1			SM	E-1
	28	Compacted subgrade	9	8	8.6			SM	E-1
	40	Compacted subgrade	21	25	10.0			SM	E-1
26+93	8	Subbase course	11	11	8.6	13.7	123.3	SP	E-1
	16	Compacted subgrade	23	25	8.1			SM	E-1
	28	Compacted subgrade	15	14	5.0			SM	E-1
	40	Compacted subgrade	20	24	5.9			SM	E-1
27+22	8	Subbase course	16	18	9.4	11.5	125.7	SP	E-1
	16	Compacted subgrade	28	36	7.8			SM	E-1
	28	Compacted subgrade	18	19	7.4			SM	E-1
	40	Compacted subgrade	16	13	5.9			SM	E-1
27+30	8	Subbase course	14	11	9.4	12.0	125.2	SP	E-1
	16	Compacted subgrade	15	16	7.7			SM	E-1
	28	Compacted subgrade	11	12	6.7			SM	E-1
	40	Compacted subgrade	16	13	4.6			SM	E-1

* In-place measurements made with nuclear density device.

Table 3

Summary of Concrete Strength Data for Replacement Slabs in the Rigid Pavement Test Site

Slab No.	Type of PCC	Slump in.	Cure Time days	Flexural Strength psi		Compressive Strength psi	
				Range	Average	Range	Average
1 & 2	3000-psi HE	2.25	7	672 to 683	678	3820 to 3926	3873
1 & 2	3000-psi HE	2.25	21	707 to 737	725	4386 to 4740	4563
3	4000-psi HE	2.50	4	--	650	--	3431
3	4000-psi HE	2.50	7	670 to 683	677	4209 to 4705	4457
3	4000-psi HE	2.50	20	713 to 755	731	4740 to 4844	4798

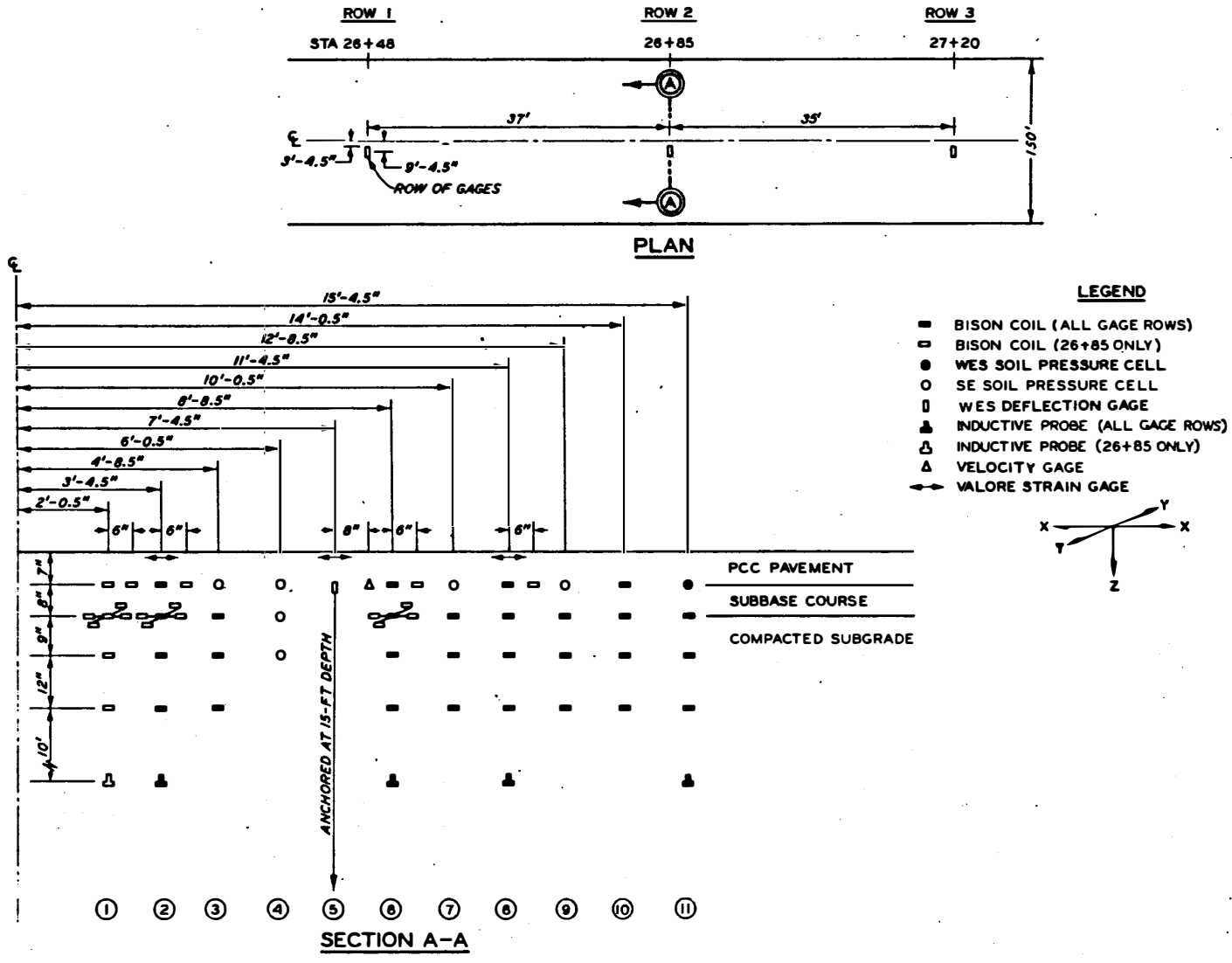

Figure 3. Typical layout of rigid pavement instrumentation

and ground data tapes. This provided the means by which the pavement response could be correlated with the corresponding aircraft load. With the exception of the thermistors, all instruments were recorded simultaneously on magnetic tapes, and all ground data tapes contained the time code and laser signals. Temperatures were recorded on paper tape.

Instrumented aircraft were used in both the initial cold weather and the subsequent warm weather tests to provide the monitored load for the pavement structures. An instrumented B-727 was used for the cold weather testing of 1972. Instrumented B-727 and C-880 aircraft were used for the warm weather testing of 1974. The B-727 aircraft were equipped with strain gages installed on the drag struts, side struts, and axles of both main gears and potentiometers installed on the torsion links of both main gears to measure the three components of force transmitted to the pavement structure. Accelerometers were the only instruments installed on the C-880 and were placed at three locations to measure the aircraft acceleration response for estimating the main gear load during dynamic tests. Similar systems of accelerometers were installed on board the B-727 aircraft as backup systems for the instrumented main gears. On-board instrumentation for all three aircraft included signal conditioning equipment, a time code generator (synchronized with the ground time code generator for correlation of test results), and a 14-track analog magnetic tape recorder.

Two series of dynamic load tests were conducted at NAFEC Airport to determine the pavement response under static and dynamic aircraft loads. The first series of tests, the cold weather tests, was conducted during the period 12 November-11 December 1972 on both the flexible and rigid pavement test sections. The second series of tests, the warm weather tests, was conducted during the period 8-15 July 1974 on only the flexible pavement since the response of rigid pavement is known to be relatively insensitive to temperature.

Data were collected for 408 aircraft operations during the cold weather tests. Of this total, 203 operations were on the flexible pavement test site and the remaining 205 were on the rigid pavement test site. During the warm weather tests, data were collected for

281 aircraft operations on the flexible pavement test site; 240 of these being with the B-727 and the remaining 41 being with the C-880.

The following types of tests were performed during both cold and warm weather tests:

a. Static load tests. The aircraft was positioned over each gage row and data collected. These tests provided data for comparison with data from dynamic load tests as well as a check of the capability of the instrumentation system.

b. Dynamic load tests. Pavement response and aircraft dynamic load data were collected at each test site under the following aircraft operating modes:

(1) Creep-speed taxi (3 to 8 knots).

(2) Low-speed taxi (15 to 30 knots).

(3) Medium-speed taxi (45 to 80 knots).

(4) High-speed taxi (85 to 130 knots).

(5) High-speed braking (130 to 45 knots).

(6) Takeoff rotation (85 to 130 knots).

(7) Touchdown.

(8) High-speed braking with reverse thrust.

(9) Turning (4 to 30 knots).

Although this particular breakdown of possible aircraft operations differs slightly from that described in Reference 1, data obtained during these operations should be directly applicable. Responses of each type of gage were recorded during tests conducted under each mode of operation. As an example of the applicability of the test modes to typical airport operations, consider a normal takeoff. At any airport, this operation involves seven of the test modes: static loading; turning; creep-, low-, medium-, and high-speed taxi; and takeoff rotation. If the takeoff was aborted, the high-speed braking modes would become applicable.

PAVEMENT STRUCTURE RESPONSE DATA

TYPICAL RESPONSES

A detailed description of the data form, automatic data processing, and data output is presented in Volume II and Appendixes A and B.[3] The data were in analog form and of two basic types, static and dynamic. Data from the static load tests were in the form of straight lines or constant voltage levels. Data from the dynamic load tests were in the form of impulses at the instant a gage row was crossed and constant voltage levels before and after.

Some gages responded in the form of both upward and downward movement data peaks, while others responded in only one direction. The WES deflection gages, Valore strain gages, and pressure cells primarily registered only one data peak. Figure 4 shows a typical digital computer reproduced recording for an SE soil pressure cell. Figure 5 shows typical analog recordings for a WES deflection gage in the flexible pavement structure. With the exception of reduced magnitudes, these figures are also typical of the rigid pavement structure response.

Bison coils primarily registered two data peaks in opposite directions. Figure 6 shows typical digital computer reproduced recordings of the Bison coils for tests on the flexible pavement test section. An upward movement peak (bow wave) occurred immediately before the aircraft wheels reached the center line of a gage location, and a downward movement peak occurred as the wheels were directly over a gage location. These two data peaks are referred to as the first and second peaks, and their positions were determined from correlations with the laser signals. A third peak, which was of lesser upward movement, occurred immediately after the wheels passed the center line of a gage location. Depending on the gear-to-gage offset distance, the second peak could be an upward movement and could be larger than the first peak. With the exception of reduced magnitudes, Bison coil recordings for the rigid pavement structure were similar to those shown in Figure 6.

Velocity gages responded in the form of two to four peaks,

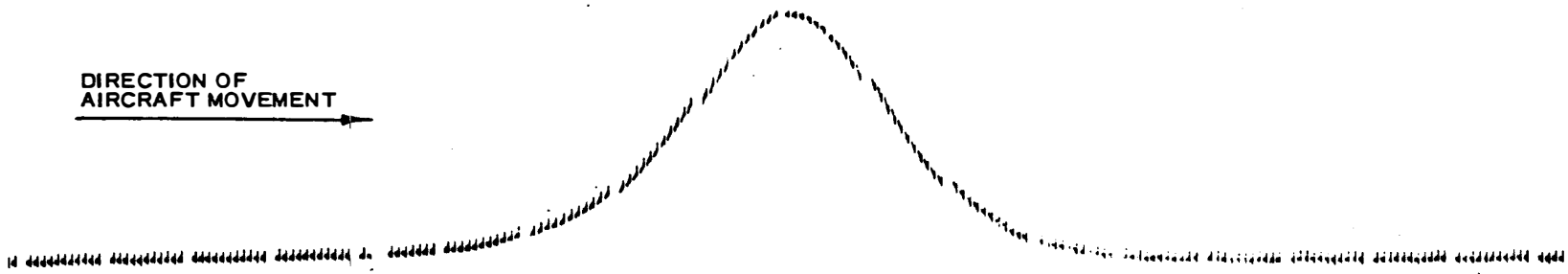

Figure 4. Typical recording for an SE soil pressure cell, 1974

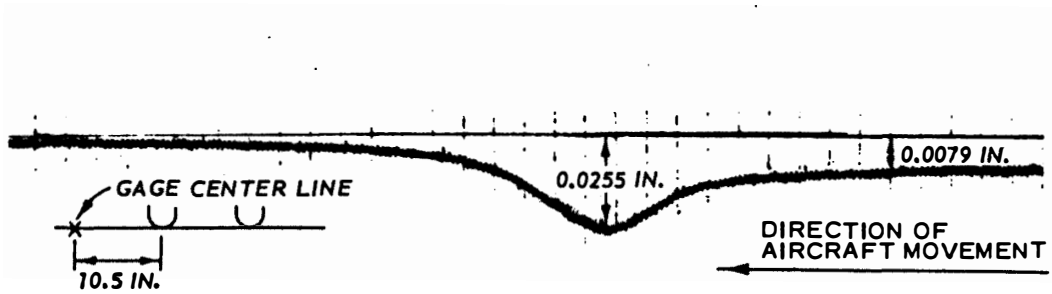

a. 10.5-IN. OFFSET

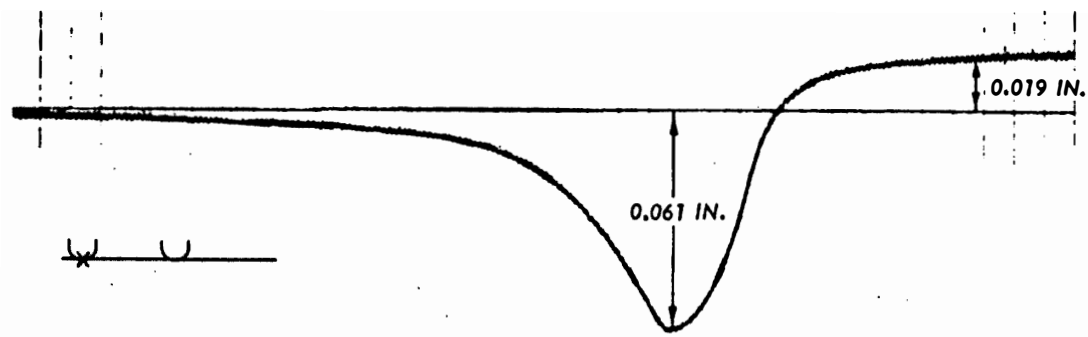

b. 0-IN. OFFSET

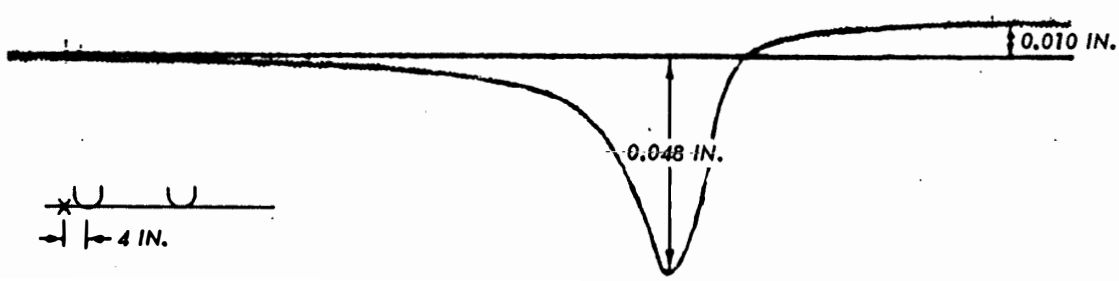

c. 4-IN. OFFSET

Figure 5. Typical analog recording for WES deflection gage (recorded for creep-speed taxi tests, 1974)

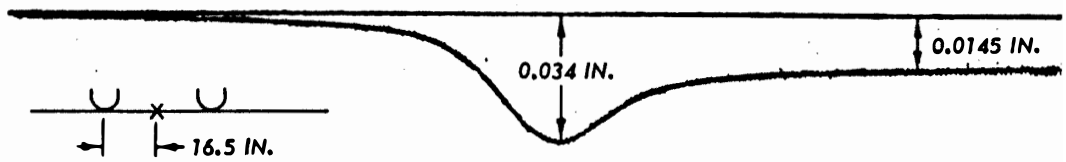

d. 16.5-IN. OFFSET

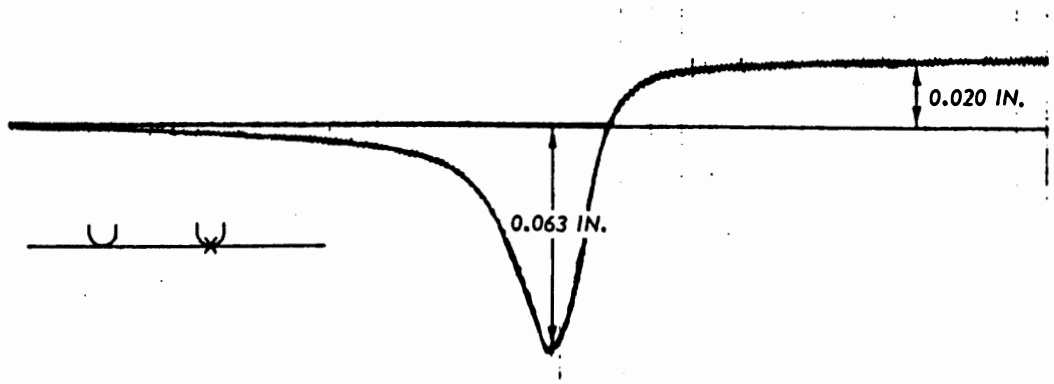

e. 0-IN. OFFSET

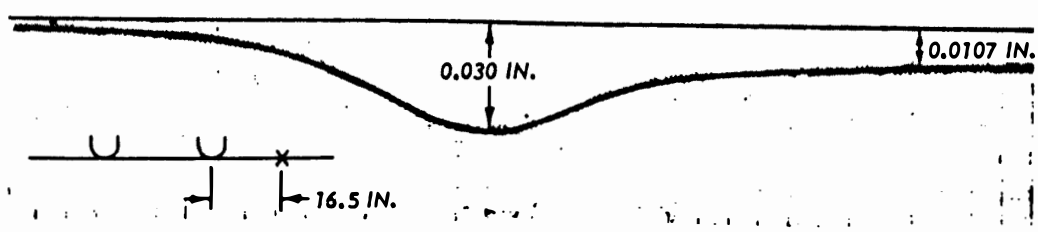

f. 16.5-IN. OFFSET

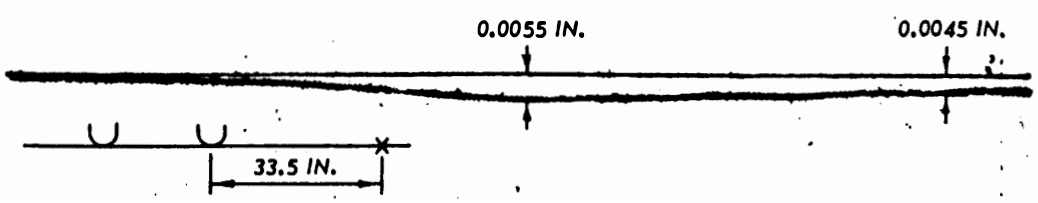

g. 33.5-IN. OFFSET

Figure 5. (Continued)

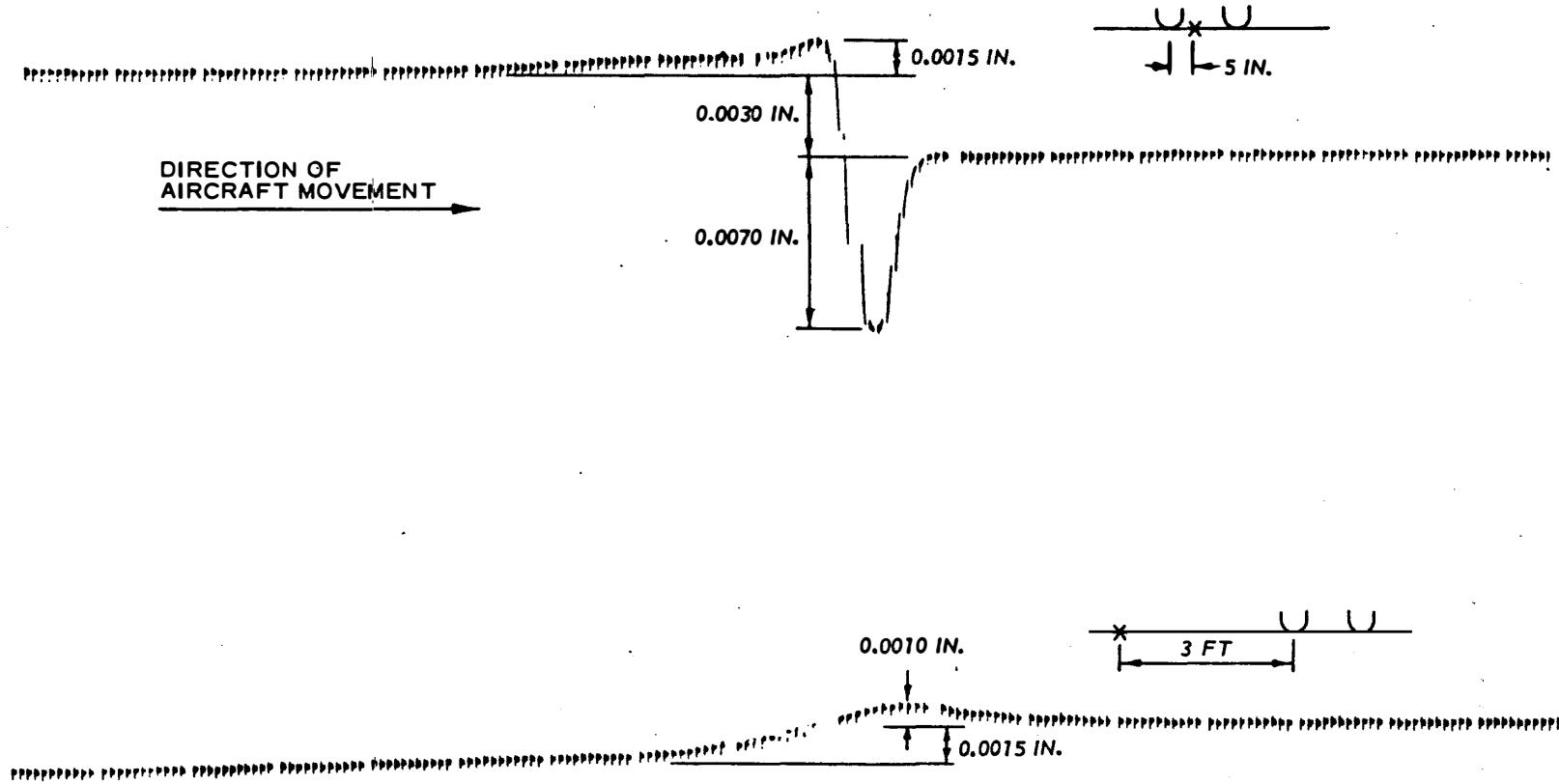

Figure 6. Typical recordings for Bison coils in creep-speed taxi tests, 1974

depending on the gear-to-gage offset distance. In the immediate gage vicinity, two upward peaks occurred immediately before the wheels reached the gage center line, and one downward and then one upward peak occurred after the wheels passed. At offset distances not within the immediate gage vicinity, only a downward and then an upward peak occurred. Figure 7 shows typical digital computer reproduced recordings of a velocity gage for 0- and 1.5-ft gear-to-gage offset distances (both real and computer expanded times are shown) for both rigid and flexible pavement structure responses.

DATA REDUCTION

The test data were reduced by digital computer, automatic data processing techniques. A detailed description of the processing is contained in Appendix A to Volume II[3] of this report.

The digital processed results were output on both hard copy (oscillograph records) and digital magnetic tapes in binary coded decimal (BCD) format, the most widely accepted input format for 7-track digital tapes. Digital BCD tapes provided the input media for dumping or further processing of the data on high-speed computers.

Desired data output varied with the type of test and the type of gage processed. Static load tests were more important in their relationship to one another than in themselves. Therefore, in addition to the magnitude of the static level, the change in each static level from the preceding calibration and static level was output. In addition to the calibration zero level, the change from the last calibration zero level was also output.

For all instruments except the velocity gages, the information that was output for the static load tests was also output for the dynamic load tests, although this was supplemented with additional information. Both data peaks were output for the Bison coils, but only one peak was output for the other gages. All data peaks were calculated from the prior-to-peak no-load level; however, the difference between the prior-to-peak and the after-peak no-load levels was also output. Another output was the change in no-load level from test to test. A description

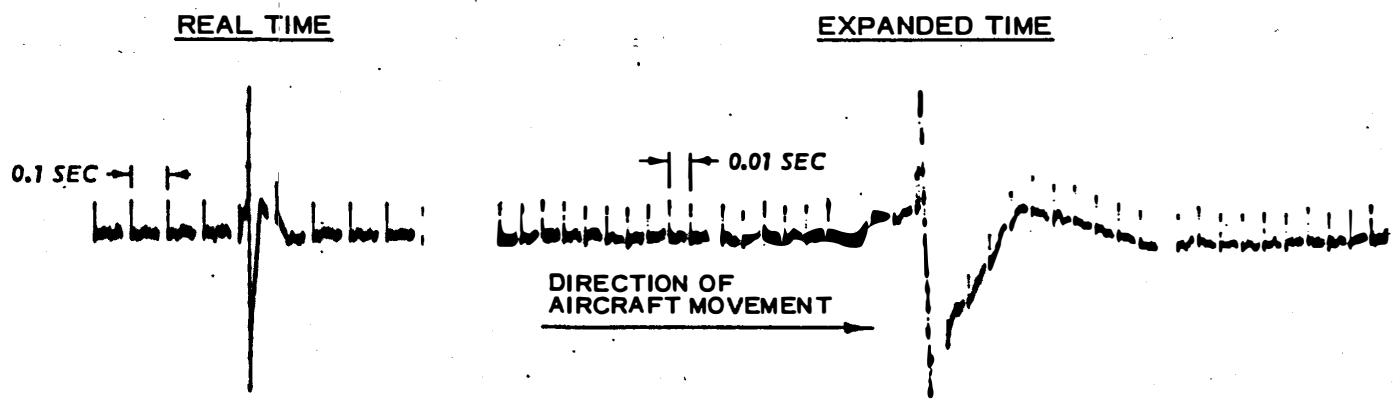

a. ZERO GEAR-TO-GAGE OFFSET

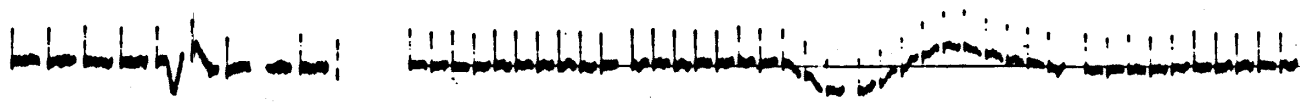

b. 1.5-FT GEAR-TO-GAGE OFFSET

Figure 7. Typical recordings for velocity gage for two different gear-to-gage offset distances, 1972

of each test in engineering units was also output. This was made by printing (with an oscillograph) groups of points 0.01 sec in length from 0.2 sec before to 0.2 sec after the peaks and recording on magnetic tape the first point of each group. The groups on hard copy containing the peak points were marked by lines on either side of the group.

A standard procedure for reducing velocity data is integration of the signals. If data response is simple, such as downward and then upward movement, this procedure is applicable and the result is the motion (displacement) that caused the velocity. For the NAFEC velocity response data at gear-to-gage offset distances not within the immediate gage vicinity (as shown in Figure 7b), integration of signals yielded the pavement displacement. However, for the velocity data in the immediate gage vicinity where multiple movement peaks occurred, direct integration was not applicable and yielded erroneous results. A description of a methodology for reduction of the velocity data to measurements of displacement is presented in Volume II.[3] The movements computed from velocity gage responses did check with those measured by WES deflection gages and Bison coils.

AIRCRAFT LOADS

Load data for the B-727 aircraft were reduced both manually and by automatic data processing as described in Appendix A to Volume II.[3] Accelerometer data for the C-880 dynamic load tests were not reduced for the four dynamic load applications with this aircraft. (Only four dynamic load tests were conducted with the C-880 before the brakes locked and five tires burst.)

Figures 8-11 summarize the B-727 aircraft dynamic loads imposed upon the flexible and rigid pavement structures. The basic operational modes are represented in these figures. A gear load ratio, which is the ratio of dynamic to static load, is used to present the aircraft vertical loading conditions in Figures 8-10. The data for each operational mode are grouped and are presented at velocity values that are representative of a specific velocity range for each mode. Creep- and low-speed taxi data are plotted at the upper ends of their velocity ranges because the majority of these tests occurred in these ranges. High-speed taxi data are plotted at the upper end of their velocity range in order to represent the highest velocities used in the tests. All other modes are plotted about the centers of their respective velocity ranges.

The dynamic load spread at each mode is represented by mean values plus or minus one standard deviation. Taxi modes are connected across the figure in order to better show their range of dynamic effects and the general decrease of the median load with an increase in taxi velocity. Also, comparisons of other operational modes with the taxi modes can be easily made with the taxi mode lines. The outer envelope represents the high and low data points for the taxi modes. The similarity between the 1972 and 1974 tests (see Figures 8 and 10) is evident.

Figure 11 shows the horizontal side thrust increase for turning operations. These results are for the 1972 tests on both the flexible and the rigid pavement test sites. Results of the 1974 tests on the flexible pavement test site are similar and within the same ranges.

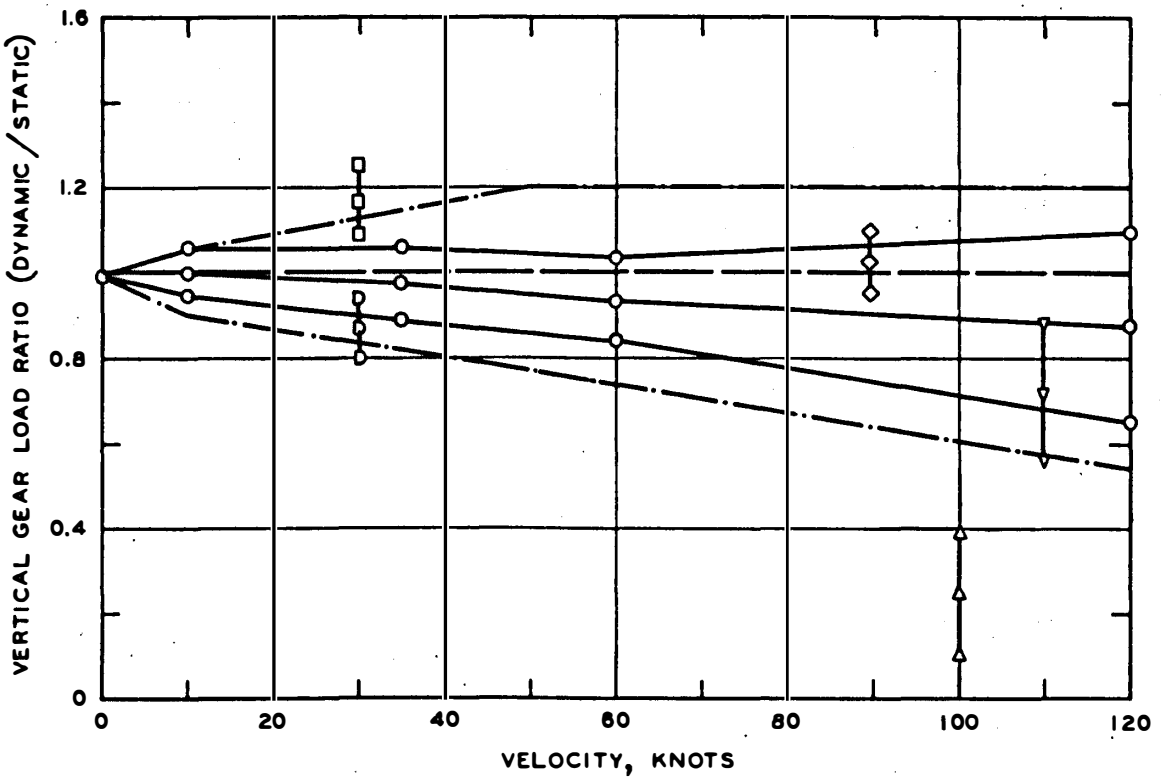

LEGEND

—·— LOAD ENVELOP FOR TAXI MODES

O STATIC LOADS AND TAXI DYNAMIC LOADS (MEAN VALUE ±1 STANDARD DEVIATION)

▽ TAKEOFF ROTATION PRIOR TO AND ON GAGES (MEAN VALUE ±1 STANDARD DEVIATION)

◇ HIGH-SPEED BRAKING WITH REVERSE THRUST (MEAN VALUE ±1 STANDARD DEVIATION)

△ TOUCHDOWN (MEAN VALUE ±1 STANDARD DEVIATION)

□ TURNING (LOAD ON GEAR ON OUTSIDE OF TURNING RADIUS ±1 STANDARD DEVIATION)

D TURNING (LOAD ON GEAR ON INSIDE OF TURNING RADIUS ±1 STANDARD DEVIATION)

Figure 8. Aircraft gear load ratios for 1972 flexible pavement tests

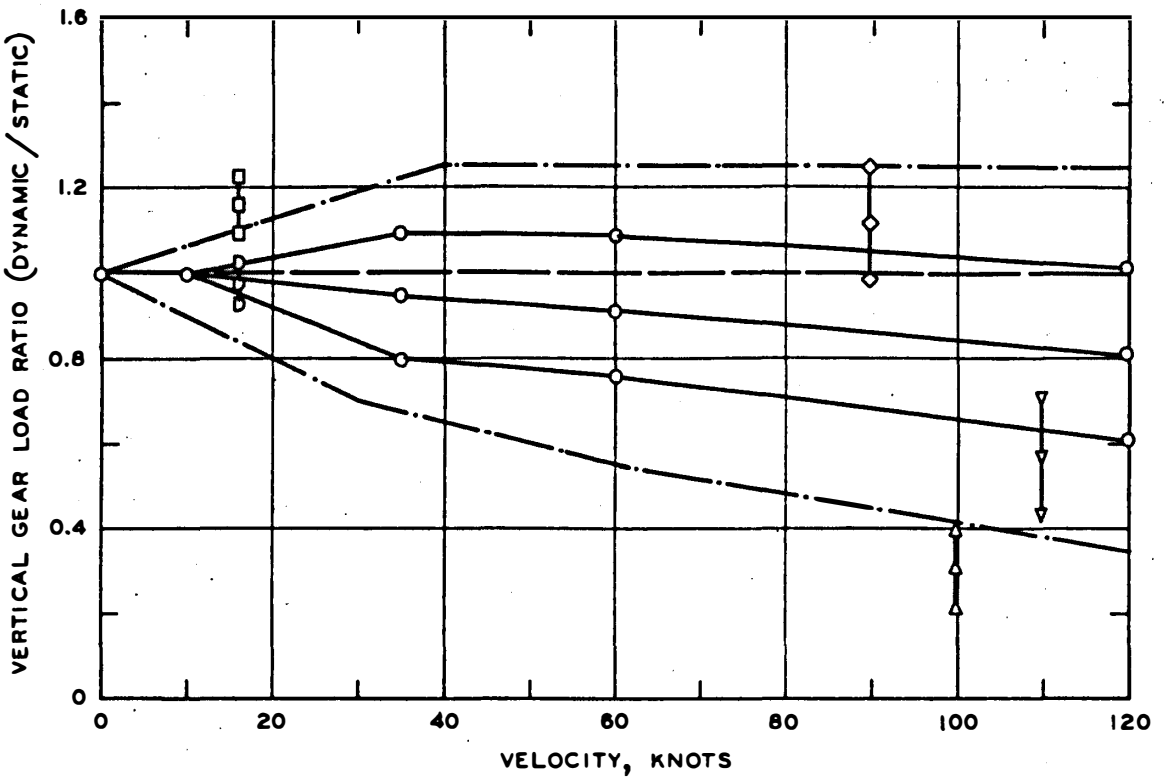

LEGEND

- LOAD ENVELOP FOR TAXI MODES
- O STATIC LOADS AND TAXI DYNAMIC LOADS (MEAN VALUE ±1 STANDARD DEVIATION)
- ▽ TAKEOFF ROTATION PRIOR TO AND ON GAGES (MEAN VALUE ±1 STANDARD DEVIATION)
- ◇ HIGH-SPEED BRAKING WITH REVERSE THRUST (MEAN VALUE ±1 STANDARD DEVIATION)
- △ TOUCHDOWN (MEAN VALUE ±1 STANDARD DEVIATION)
- □ TURNING (LOAD ON GEAR ON OUTSIDE OF TURNING RADIUS ±1 STANDARD DEVIATION)
- D TURNING (LOAD ON GEAR ON INSIDE OF TURNING RADIUS ±1 STANDARD DEVIATION)

Figure 9. Aircraft gear load ratios for 1972 rigid pavement tests

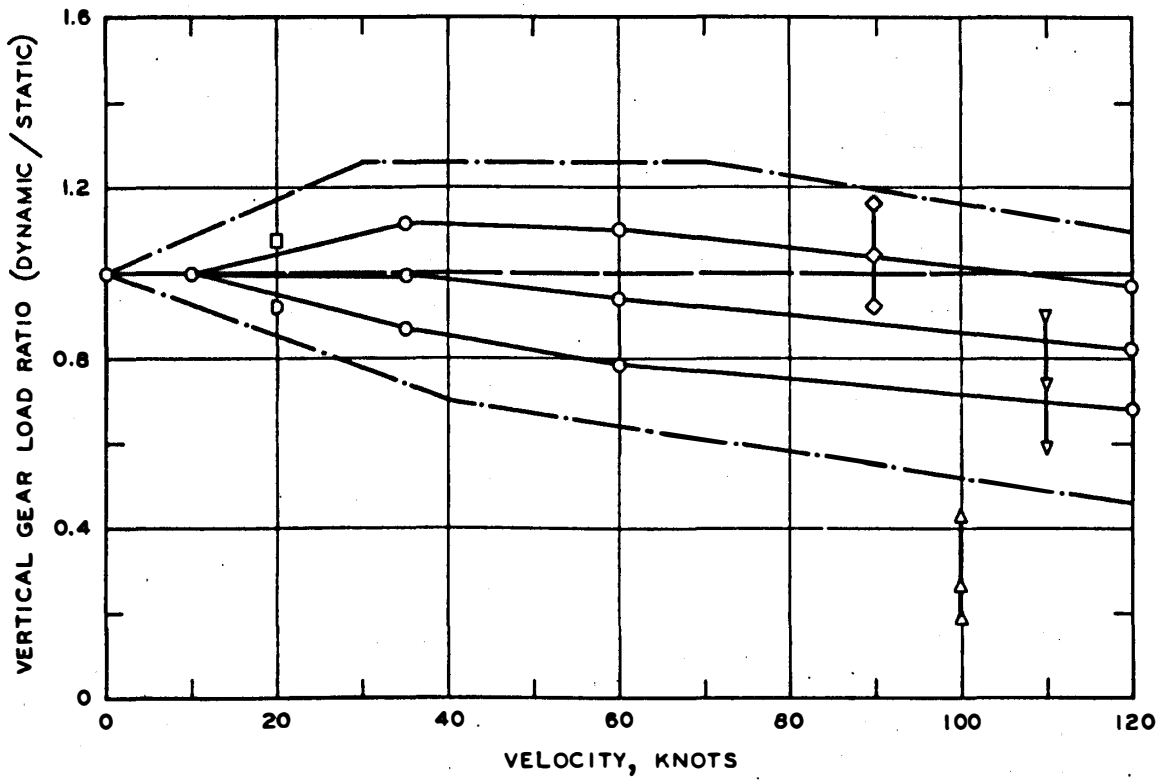

LEGEND

—·— LOAD ENVELOP FOR TAXI MODES

o STATIC LOADS AND TAXI DYNAMIC LOADS (MEAN VALUE ±1 STANDARD DEVIATION)

▽ TAKEOFF ROTATION PRIOR TO AND ON GAGES (MEAN VALUE ±1 STANDARD DEVIATION)

◇ HIGH-SPEED BRAKING WITH REVERSE THRUST (MEAN VALUE ±1 STANDARD DEVIATION)

△ TOUCHDOWN (MEAN VALUE ±1 STANDARD DEVIATION)

□ TURNING (LOAD ON GEAR ON OUTSIDE OF TURNING RADIUS ±1 STANDARD DEVIATION)

D TURNING (LOAD ON GEAR ON INSIDE OF TURNING RADIUS ±1 STANDARD DEVIATION)

Figure 10. Aircraft gear load ratios for 1974 flexible pavement tests

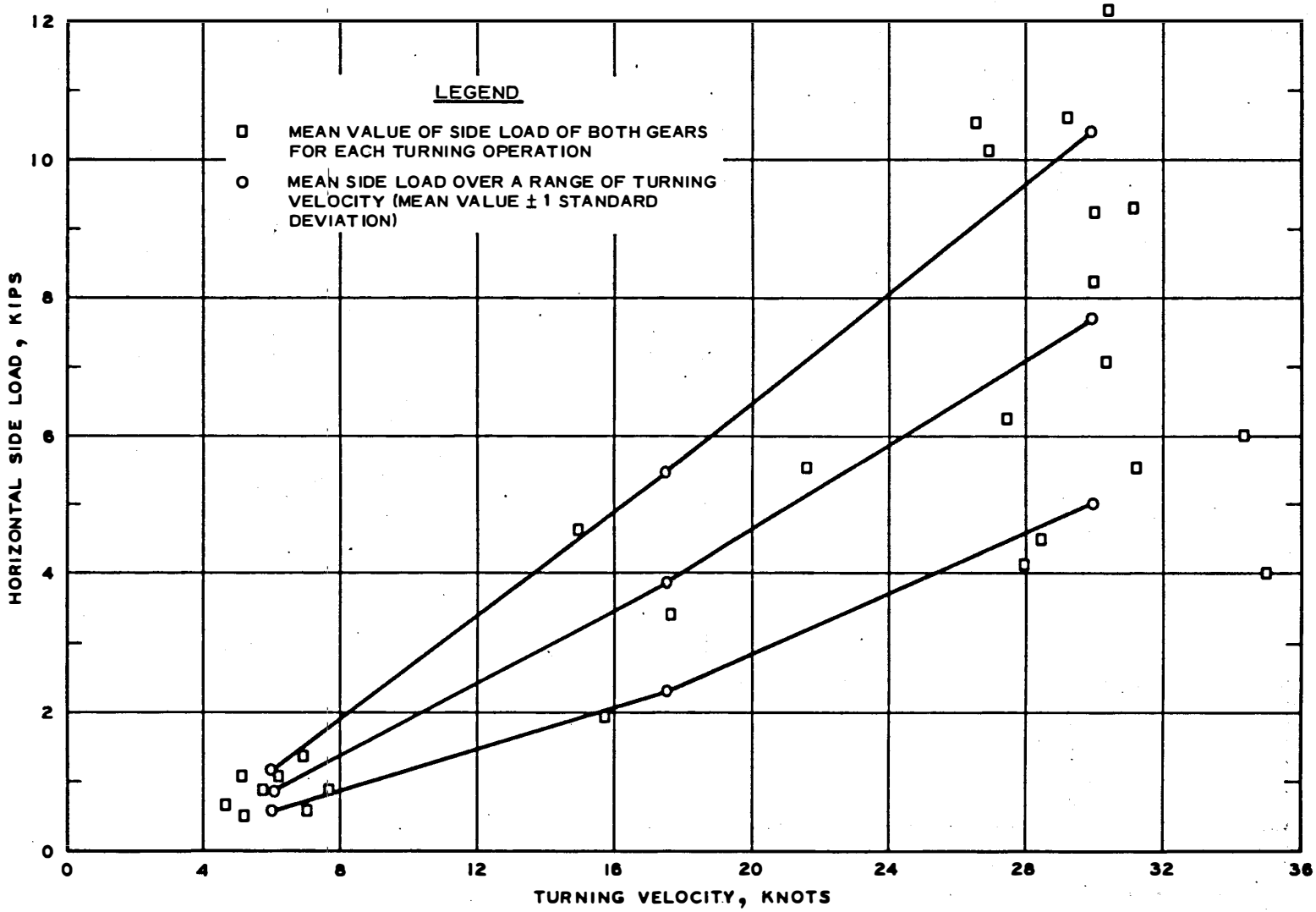

Figure 11. Horizontal side loads for turning operations in 1972 tests

Table 4 presents the aircraft average wheel loads for both the 1972 and the 1974 test series. The average loads are for both static and dynamic test conditions.

Table 4

Average Aircraft Wheel Loads

Aircraft	Test	Average Vertical Wheel Load, lb	Standard Deviation, lb
B-727	1972 flexible pavement	28,073	2,990
B-727	1972 rigid pavement	28,588	1,971
B-727	1974 flexible pavement	30,286	2,938
C-880	1974 flexible pavement	18,050	--

Note: For the B-727 tests on the flexible and rigid pavements in 1972 and 1974, the average horizontal side load for normal taxiing at 45 knots was 1000 lb with a standard deviation of 100 lb.

DATA INTERPRETATION AND ANALYSIS

A large amount of data was collected during the study, all of which has been reduced. With the exception of the velocity gage responses, all data are presented in Reference 3. The velocity gage data were not presented (as explained in Reference 3) because of their agreement with the behavior of the deflection gages and Bison coils. Two methods of data interpretation were used. The first method, which might be referred to as the standard method, considered a zero reference point of the gage and pavement structure from which all subsequent readings were taken and used to represent the pavement response. This method of interpretation provided data which led to confusion in analysis. The confusion resulted from the fact that the gage and pavement structure, and thus the zero reference point, physically moved as the soil and pavement structure mass was kneaded by randomly distributed traffic. This phenomenon has been suspected for some time and was actually reported in Reference 6. The second method of data interpretation consisted of using a floating reference and separating the response data into elastic and inelastic phases. Volume II[3] of this report presents in detail the methodologies used in the interpretation and analysis of data, and Appendix B of Volume II presents plots of the reduced test data.

As an example of the two data interpretation methods, consider the two series of static load tests shown in Figure 12. This figure represents the initial no-load reading, load on reading, and load off (rebound) reading of a WES deflection gage measuring between the 0- and 15-ft depths of the flexible pavement structure during the warm weather tests in 1974. The data shown in Figure 12 were obtained by performing successive sequences of B-727 load application (load off, load on, load off) for both series of tests with the left (crosshatched) wheel of the dual-wheel main gear located at the distances from the runway center line at which the data are plotted. For example, for the first load series, the left wheel was located at approximately 15, 11.3, 9.6, 6.1, and 4.2 ft from the runway center line for load sequences 1, 2, 3, 4, and 5, respectively. At each location of the gear, the pavement

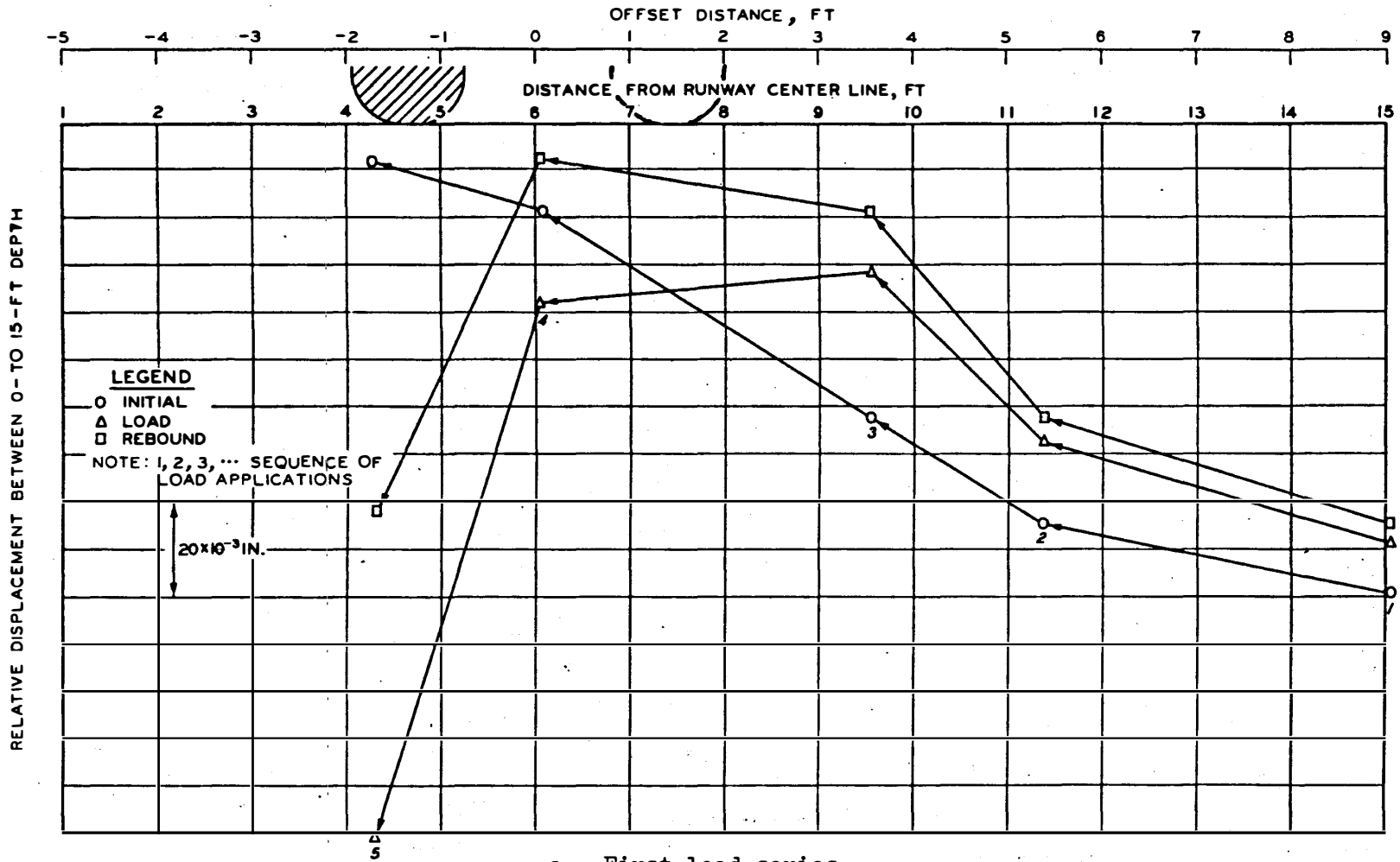

a. First load series

Figure 12. Typical static load test measurements with a WES deflection gage (0- to 15-ft depth)

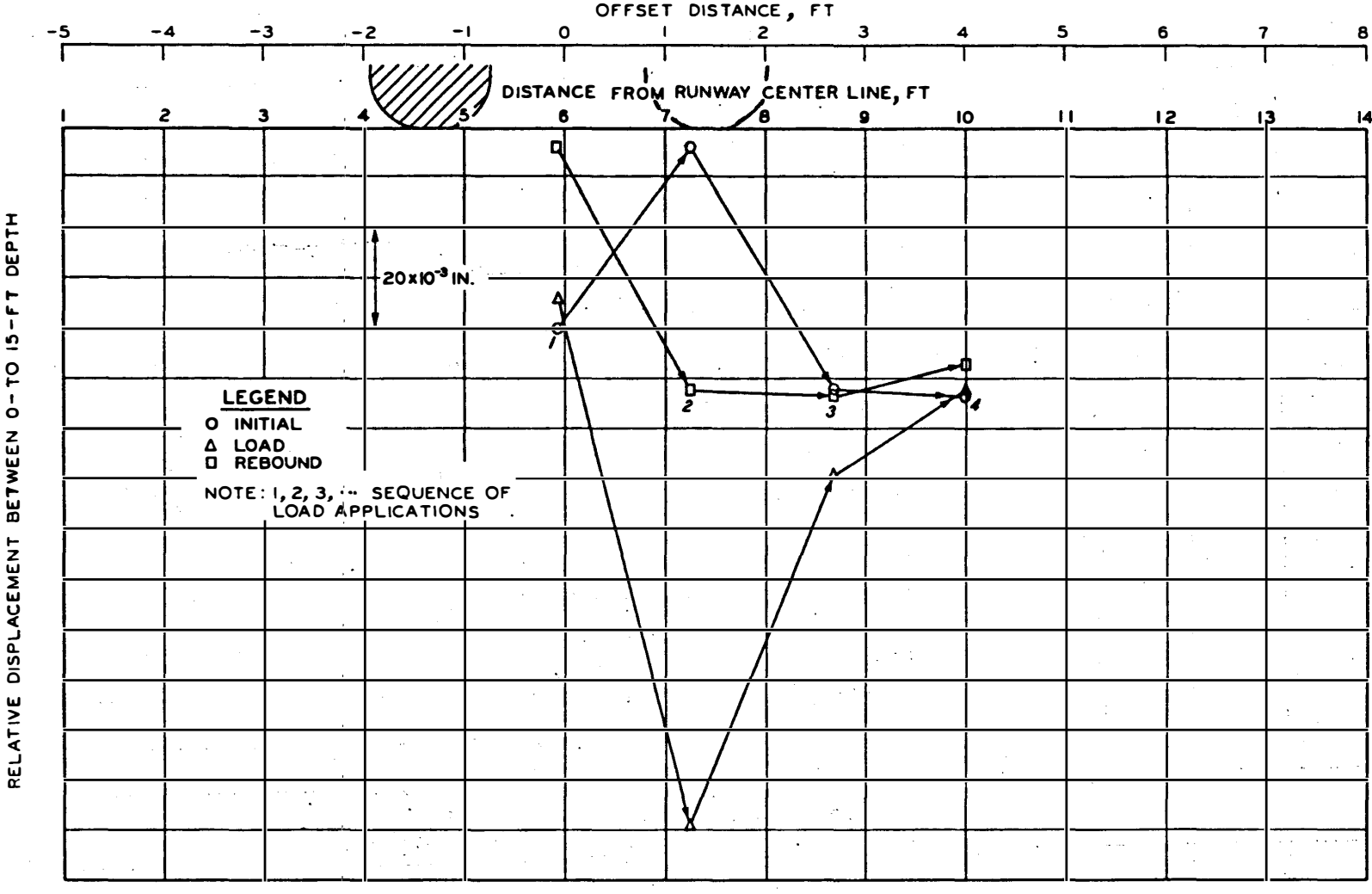

b. Second load series

Figure 12. (Sheet 2 of 2)

response was measured by the WES deflection gage located 7 ft 4.5 in. from the runway center line. Assuming a relationship of reciprocal displacement exists, information can be plotted as shown in Figure 12 as the response of the pavement structure when the aircraft main gear passes at the indicated distance from the runway center line. The information for the second series of tests was developed in the same manner except that the load sequences (1, 2, 3, and 4) were applied from left to right. An elapsed period of 1 day occurred between the first and second load series during which time 23 dynamic load applications (including creep-speed taxis) had occurred on the instrumented area. The behavior (not the magnitude) shown in Figure 12 is typical for both rigid and flexible pavement structures and for the Bison coil and Valore strain gage responses.

For the first method of analysis, the initial reading for load sequence 1 for each load series is used as the zero reference for the entire load series. This method of data interpretation results in relative displacements as shown in Figure 13. As can be seen, the displacements are significantly different even though the aircraft gear load, location, and pavement structure were the same. There was no logical explanation for these differences based upon the data interpretation method. Based upon past experience with interpretation of instrumentation data from carefully controlled testing of test sections, the data were reinterpreted using the methodology explained in Volume II[3] of this report. This method of interpretation, in summary, consists of using a floating reference and separating the response data for each load sequence into the elastic and inelastic phases. This is accomplished by considering the elastic phase to be the difference between the load and rebound readings for each load sequence and the inelastic phase to be the difference between the initial and rebound readings for each load sequence. Using this method for interpretation of data, the elastic displacements for each load sequence and both series of static load tests shown in Figure 12 can be plotted as shown in Figure 14. It can be seen that the elastic displacements agree quite well for both series of tests. The inelastic displacements are also shown plotted in Figure 14;

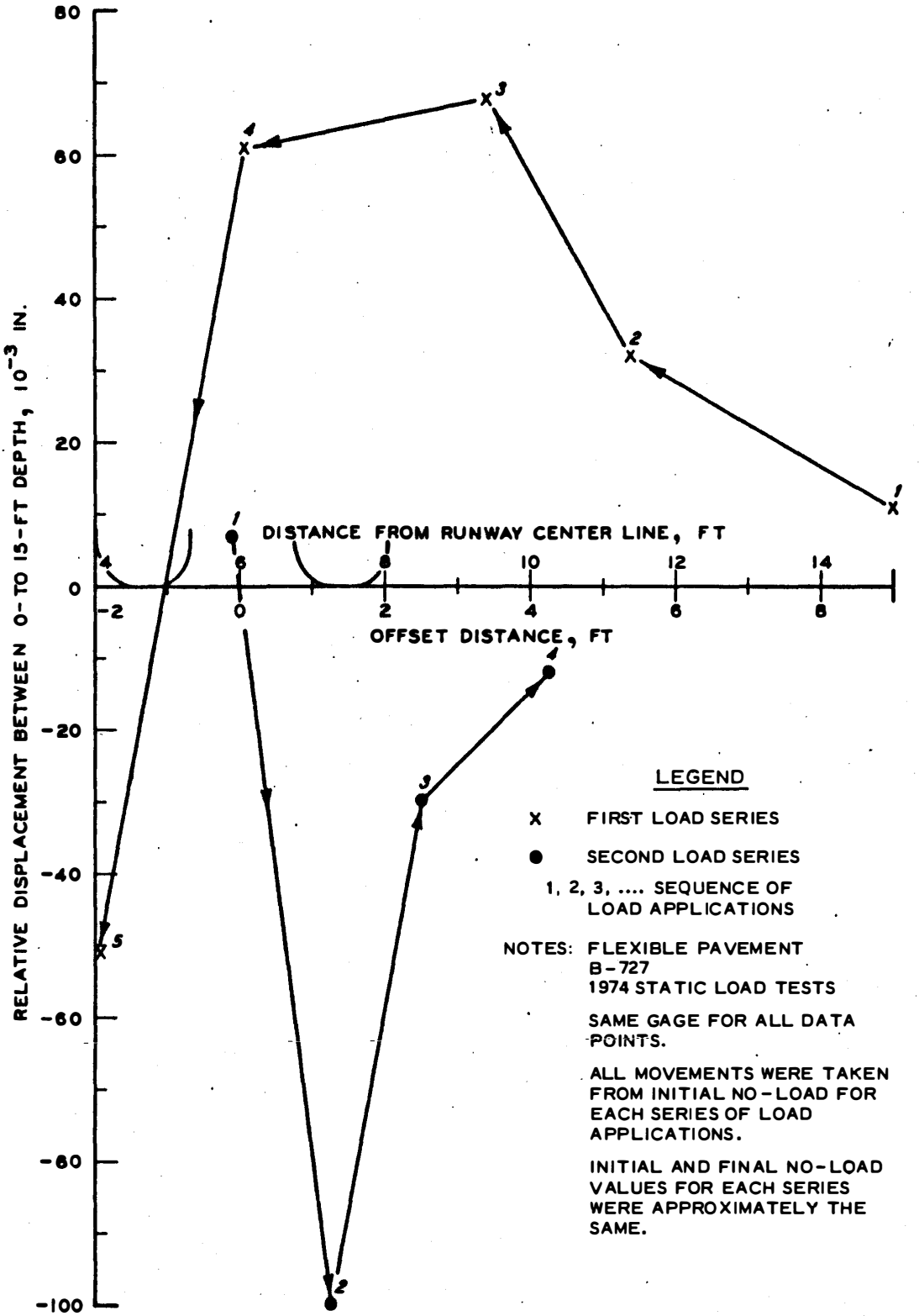

Figure 13. Relative displacements from a common reference (from Figure 12)

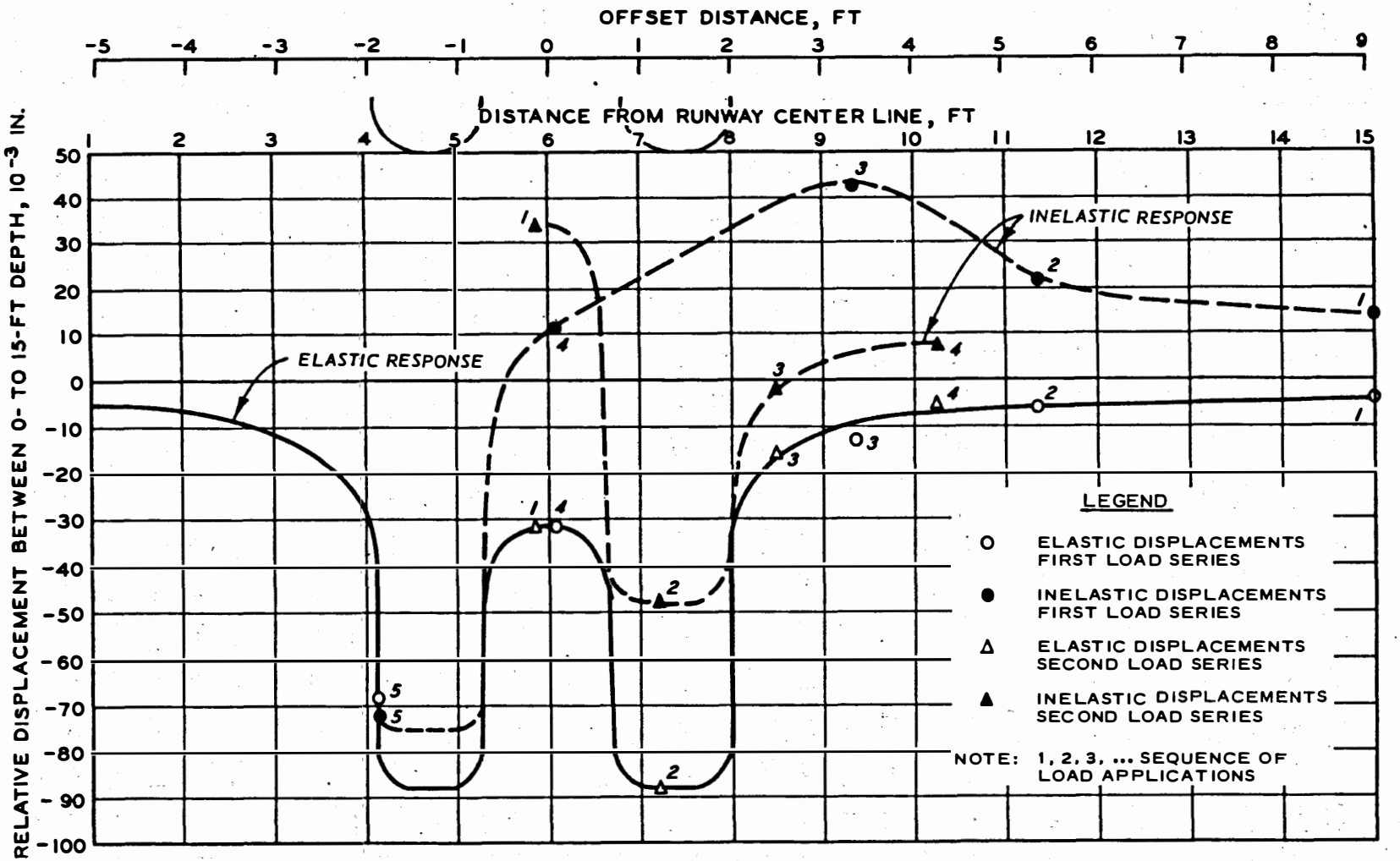

Figure 14. Typical static load test results measured with a WES deflection gage (from Figure 12)

however, these displacements cannot be combined into a single plot since their magnitudes are (as illustrated in Figure 14) dependent upon the loading history, i.e., the traffic distribution pattern. For the data illustrated, it should be remembered that the loading sequences for the first load series were performed from right to left while for the second load series the loading sequences were performed from left to right. The phenomenon depicted in these illustrations (Figures 12-14) was observed for every load series performed, whether the operating mode was static load, creep-speed taxi, high-speed taxi, rotation, or high-speed turn. All of the displacement data collected were interpreted in the manner illustrated in Figures 12 and 14, and the results are presented in Appendix B to Volume II[3] of this report.

Another illustration is shown in Figure 15 where the elastic movements (static load curve superimposed) for the creep-speed tests of Figure 5 are plotted. Figure 16 shows the inelastic movements illustrated in Figure 5. The elastic and inelastic responses occur simultaneously but were separated in this manner for analysis.

The data acquired for this study represent nonconditioned pavement structures. Pavement structure conditioning is a test procedure in which a pavement is loaded repeatedly before instrument responses are recorded. By conditioning, the inelastic response, which can be erratic, can be made to approach zero. That is, after repeated load application at the same point, the response becomes entirely elastic. Conditioning of the pavement has often been used in the belief that it causes instrument responses to be stable. While this type conditioning temporarily eliminates the inelastic movements, it is not really representative of behavior under actual traffic loading, since traffic is randomly distributed and approaches a normal distribution with time. Therefore, in actual use, the pavement never becomes conditioned and the inelastic displacements are continually occurring at varying magnitudes, depending upon the loading history, as can be seen in Figure 14.

In order to be able to fully interpret and analyze the nonconditioned pavement structure response data, the elastic and inelastic phases had to be separated and treated independently in the investigation

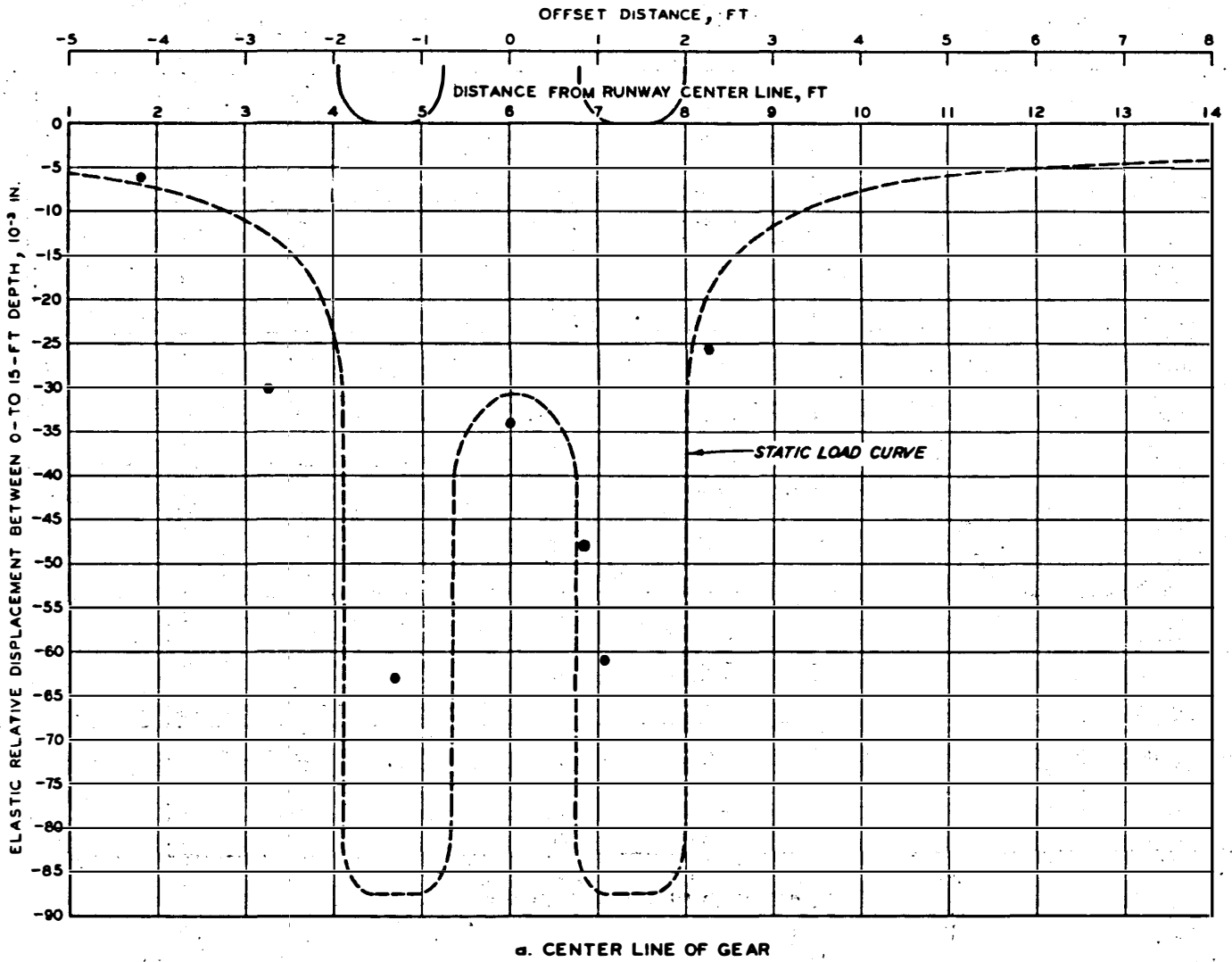

Figure 15. Typical creep-speed taxi test elastic relative displacements corresponding to Figure 5

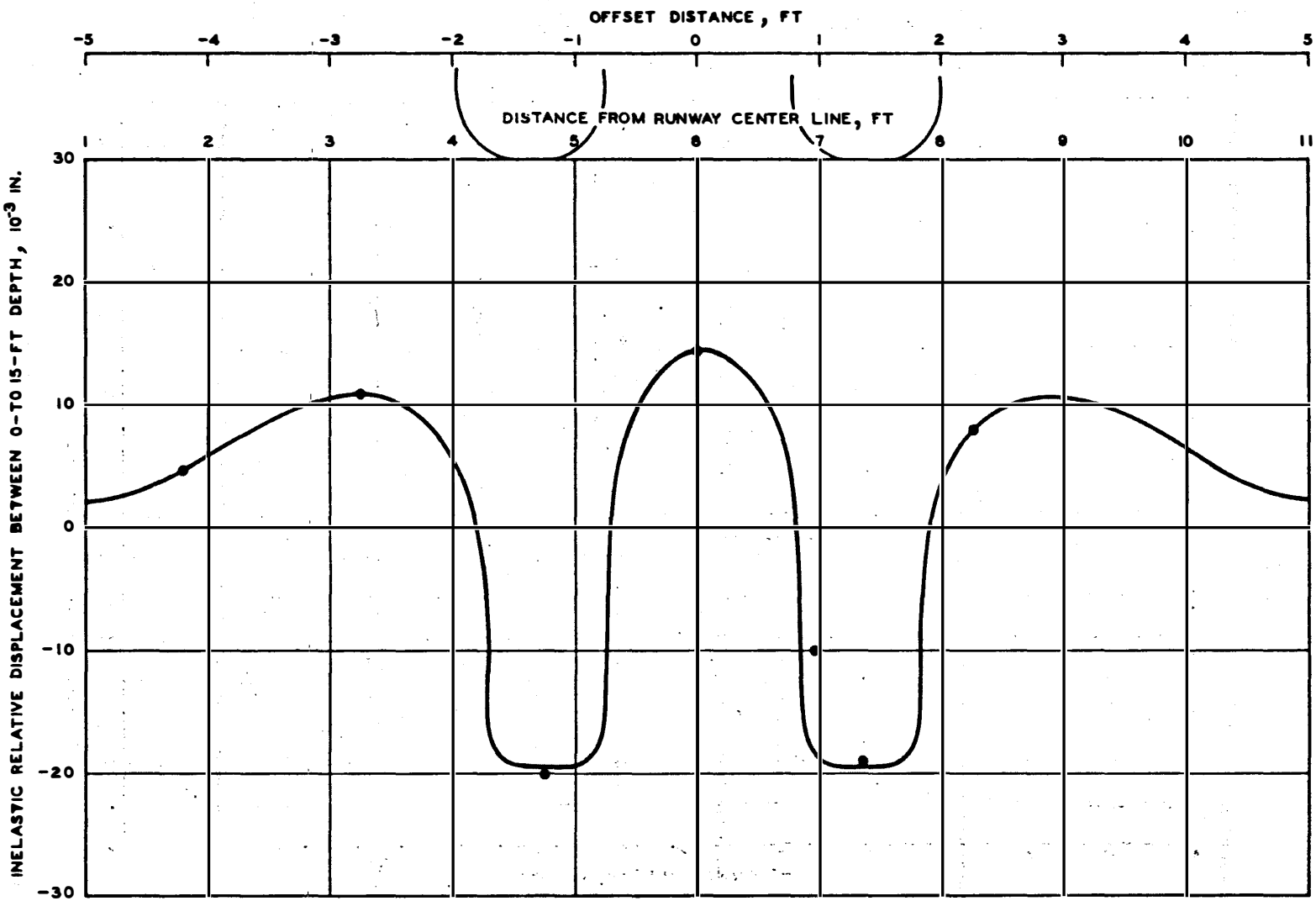

Figure 16. Inelastic wave form for creep-speed taxi tests illustrated in Figure 5.

of static and dynamic load test results. Instrument responses could not be completely analyzed unless the inelastic behavior was fully recognized and utilized.

Two different types of displacement responses were identified as acting in both flexible and rigid pavements. The two types are total pavement structure response as assumed to be referenced to infinity (inertial reference) and individual pavement structure element response referenced internally to each element (noninertial reference). Each type of response exhibited both elastic and inelastic material behavioral phases.

Bow waves in front of the wheels and elastic vertical expansions behind and adjacent to each wheel were found to occur within the structural elements (noninertial reference) of both pavement structures under moving aircraft operations.

The three different types of displacement and motion measuring instruments (WES deflection gages, Bison coils, and velocity gages) were compatible and complemented each other in their indications of pavement structure responses.

The vertical pressure data for both flexible and rigid pavements were found to be totally recovered, i.e. elastic (corresponding to the elastic phase of behavior), upon removal or passage of a load. No residual pressures appeared to be acting; therefore, the inelastic displacement behavior did not seem to induce residual vertical pressures. The pressure cells appeared to be carried with or ride within the pulsating structures.

SUMMARY OF PAVEMENT STRUCTURE RESPONSES TO AIRCRAFT DYNAMIC LOADS

Volume II[3] of this report presents summary figures of the nonconditioned pavement structure response to aircraft dynamic loads for all instrumented gage rows. Only summary figures for gage row 2 in the nonconditioned flexible and rigid pavement structures will be presented in this section. The summary figures are for the maximum load points of the aircraft gear. At the pavement surface and in upper layers, these maximum load points are beneath one of the dual wheels. The maximum load point then migrates with depth into the geometric centroid of the gear, which occurred at a depth of about 3 ft in the flexible pavement structure and at the bottom of the concrete slabs in the rigid pavement structure.

Figures 17-20 present the static load and relative displacement distributions with depth for the gear maximum load points on gage row 2 of both nonconditioned pavement structures. The data in Figures 17 and 19 are accumulated vertical relative displacements measured by the Bison coils. To permit accumulating and plotting of the data, the Bison coils at the 51- and 36-in. depths of the flexible and rigid pavement structures, respectively, had to be assumed as zero reference points since no measurements were made below these depths. However, this assumption does not mean that no displacements occurred below the 51- and 36-in. depths. Figures 17 and 19 show the maximum elastic response that was measured. They also show the maximum elastic plus the maximum inelastic response that was measured, because the elastic and inelastic responses do occur simultaneously. For a single static load application of the aircraft on the pavements, the maximum elastic plus inelastic curves represent the maximum relative displacements that could be expected. However, depending on the load history, the actual displacement for any specific loading could be anywhere between the elastic and elastic plus inelastic curves. (Load history means the magnitude of the previous load and the offset position with respect to a point in the pavement structure.) Load tests conducted after first conditioning the

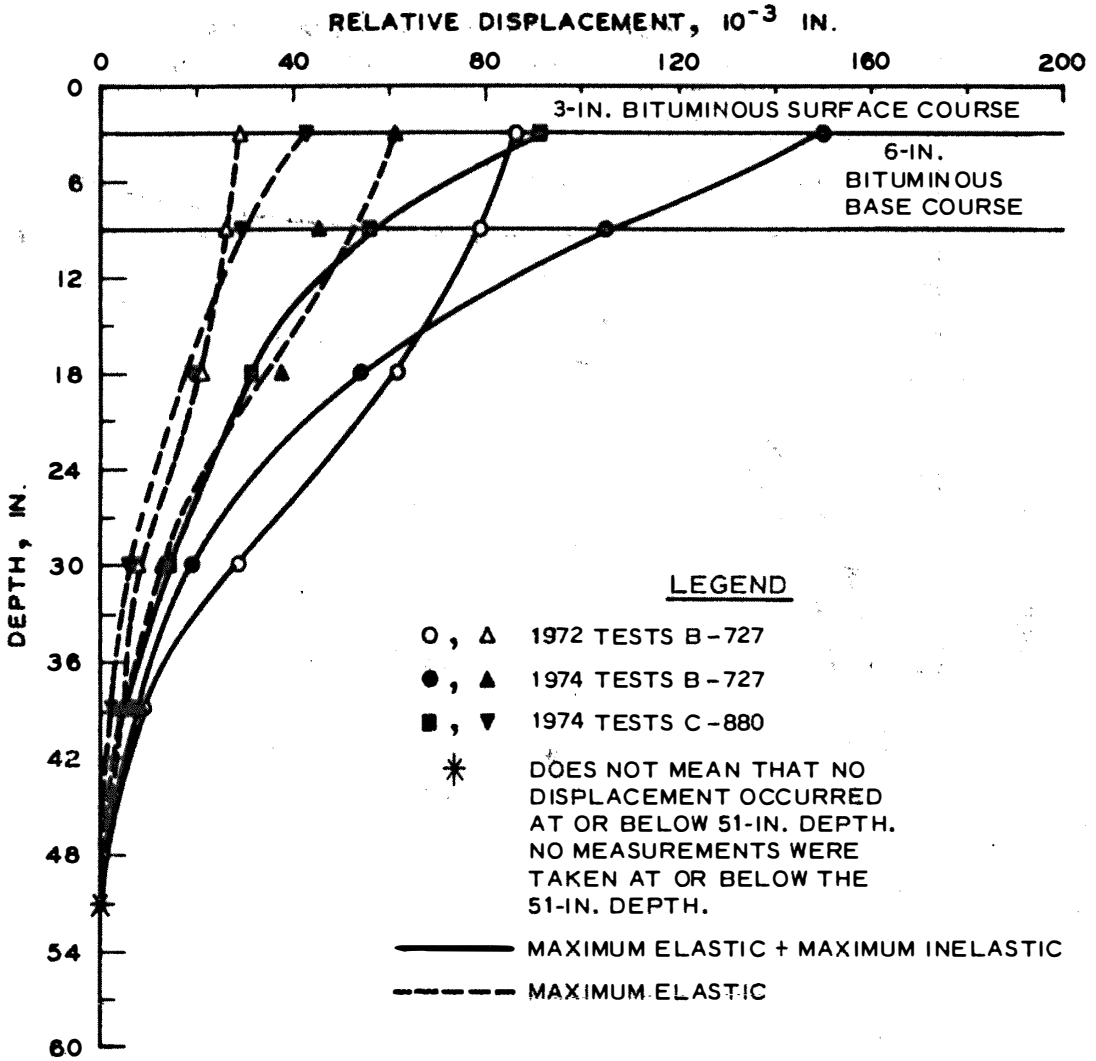

Figure 17. Vertical relative displacement versus depth, flexible pavement structure

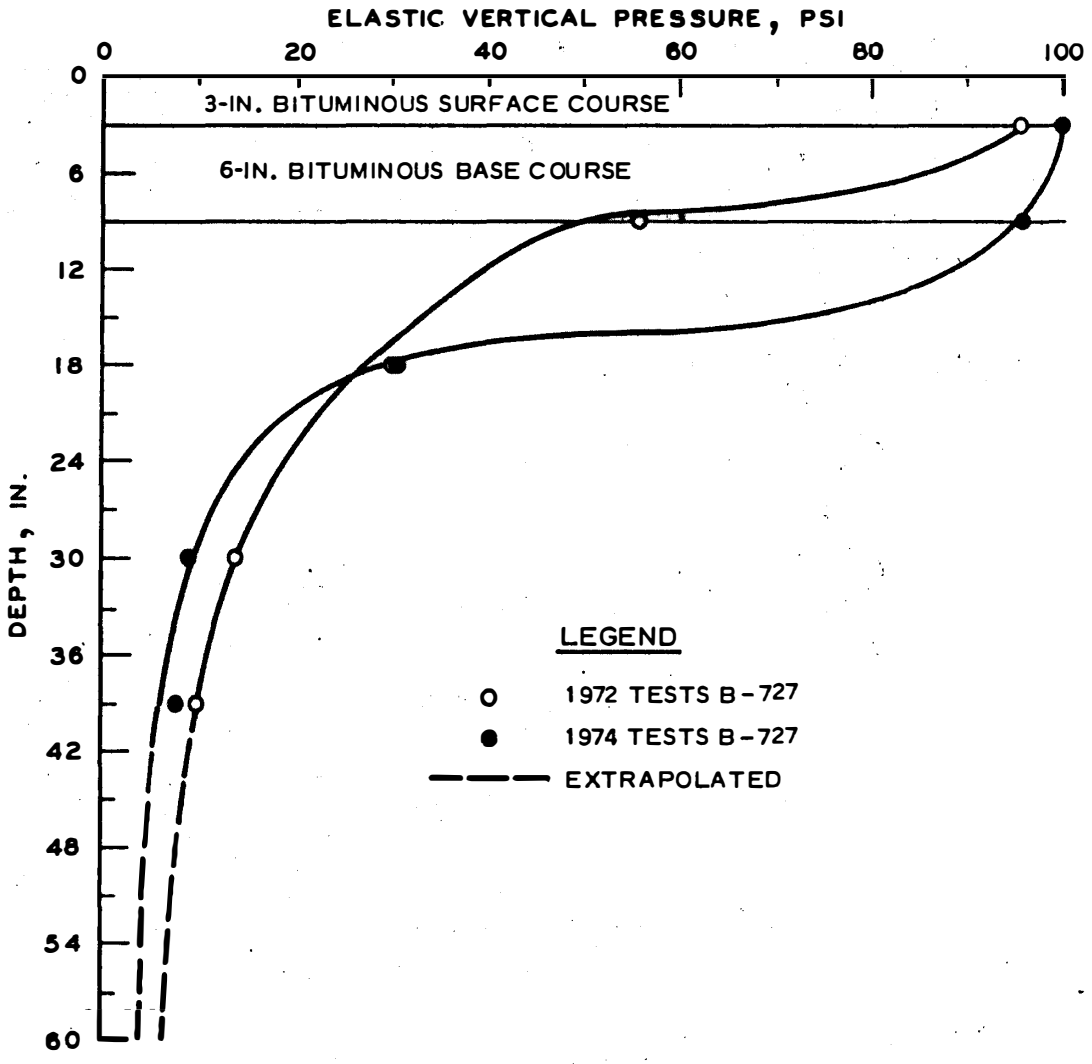

Figure 18. Vertical pressure versus depth, flexible pavement structure

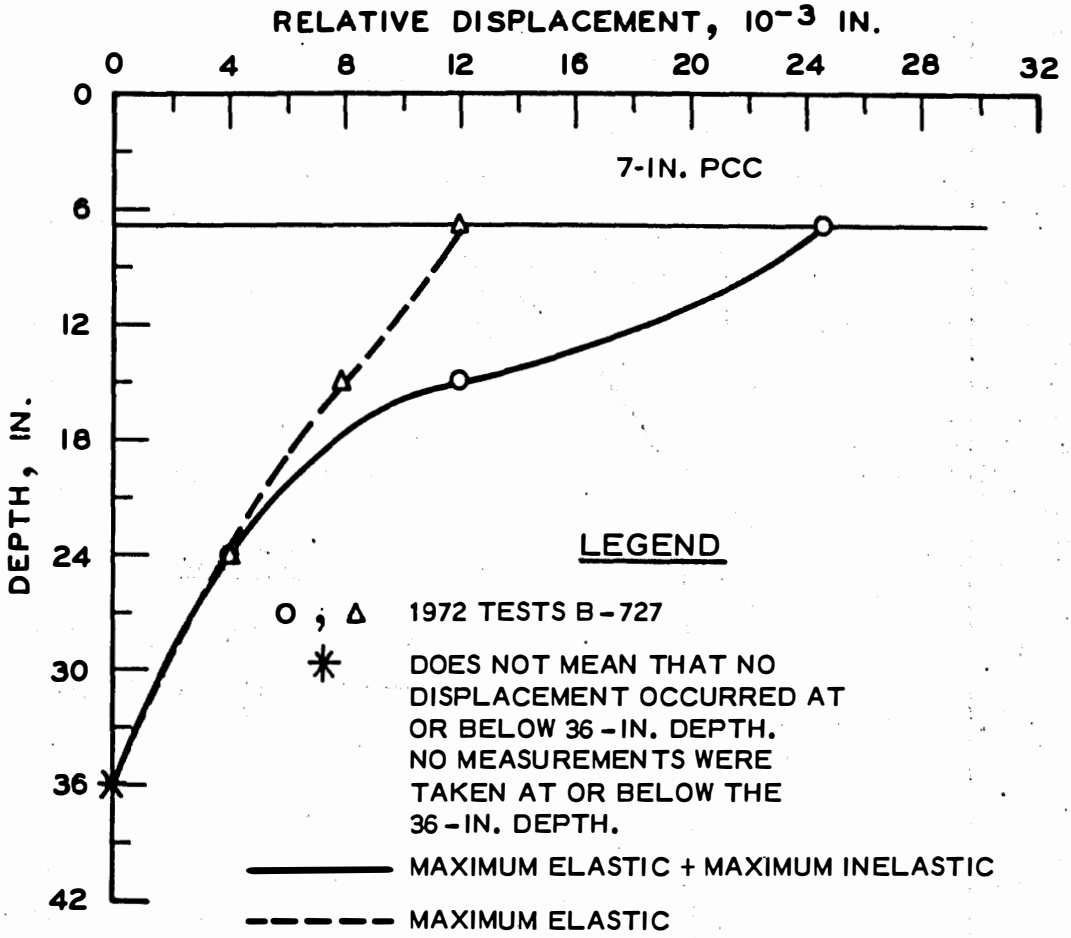

Figure 19. Vertical relative displacement versus depth, rigid pavement structure

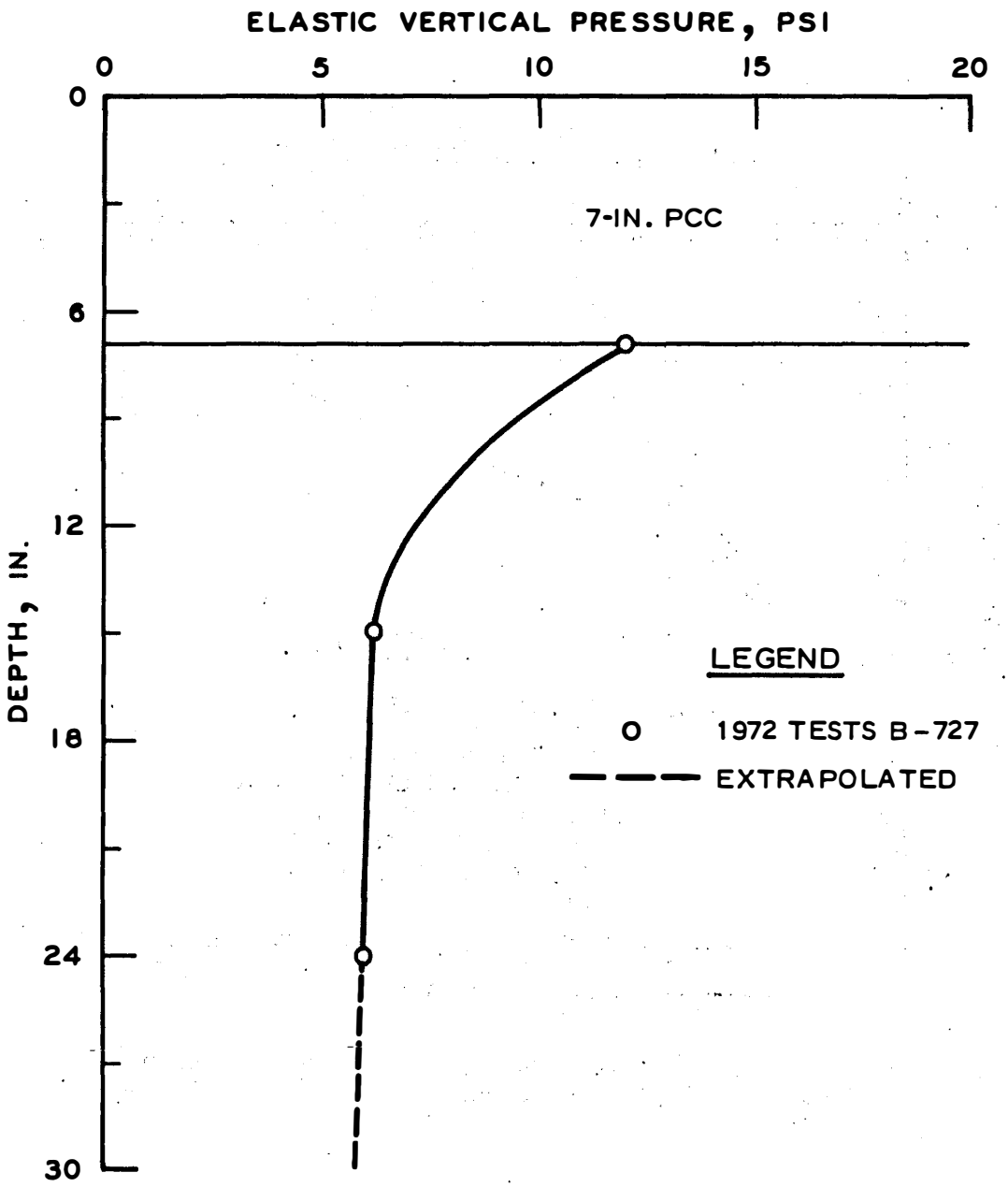

Figure 20. Vertical pressure versus depth, rigid pavement structure

pavement structures would only produce the elastic response curves and a significant displacement (inelastic) would not be obtained.

Figures 21-36 summarize relative displacements for the nonconditioned flexible pavement structure for both 1972 and 1974 test results. All basic airport operating modes for which data existed at the maximum load points are represented. If no data points are shown for an operational mode, either no data were acquired at the maximum load point or no data were recorded on the gage or gages for that mode, and the figures in Appendix B to Volume II[3] should be checked for the results. Static and dynamic load test comparisons can be seen in the figures in Appendix B for regions outside the maximum load points. A single data point in the summary figures indicates that either only one test was recorded or no data spread existed on the gage or gages at the maximum load point.

As was the case for the aircraft load data, the data for each operational mode were grouped and are presented in the summary figures at velocity values that are representative of the specific velocity range for each mode. Creep- and low-speed taxi data are plotted at the upper ends of their velocity ranges because the majority of these tests occurred in these ranges. High-speed taxi data are plotted at the upper end of their velocity range in order to represent the highest velocities used in the tests. All other modes are plotted about the centers of their respective velocity ranges. The data points shown represent, for each operational mode, the spread of the pavement response from an upper to a lower value.

For each distance across which the relative displacements were measured, figures for elastic and inelastic responses are presented. However, the method of presentation should not be construed to mean that elastic and inelastic behavior occur separately; they occur simultaneously. The elastic response spreads for each mode are represented by the high and low points being connected by vertical dashed lines. Only elastic high points of the taxi modes are connected across the figures. These lines show the relationship of other modes to the taxi modes and the relationship between the 1972 and the 1974 tests.

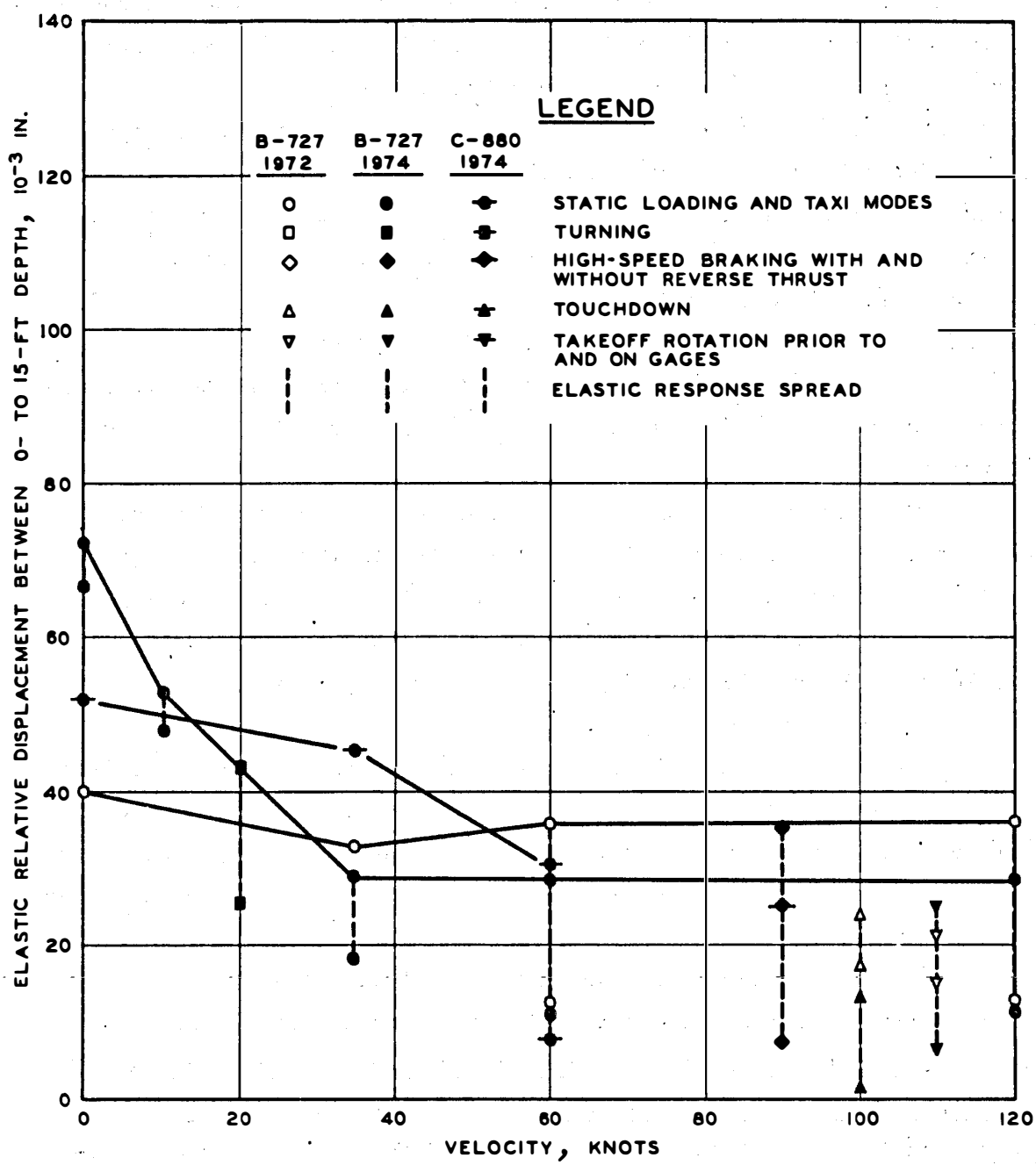

Figure 21. Maximum elastic vertical relative displacement between 0- to 15-ft depth versus velocity, flexible pavement

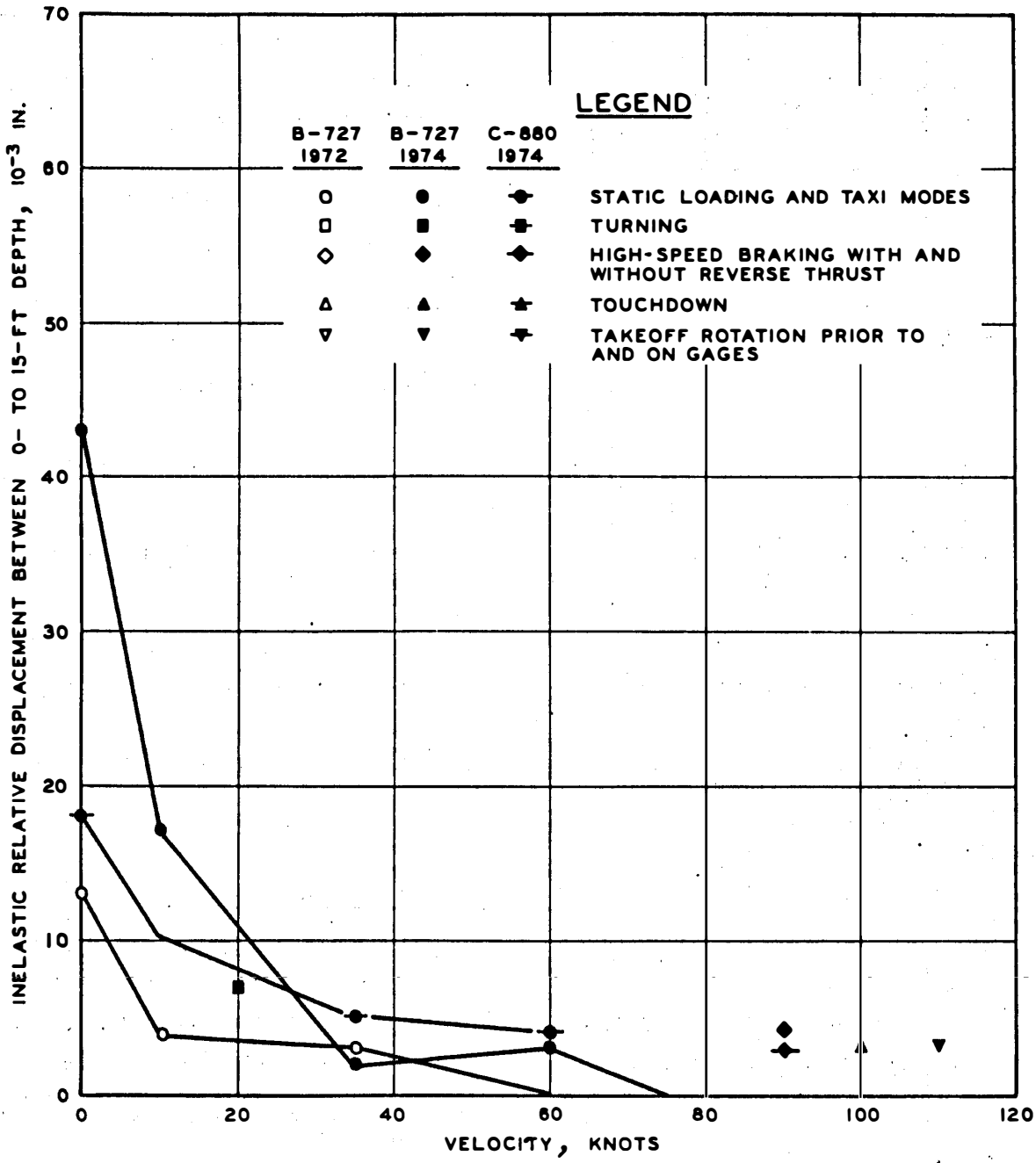

Figure 22. Maximum inelastic vertical relative displacement between 0- to 15-ft depth versus velocity, flexible pavement

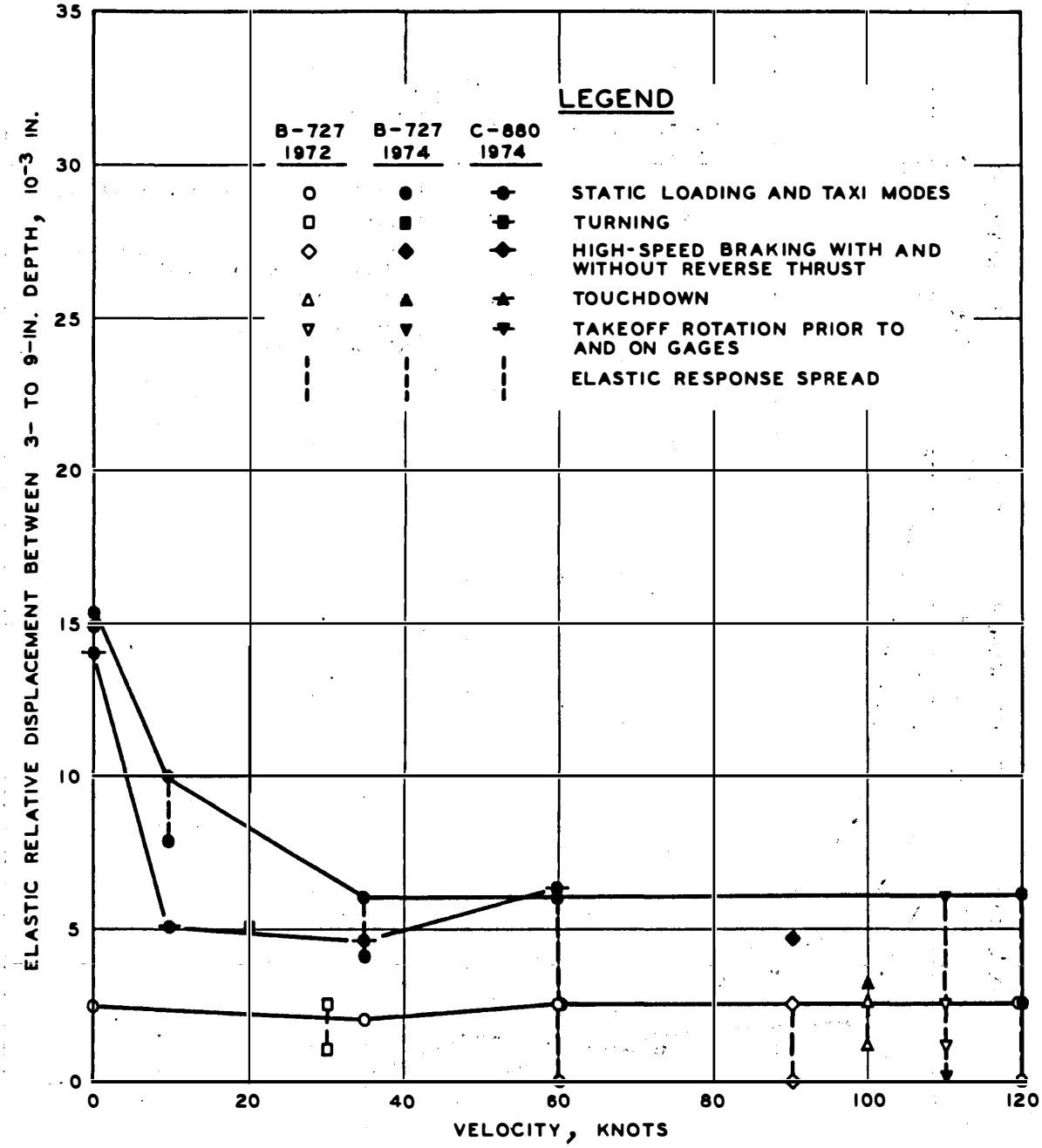

Figure 23. Maximum elastic vertical relative displacement between 3- to 9-in. depth versus velocity, flexible pavement

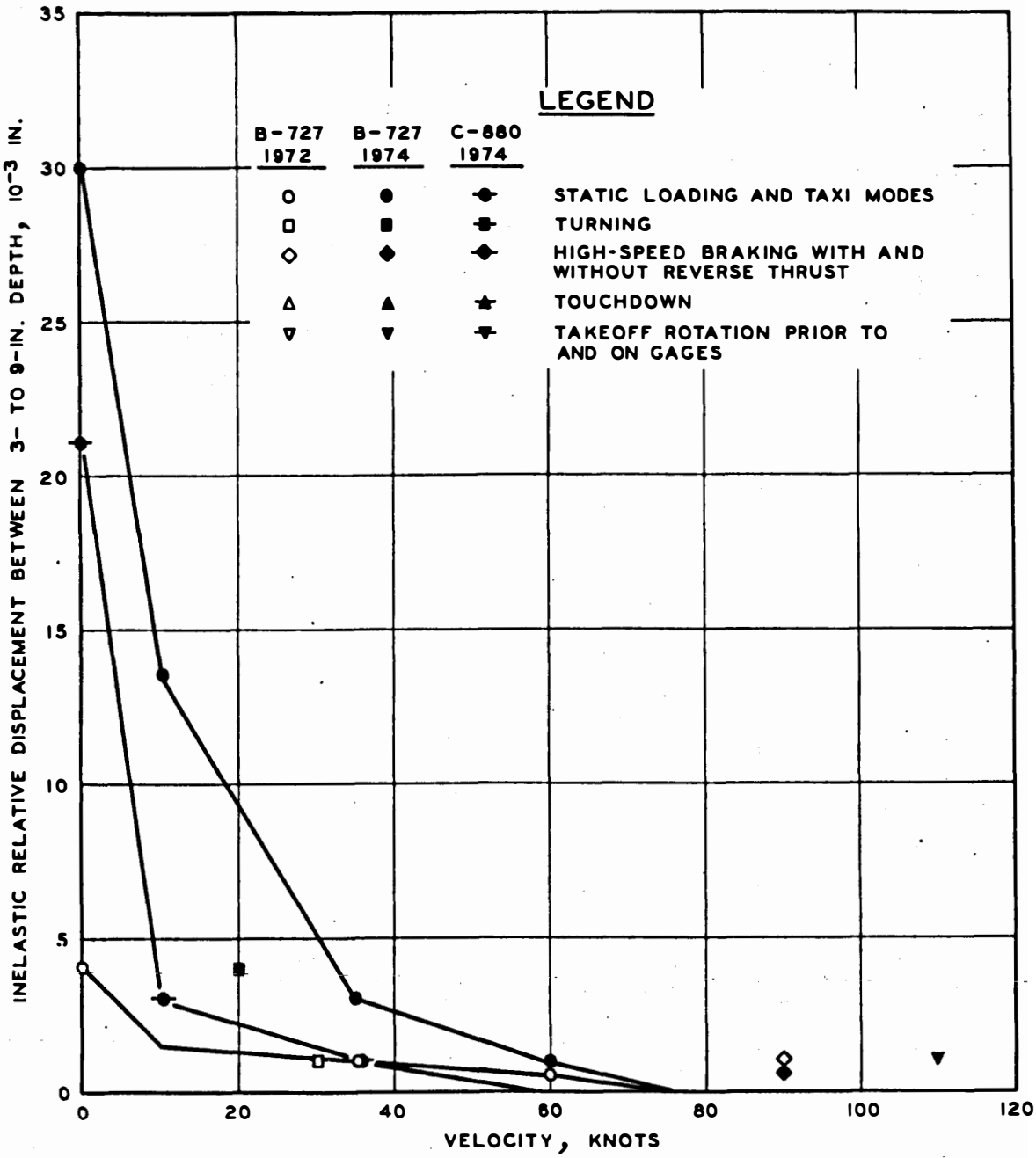

Figure 24. Maximum inelastic vertical relative displacement between 3- to 9-in. depth versus velocity, flexible pavement

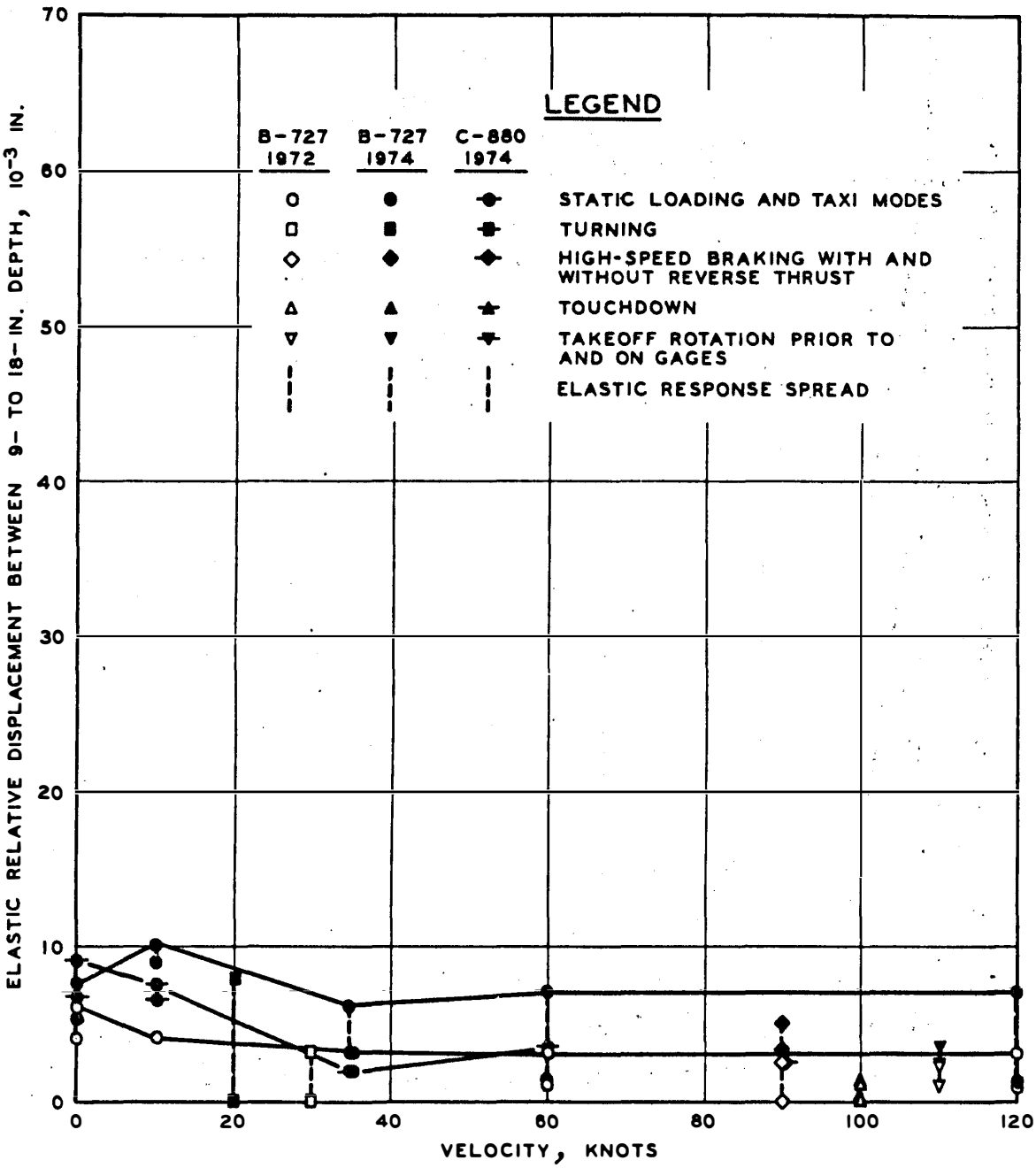

Figure 25. Maximum elastic vertical relative displacement between 9- to 18-in. depth versus velocity, flexible pavement

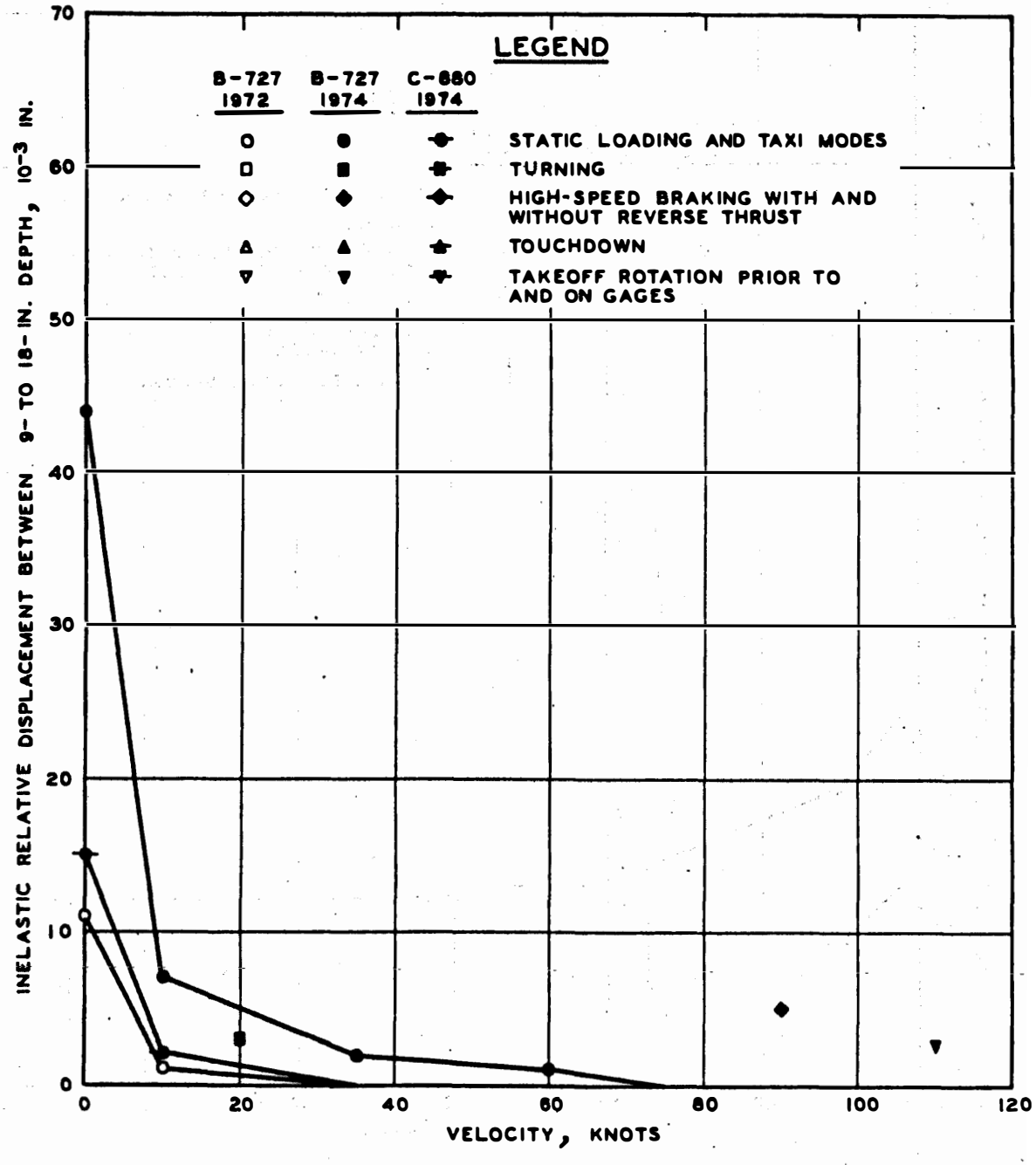

Figure 26. Maximum inelastic vertical relative displacement between 9- to 18-in. depth versus velocity, flexible pavement

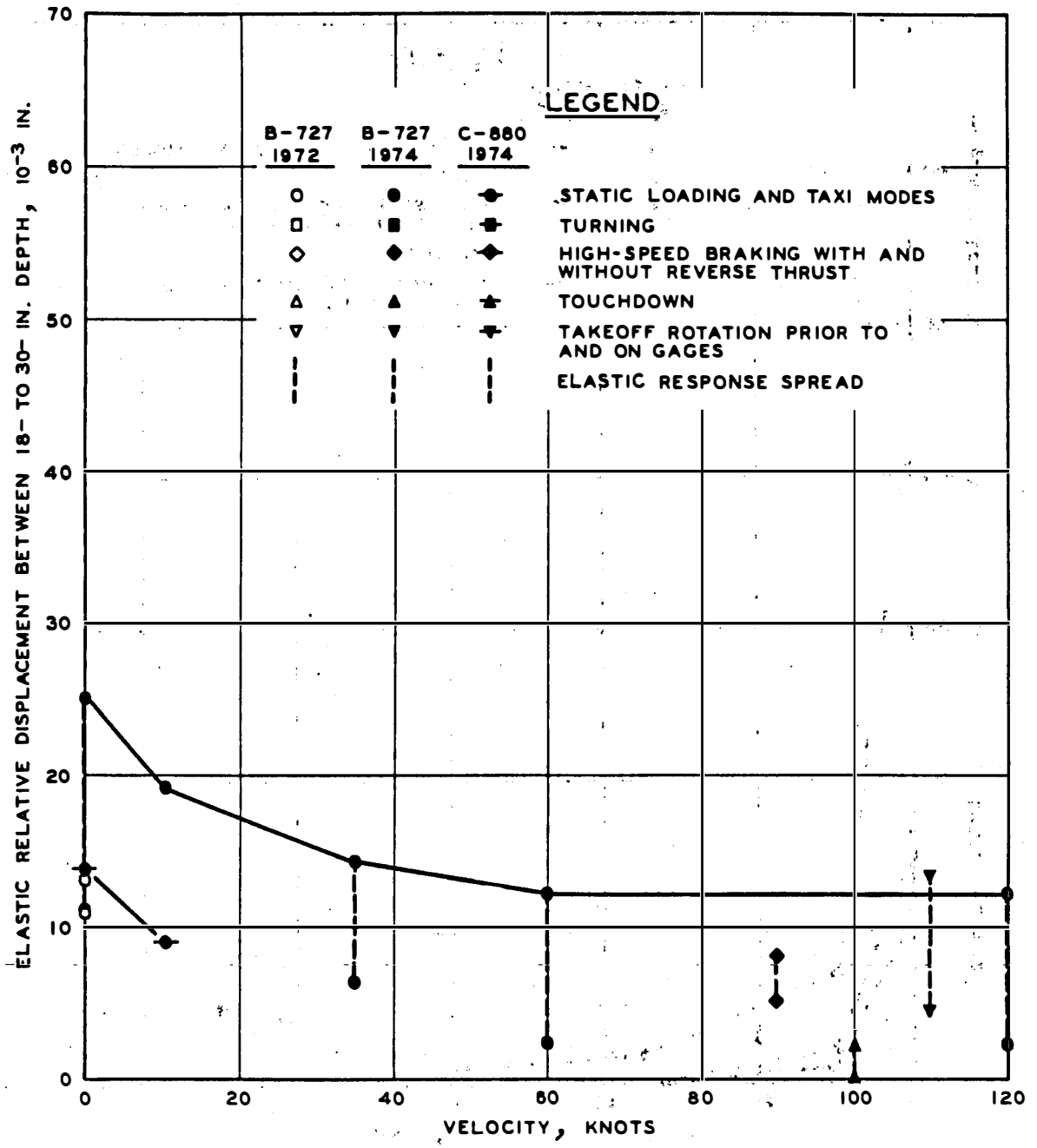

Figure 27. Maximum elastic vertical relative displacement between 18- to 30-in. depth versus velocity, flexible pavement

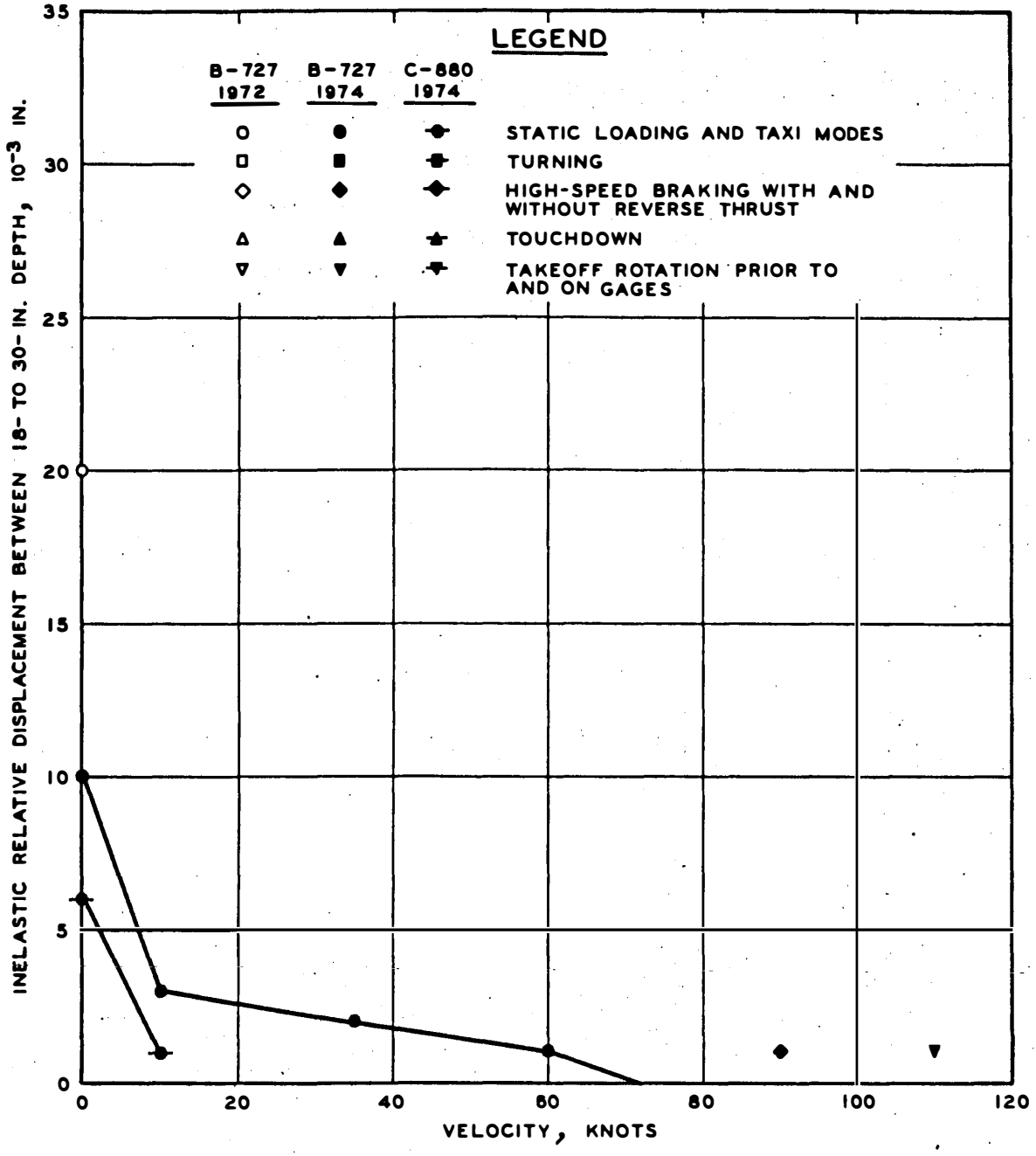

Figure 28. Maximum inelastic vertical relative displacement between 18- to 30-in. depth versus velocity, flexible pavement

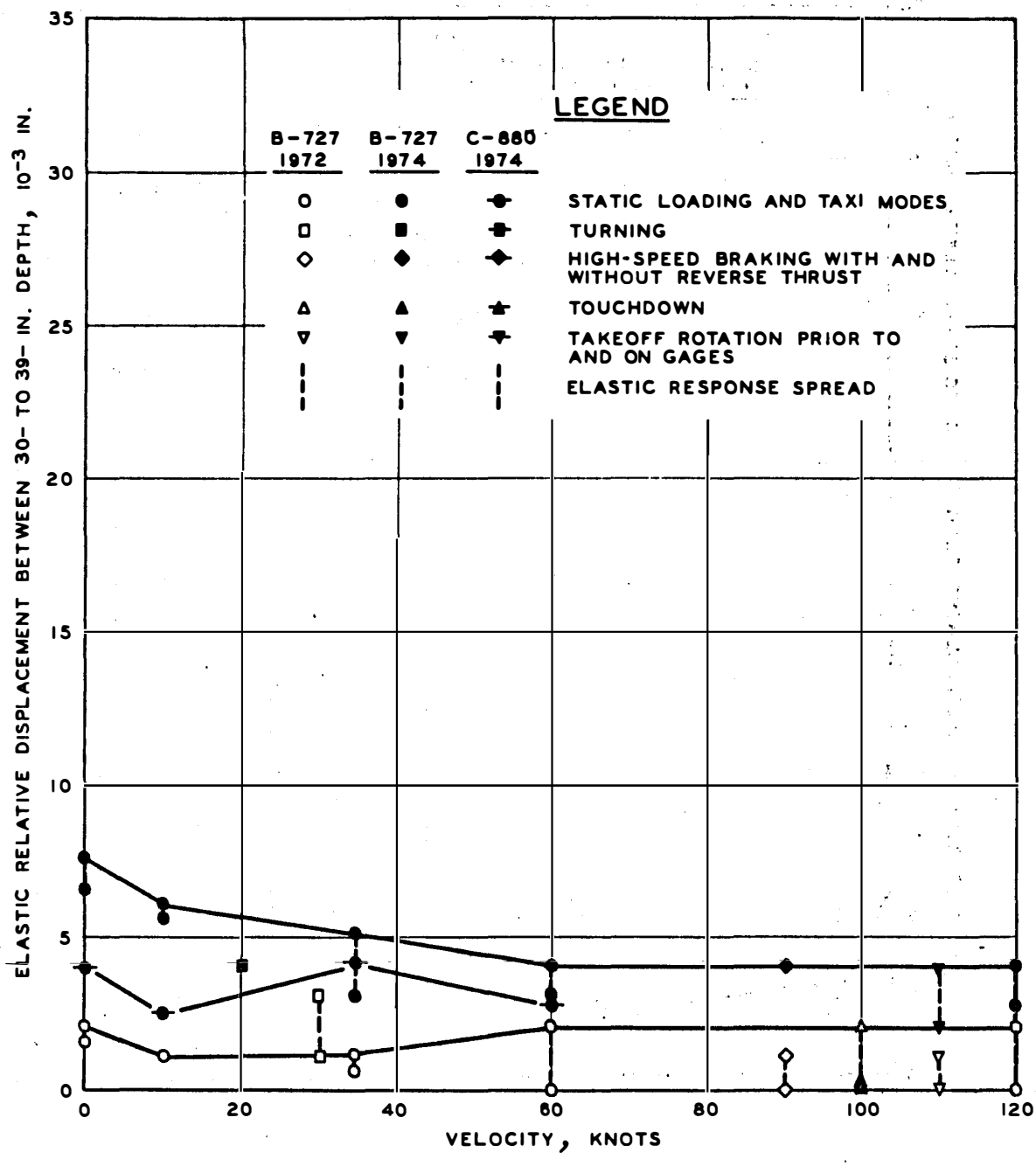

Figure 29. Maximum elastic vertical relative displacement between 30- to 39-in. depth versus velocity, flexible pavement

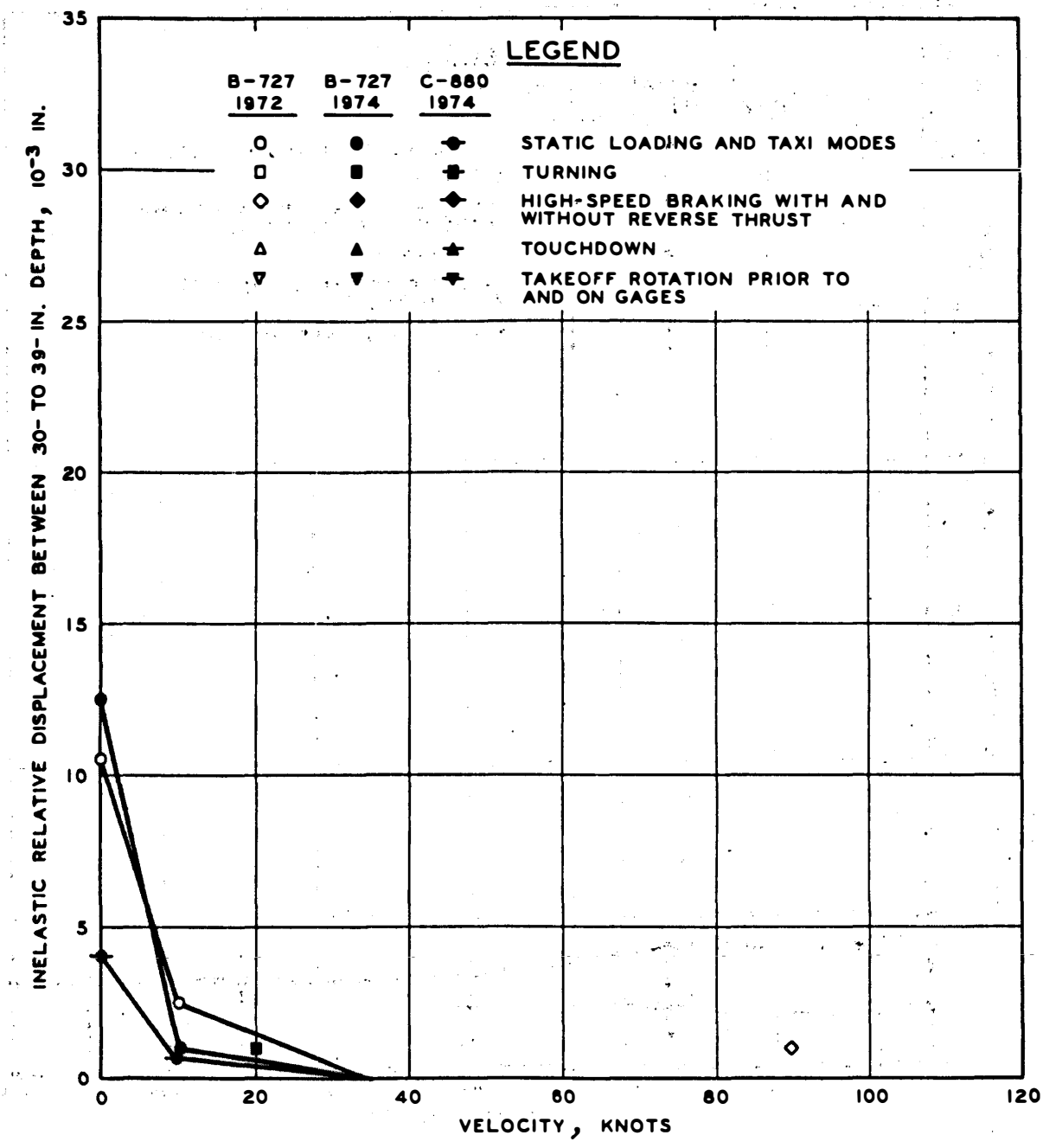

Figure 30. Maximum inelastic vertical relative displacement between 30- to 39-in. depth versus velocity, flexible pavement

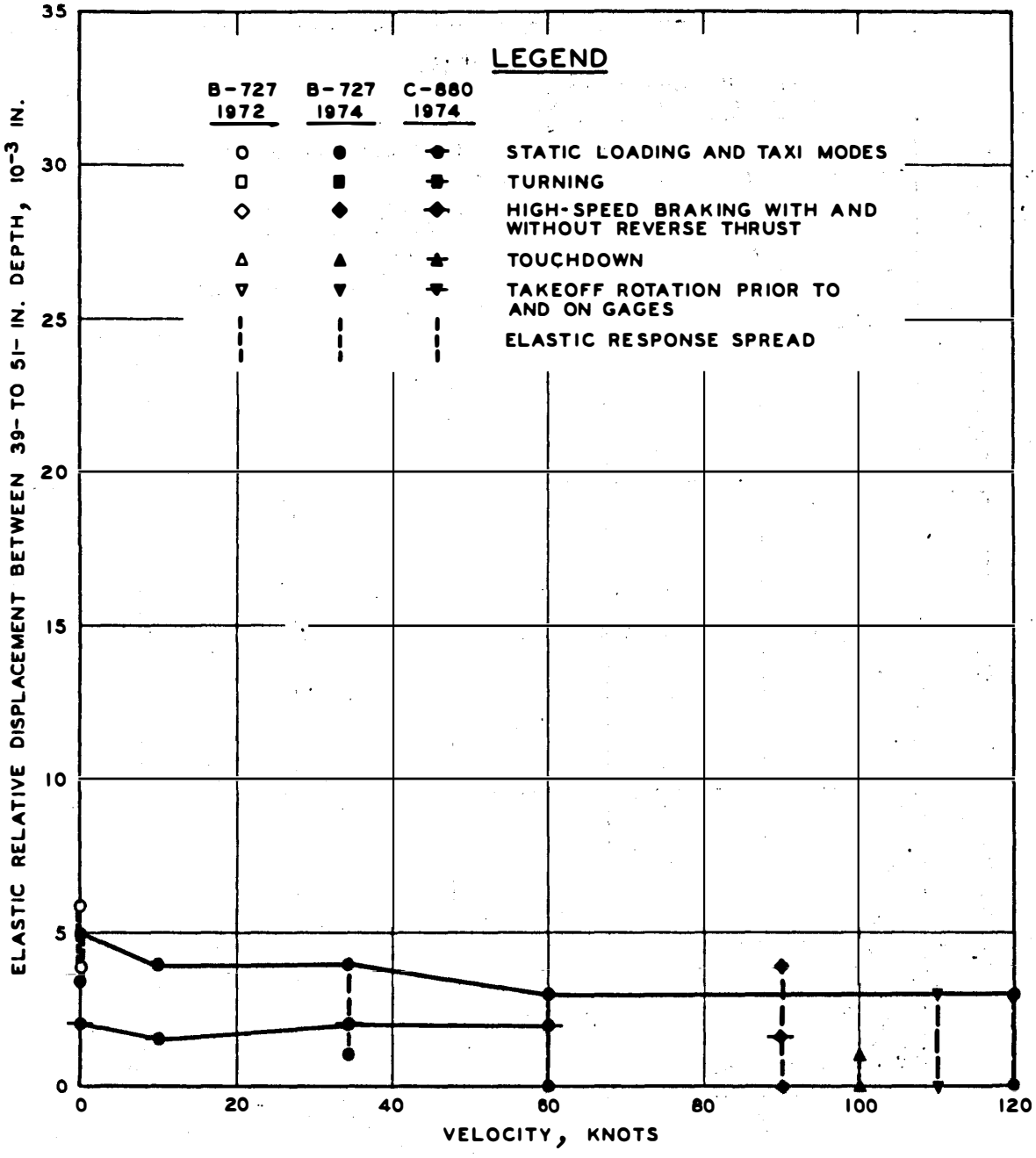

Figure 31. Maximum elastic vertical relative displacement between 39- to 51-in. depth versus velocity, flexible pavement

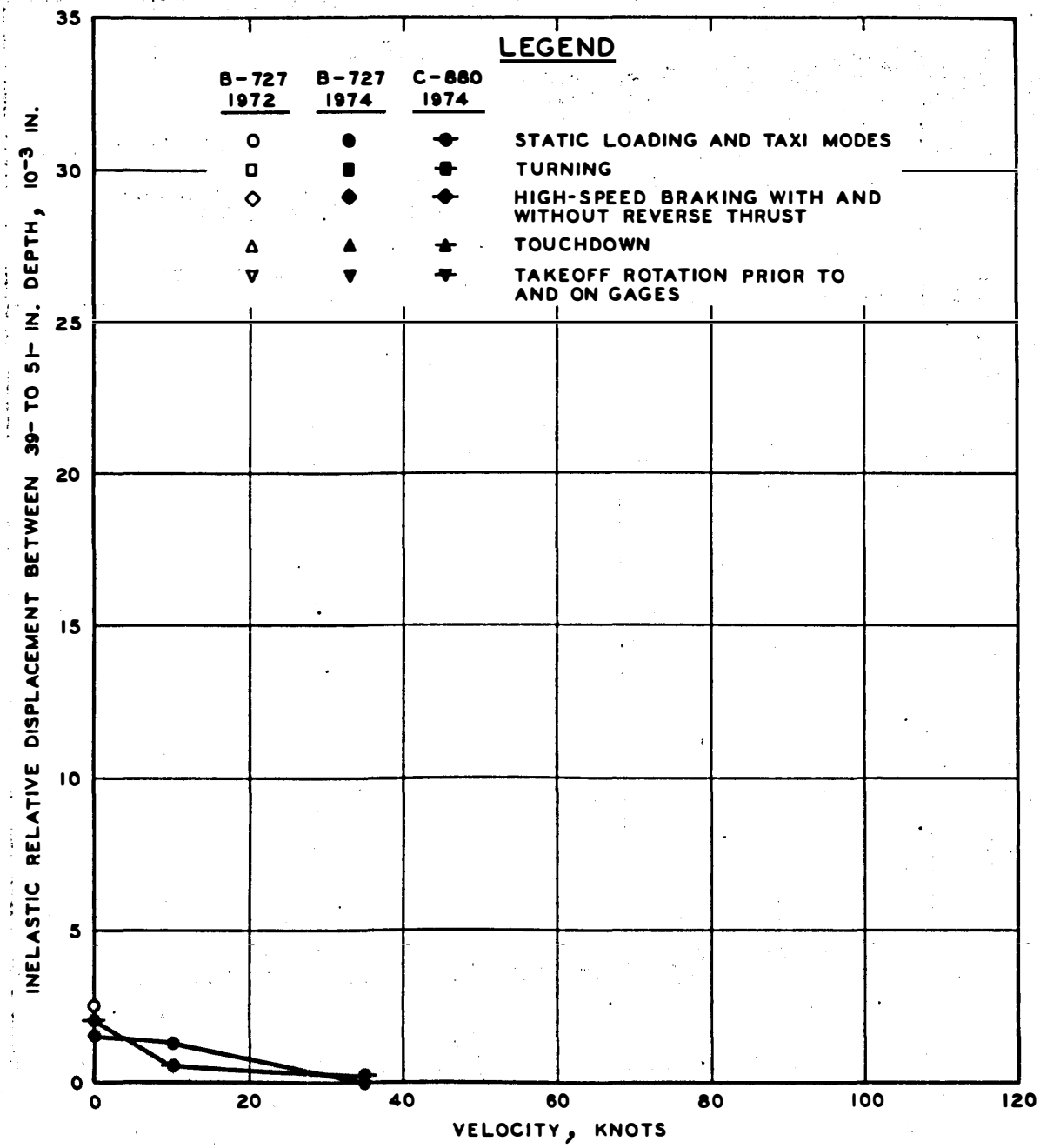

Figure 32. Maximum inelastic vertical relative displacement between 39- to 51-in. depth versus velocity, flexible pavement

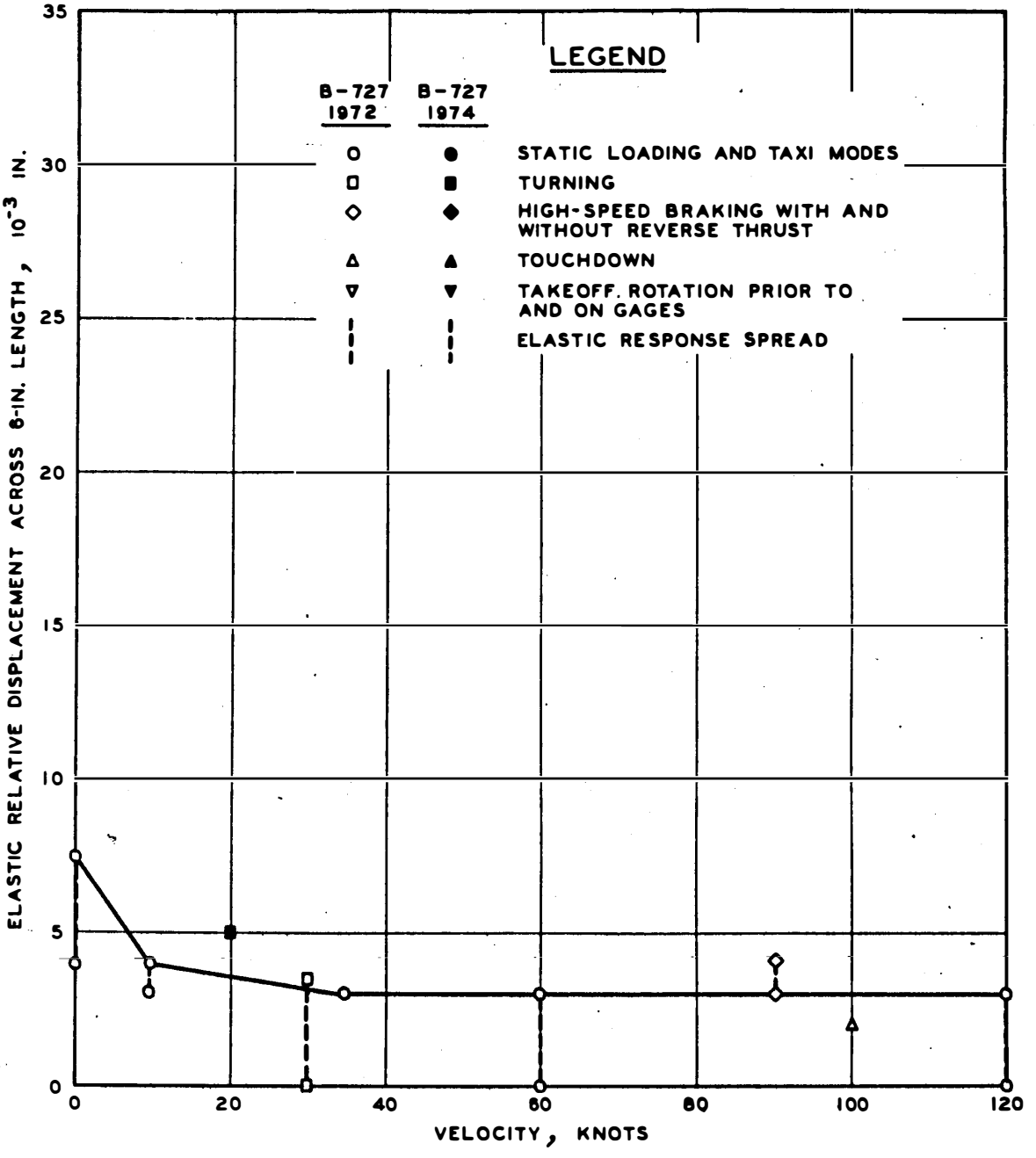

Figure 33. Maximum elastic horizontal (longitudinal) relative displacement across 6-in. length at 9-in. depth versus velocity, flexible pavement

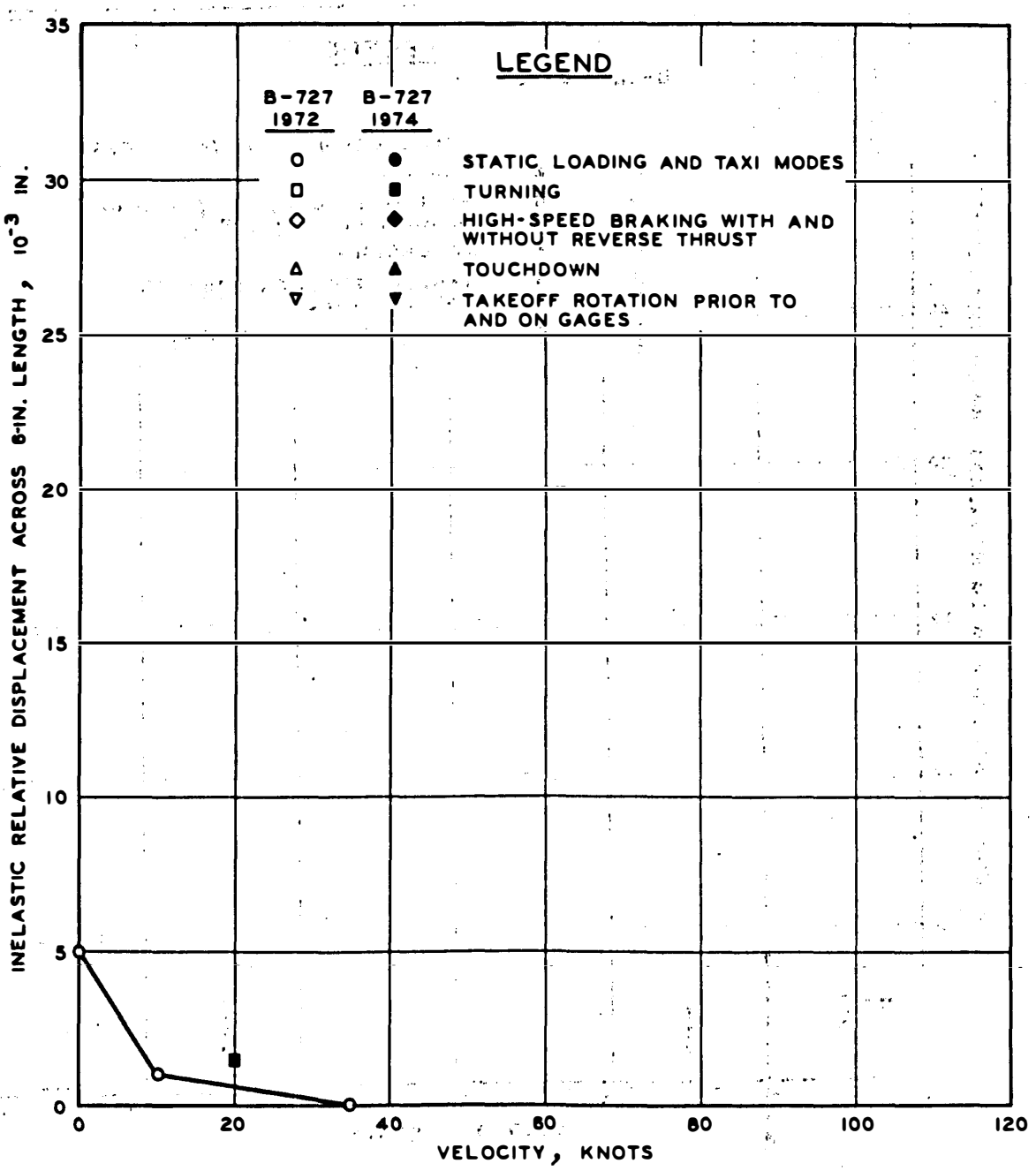

Figure 34. Maximum inelastic horizontal (longitudinal) relative displacement across 6-in. length at 9-in. depth versus velocity, flexible pavement

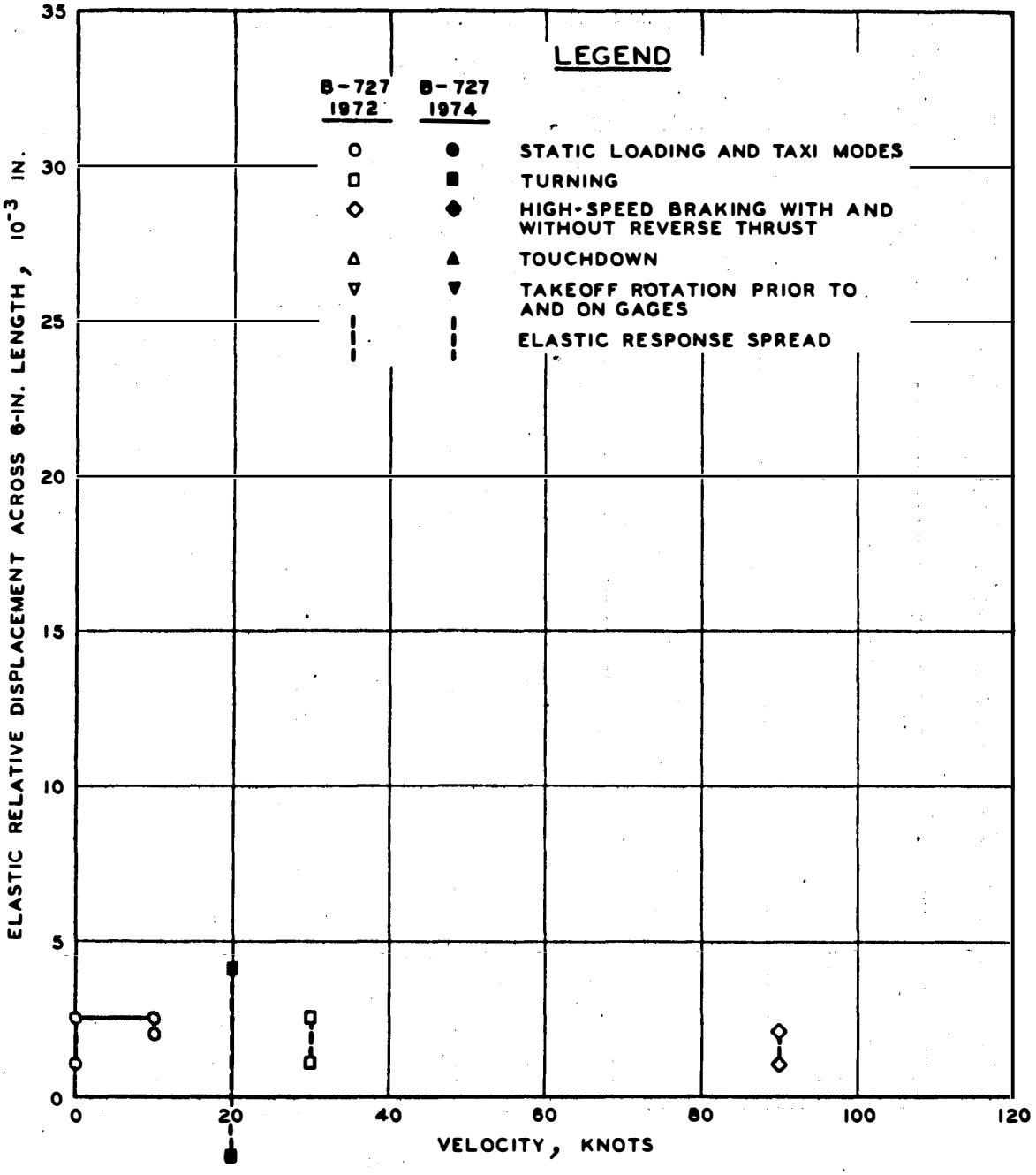

Figure 35. Maximum elastic horizontal (transverse) relative displacement across 6-in. length at 9-in. depth versus velocity, flexible pavement

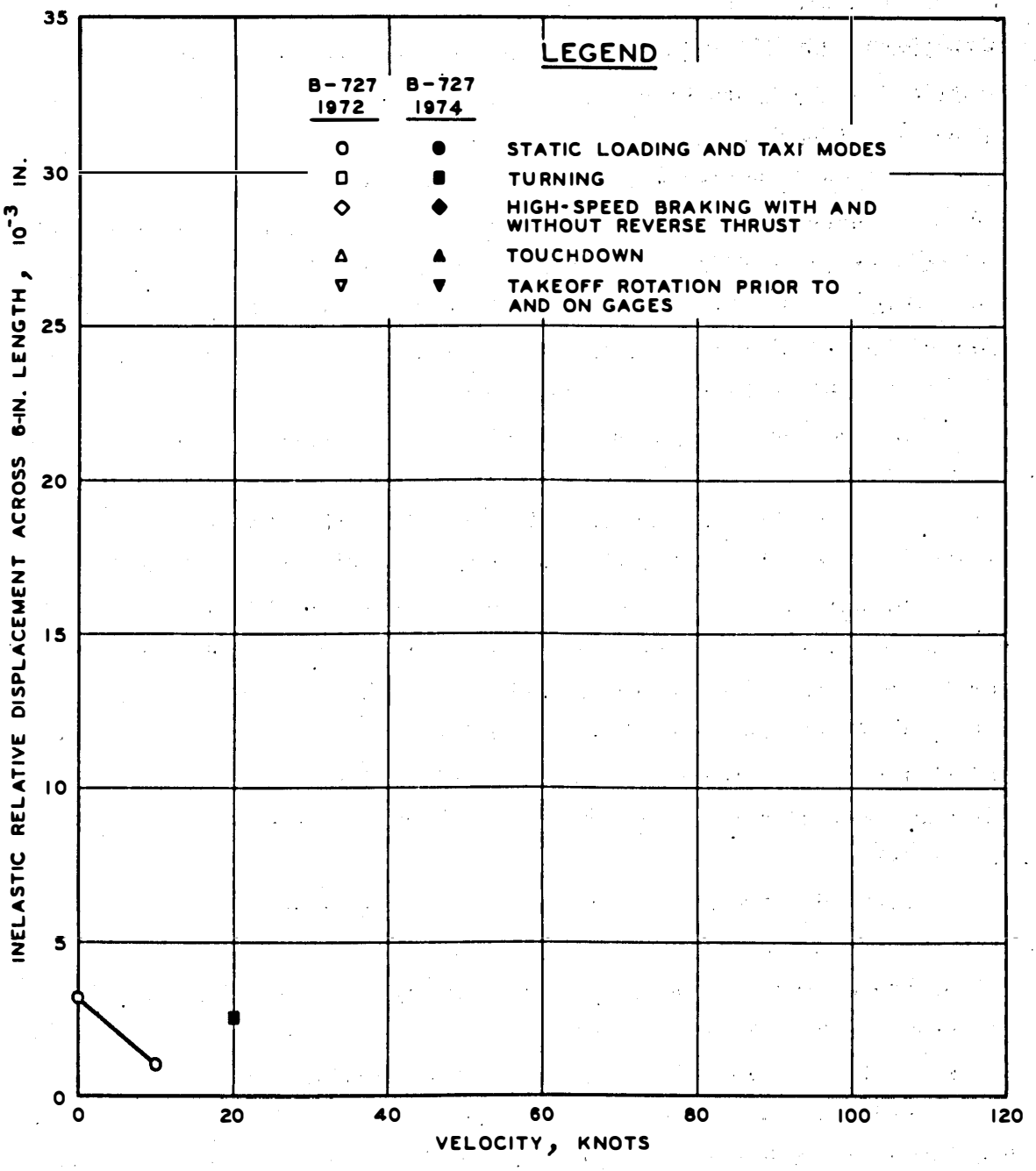

Figure 36. Maximum inelastic horizontal (transverse) relative displacement across 6-in. length at 9-in. depth versus velocity, flexible pavement

The inelastic responses are the largest magnitudes measured at the gear maximum load point for a single pass over a gage row. Minimum inelastic response is zero, and the taxi modes are connected across the figures as for the elastic responses. A distributed series of loadings with the same gear loads as those for the data shown could result in larger inelastic displacements at a given point if the reference were considered to be the highest peak occurring in the sequence. However, no matter what the loading series is, the elastic movement as defined herein would not be greater than what is shown for the same load ranges. For a single pass of the aircraft, the sum of the elastic and inelastic responses for a gage would represent the approximate maximum nonconditioned pavement structure displacement that could be expected. However, depending on the load history, the displacement could be less than the above sum.

Noticeable in Figures 21-36 are the increases in elastic and inelastic responses in 1974 and their decreases with increased velocity and depth to about the same levels as the 1972 responses. This is believed to be due to a viscoelastic effect and plastic behavior increases in the bituminous layers due to the higher temperatures and not due to a temperature effect in the soil materials. In other words, the behavior in the bituminous layers was controlling the deeper material behaviors. These figures imply that the viscoelastic response can be separated from the approximately constant elastic (without viscoelastic) response by projecting back the elastic response at high aircraft velocities.

Figures 33-36 summarize the flexible pavement structure horizontal responses as measured by Bison coils. The 1972 results include almost all of the operating modes, but only turning data were recorded in 1974. All previous remarks also apply to these figures, and the behavior shown is basically the same as that shown by the vertical response figures.

Figures 37-41 summarize the flexible pavement structure vertical pressures for both 1972 and 1974 test results. The data are presented as previously described for the relative displacements. Noticeable in these figures are the sharp initial decreases in elastic pressures with increases in velocity and the increased pressure magnitudes of 1974.

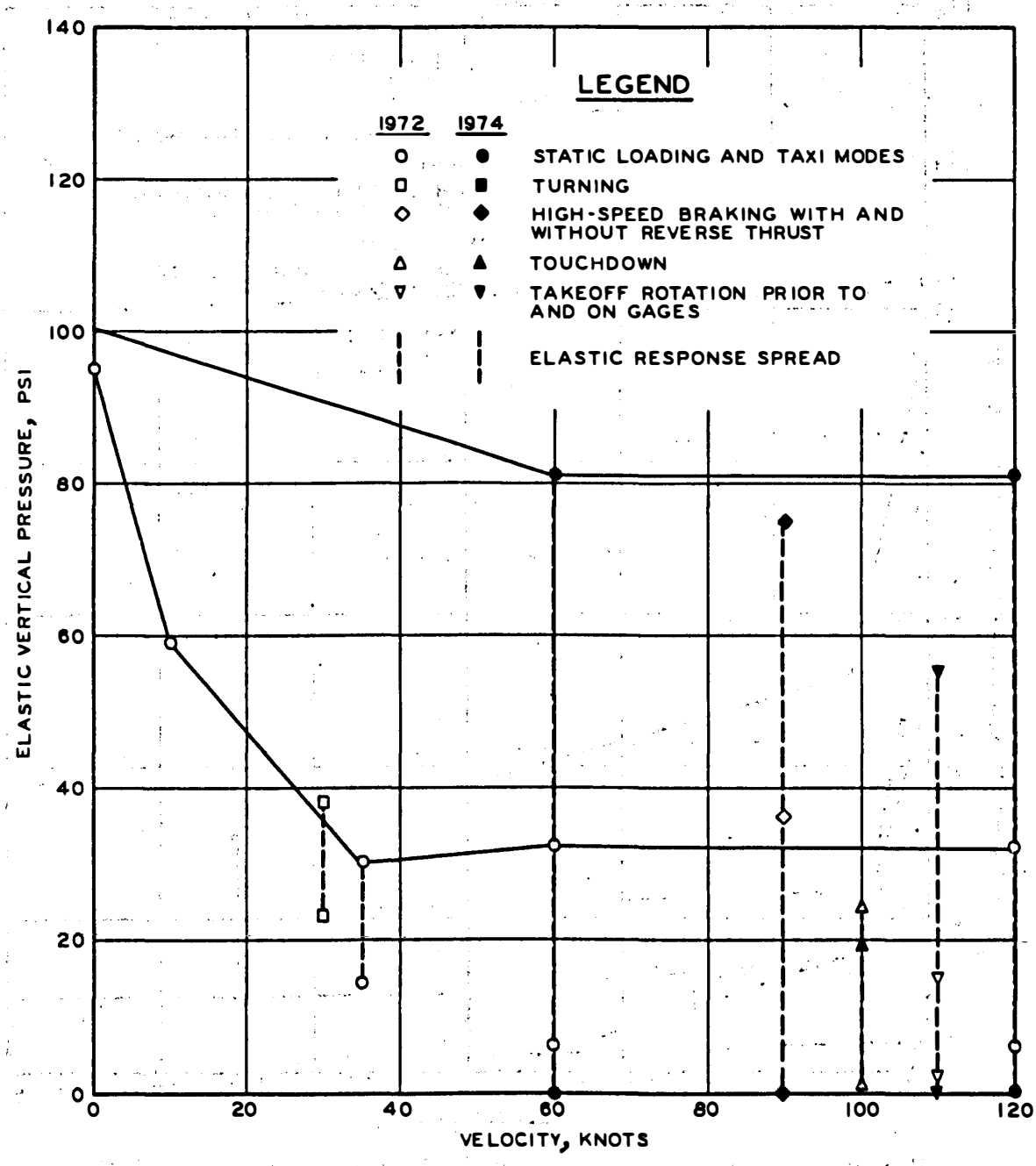

Figure 37. Maximum elastic vertical pressure at 3-in. depth versus velocity, flexible pavement, B-727

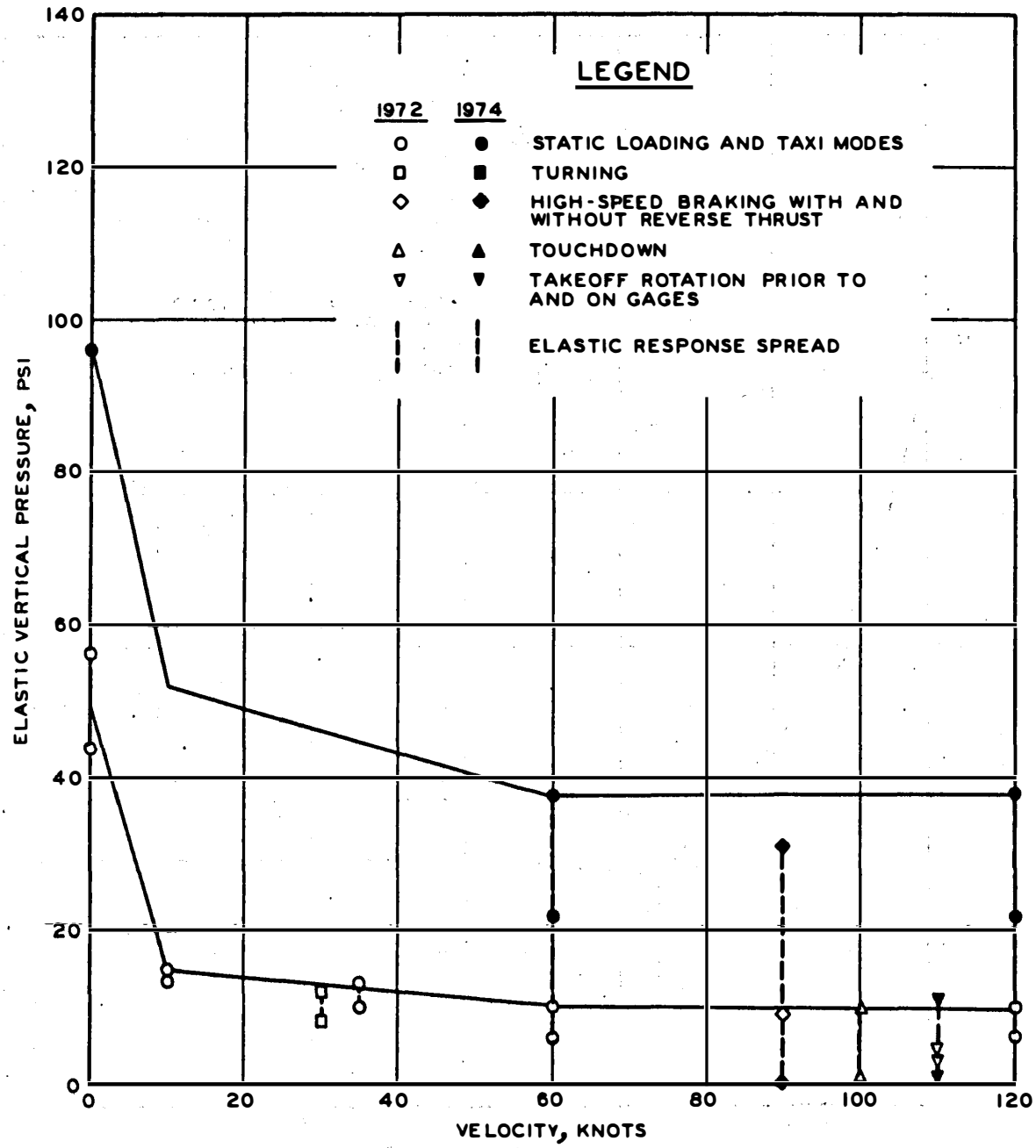

Figure 38. Maximum elastic vertical pressure at 9-in. depth versus velocity, flexible pavement, B-727

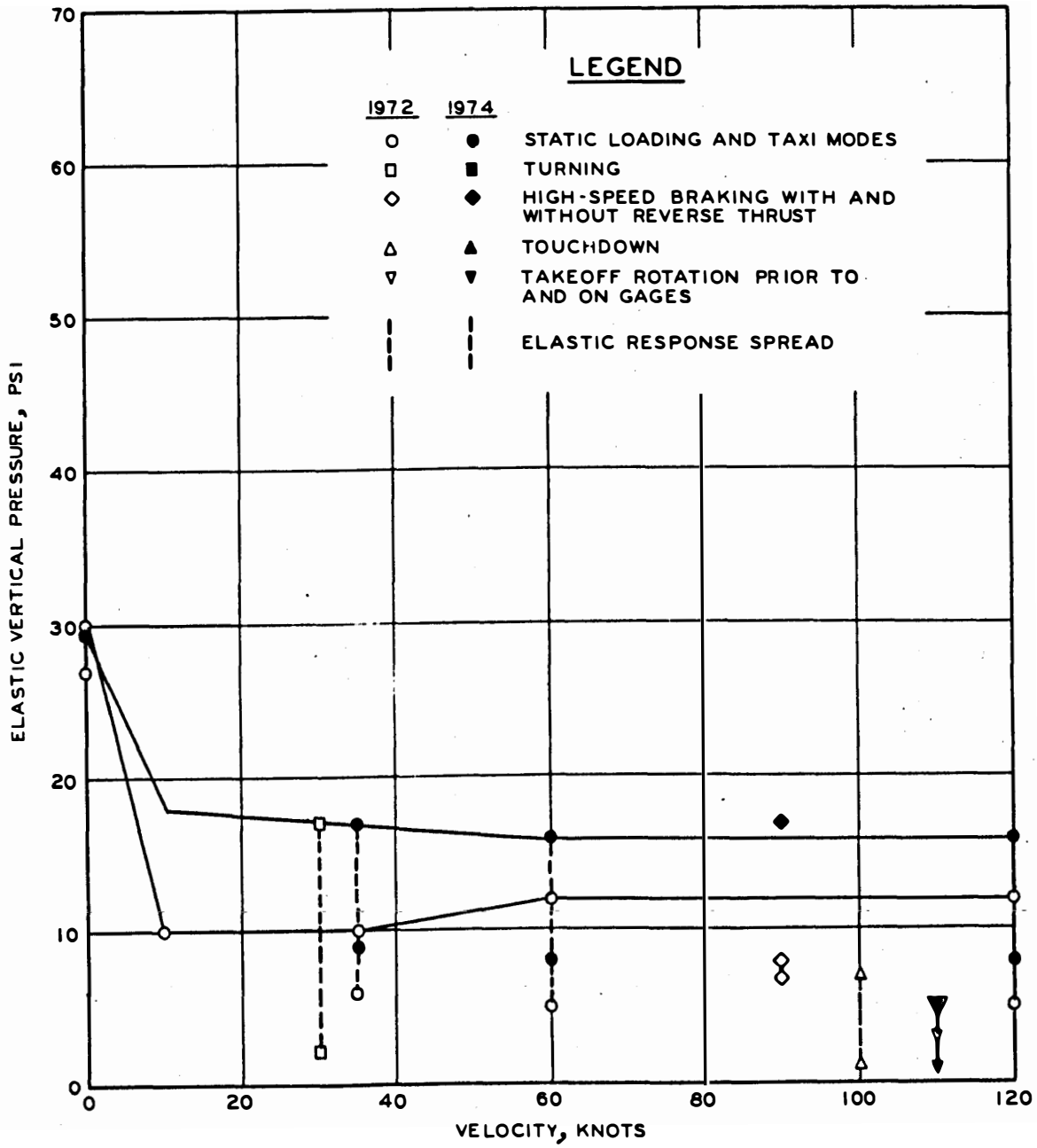

Figure 39. Maximum elastic vertical pressure at 18-in. depth versus velocity, flexible pavement, B-727

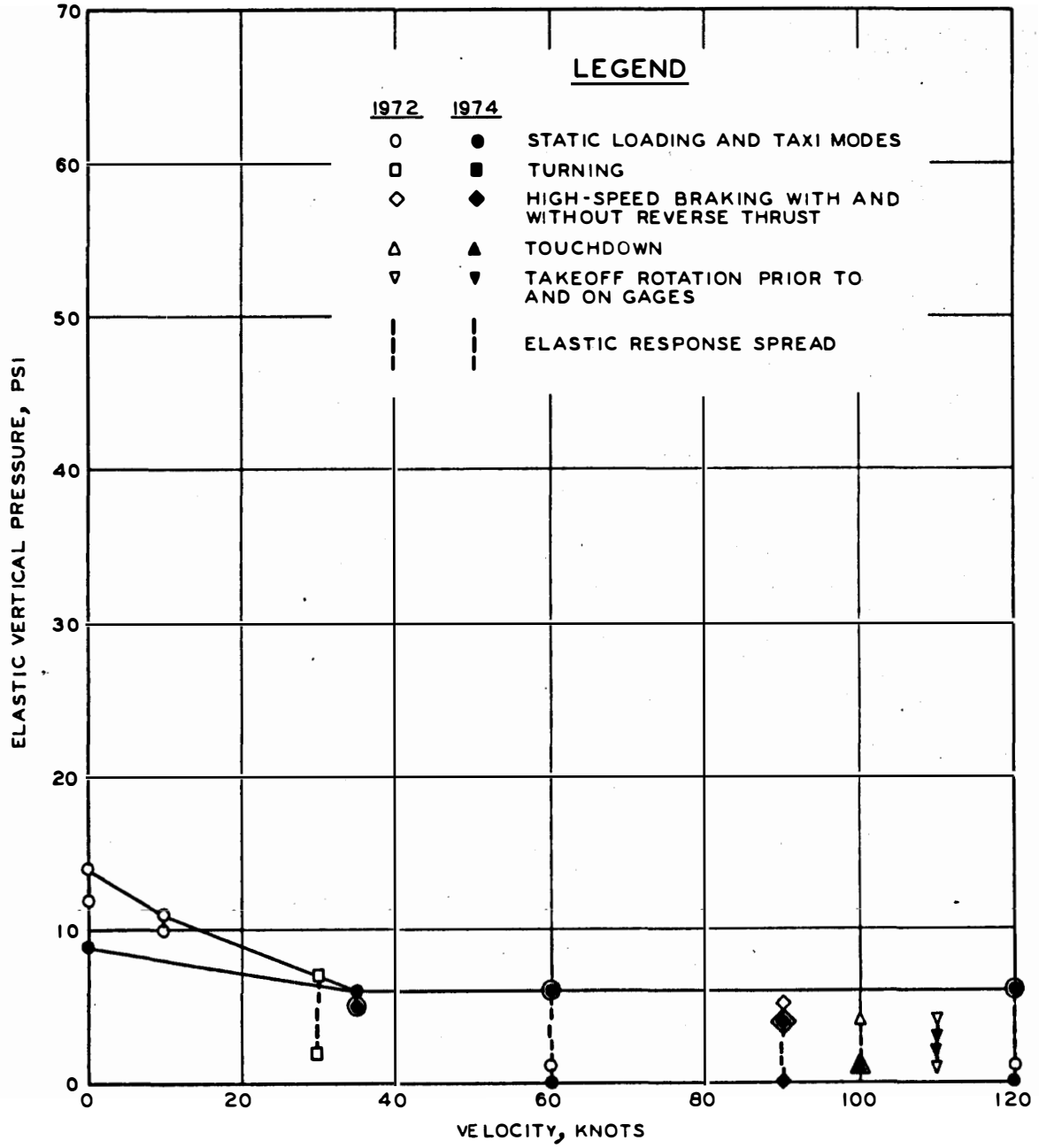

Figure 40. Maximum elastic vertical pressure at 30-in. depth versus velocity, flexible pavement, B-727

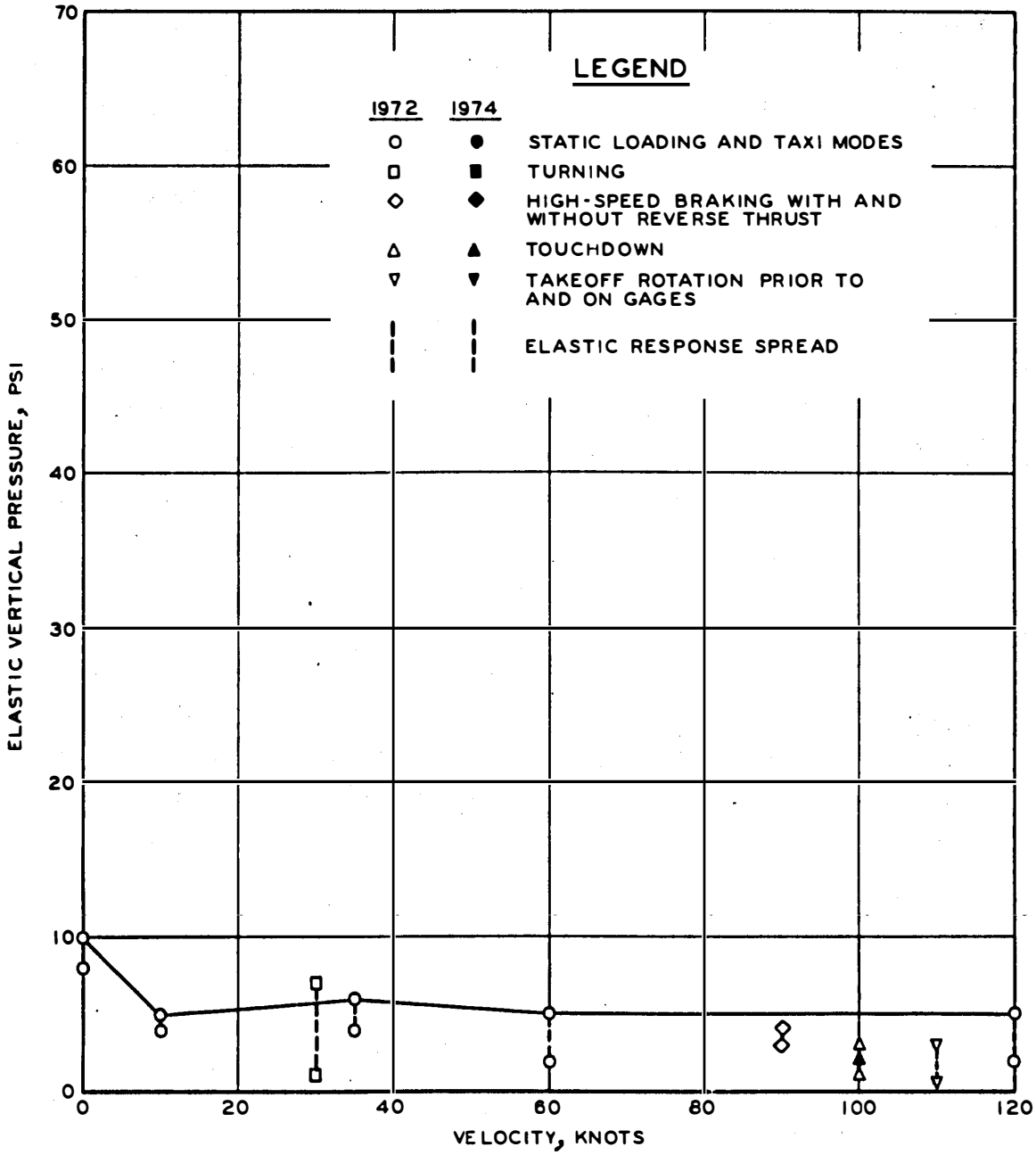

Figure 41. Maximum elastic vertical pressure at 39-in. depth versus velocity, flexible pavement, B-727

However, also noticeable are the decreases with increases in depth of the 1974 pressure magnitudes to about the same level as 1972 results at the 30- and 39-in. depths. This behavior is fairly consistent with that of the individual pavement structure element displacements.

Figures 42-53 summarize the nonconditioned rigid pavement structure relative displacement test results. Previous remarks concerning the methods of presentation and the elastic and inelastic responses are also applicable here. There was a small amount of inelastic behavior of the concrete slabs, but they acted primarily as elastic plates, as shown. The pavement foundation material showed inelastic responses of the rigid pavement structure even though the concrete slabs responded almost entirely elastically. The response decrease around 20 knots shown in some of the figures is probably due to a lack of maximum load point data, as can be seen in Appendix B to Volume II.[3]

Figures 48-53 summarize the rigid pavement structure horizontal responses as measured by Bison coils at a depth of 15 in. and the responses measured by Valore strain gages at the surface of the concrete slabs. The horizontal responses show about the same static to dynamic load comparisons as the vertical displacements. Noticeable in Figures 48-53 are the inelastic responses of the rigid pavement structure.

Figures 54-56 summarize the rigid pavement structure vertical pressures. Noticeable in these figures are the nearly constant vertical pressures. This behavior is fairly consistent with the displacement results.

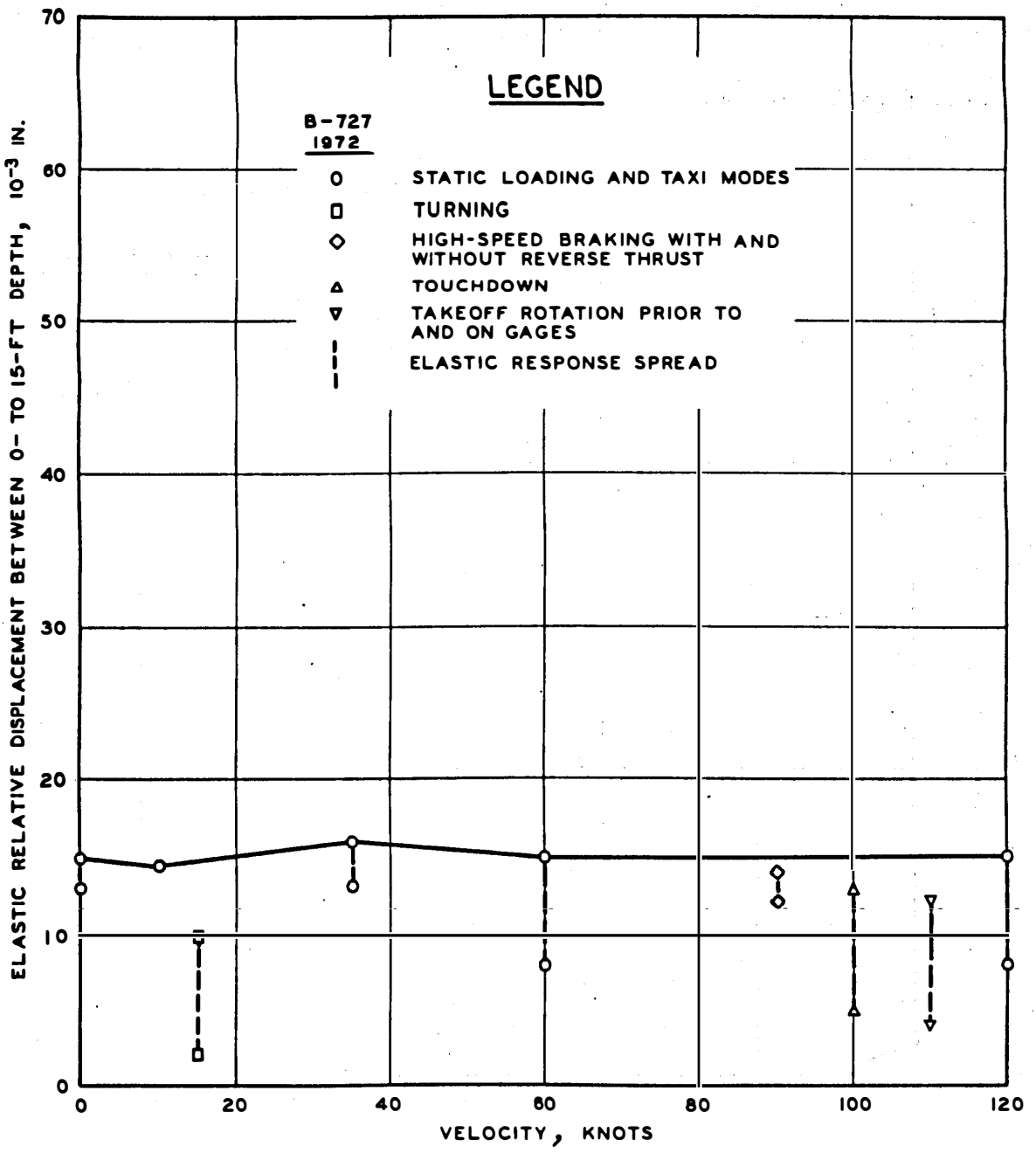

Figure 42. Maximum elastic vertical relative displacement between 0- to 15-ft depth versus velocity, rigid pavement

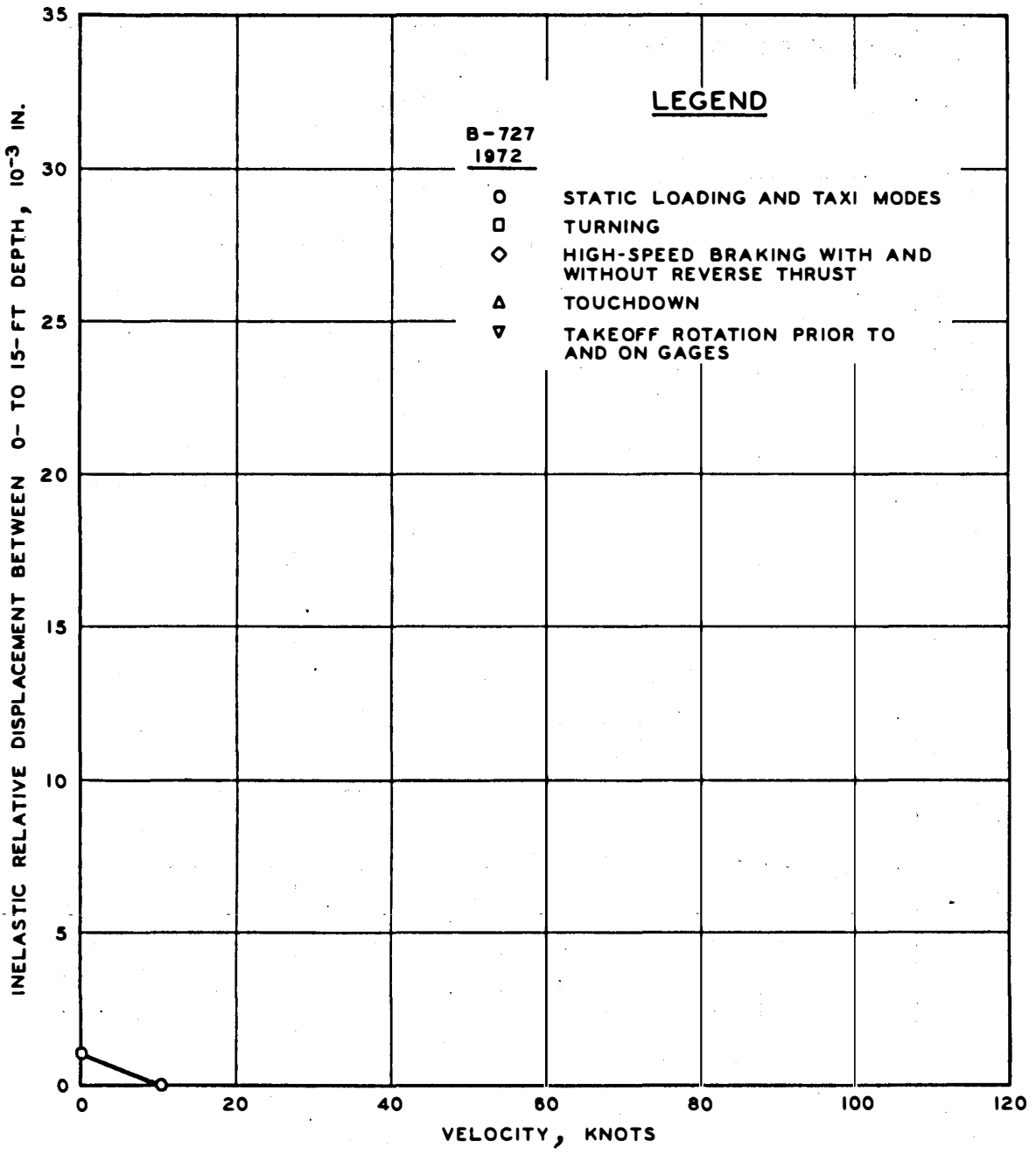

Figure 43. Maximum inelastic vertical relative displacement between 0- to 15-ft depth versus velocity, rigid pavement

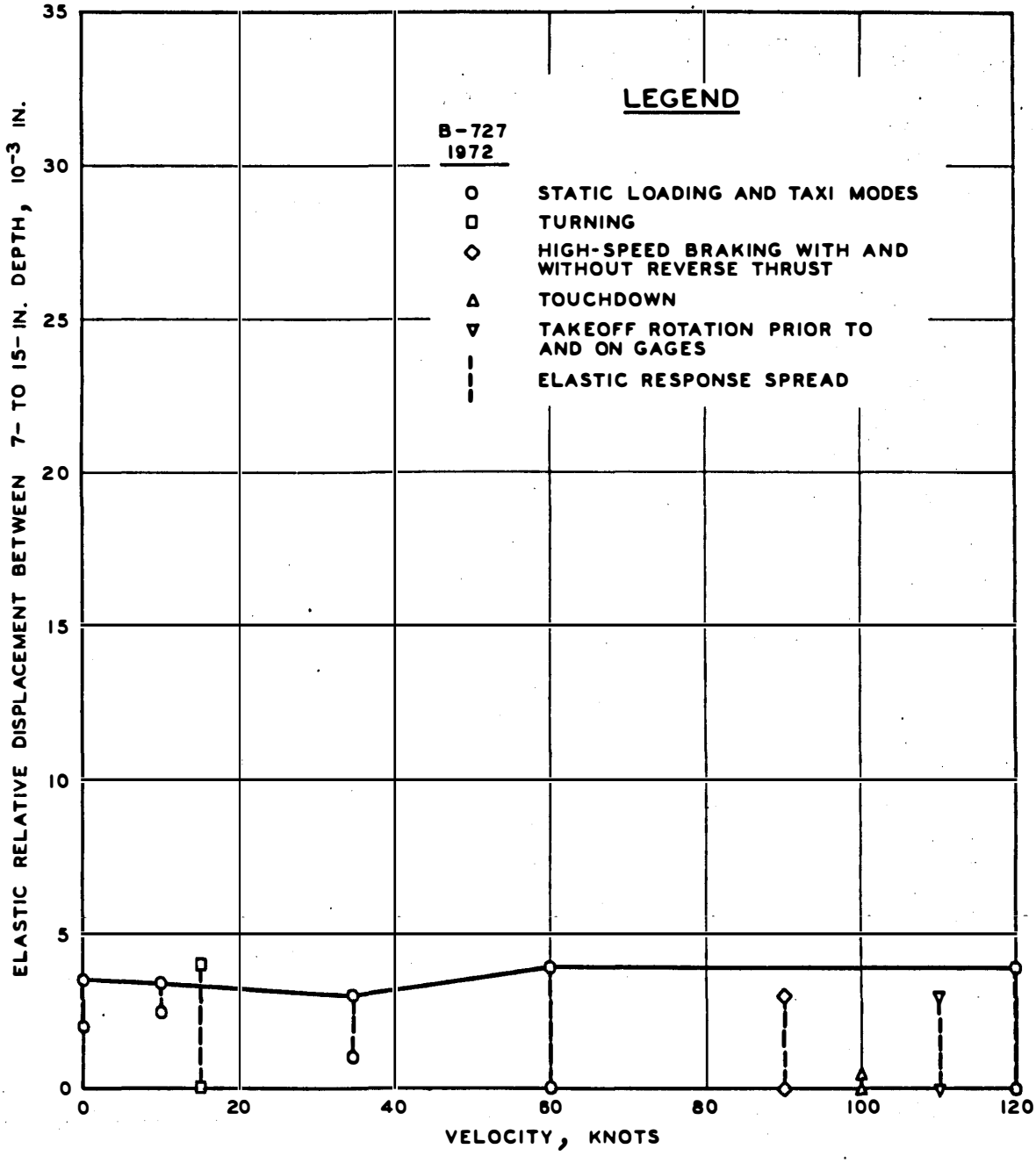

Figure 44. Maximum elastic vertical relative displacement between 7- to 15-in. depth versus velocity, rigid pavement

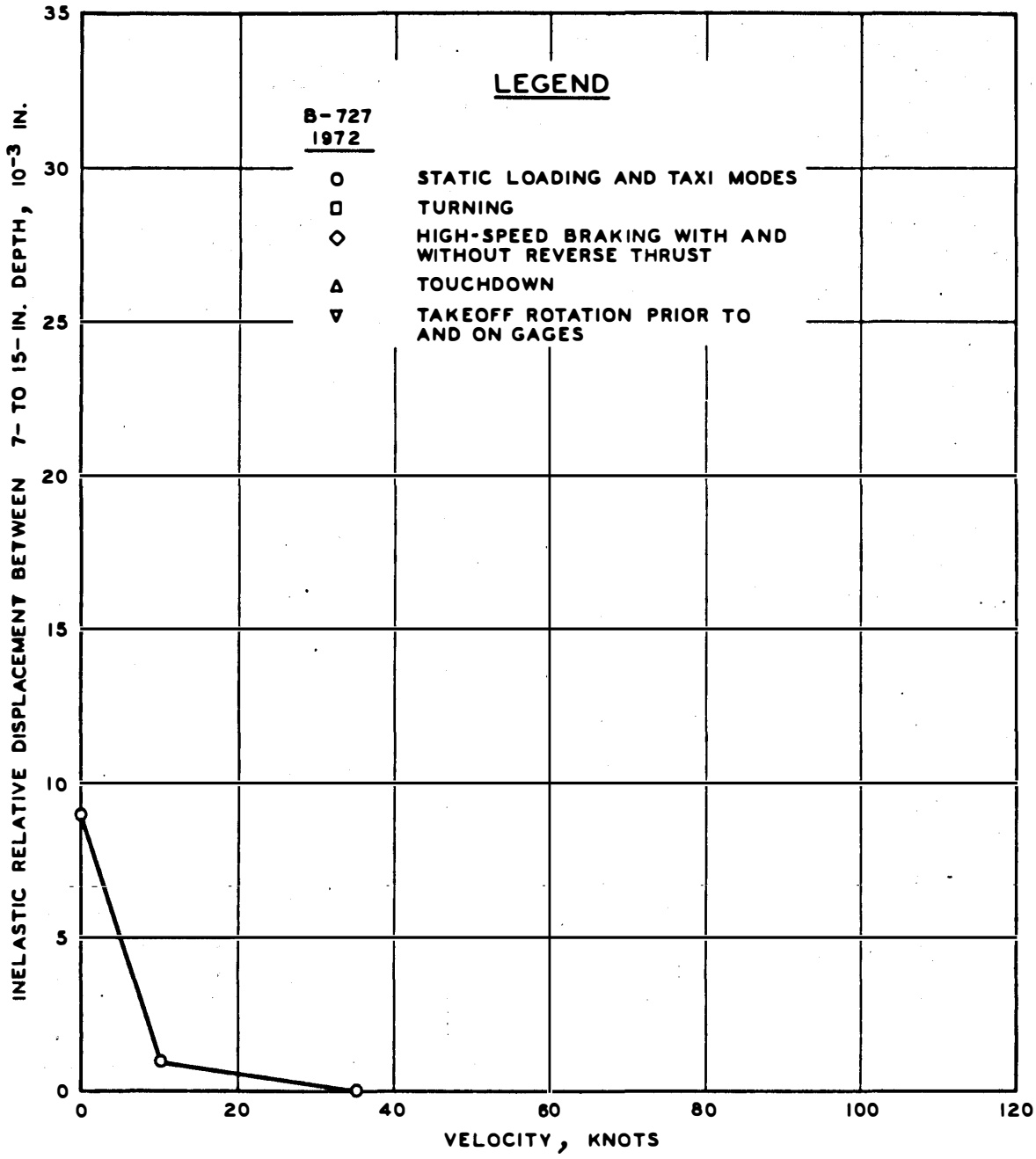

Figure 45. Maximum inelastic vertical relative displacement between 7- to 15-in. depth versus velocity, rigid pavement

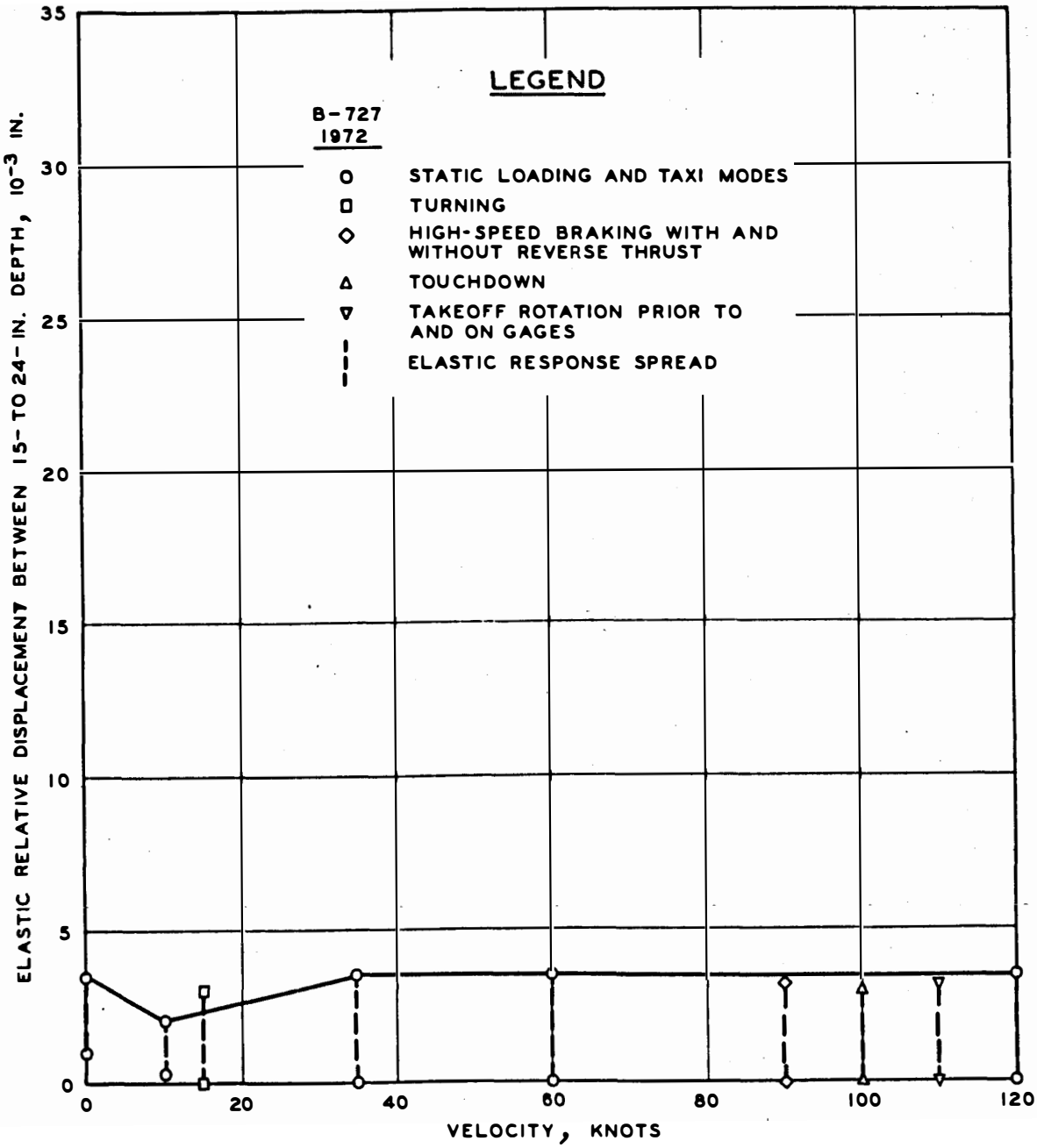

Figure 46. Maximum elastic vertical relative displacement between 15- to 24-in. depth versus velocity, rigid pavement

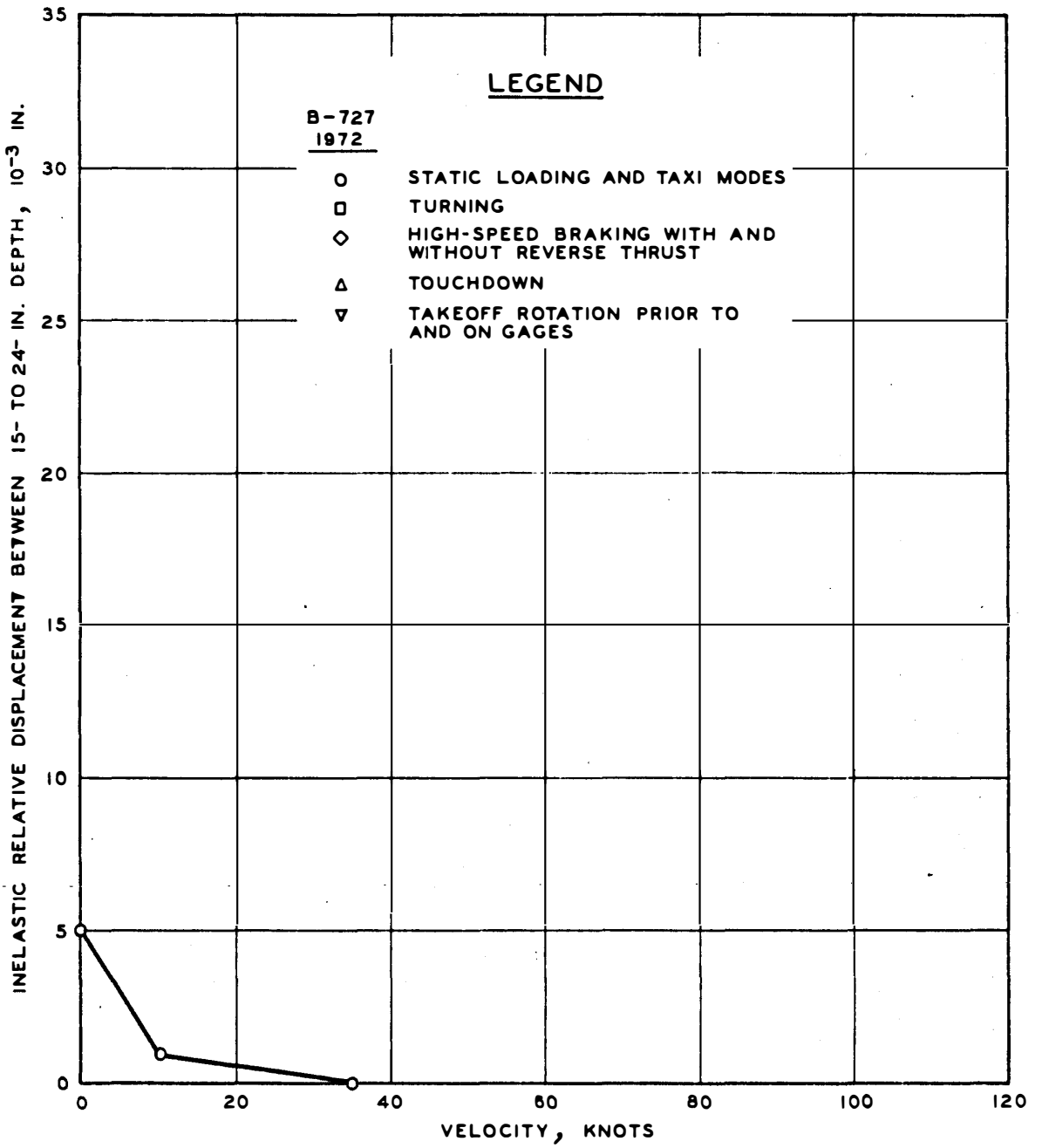

Figure 47. Maximum inelastic vertical relative displacement between 15- to 24-in. depth versus velocity, rigid pavement

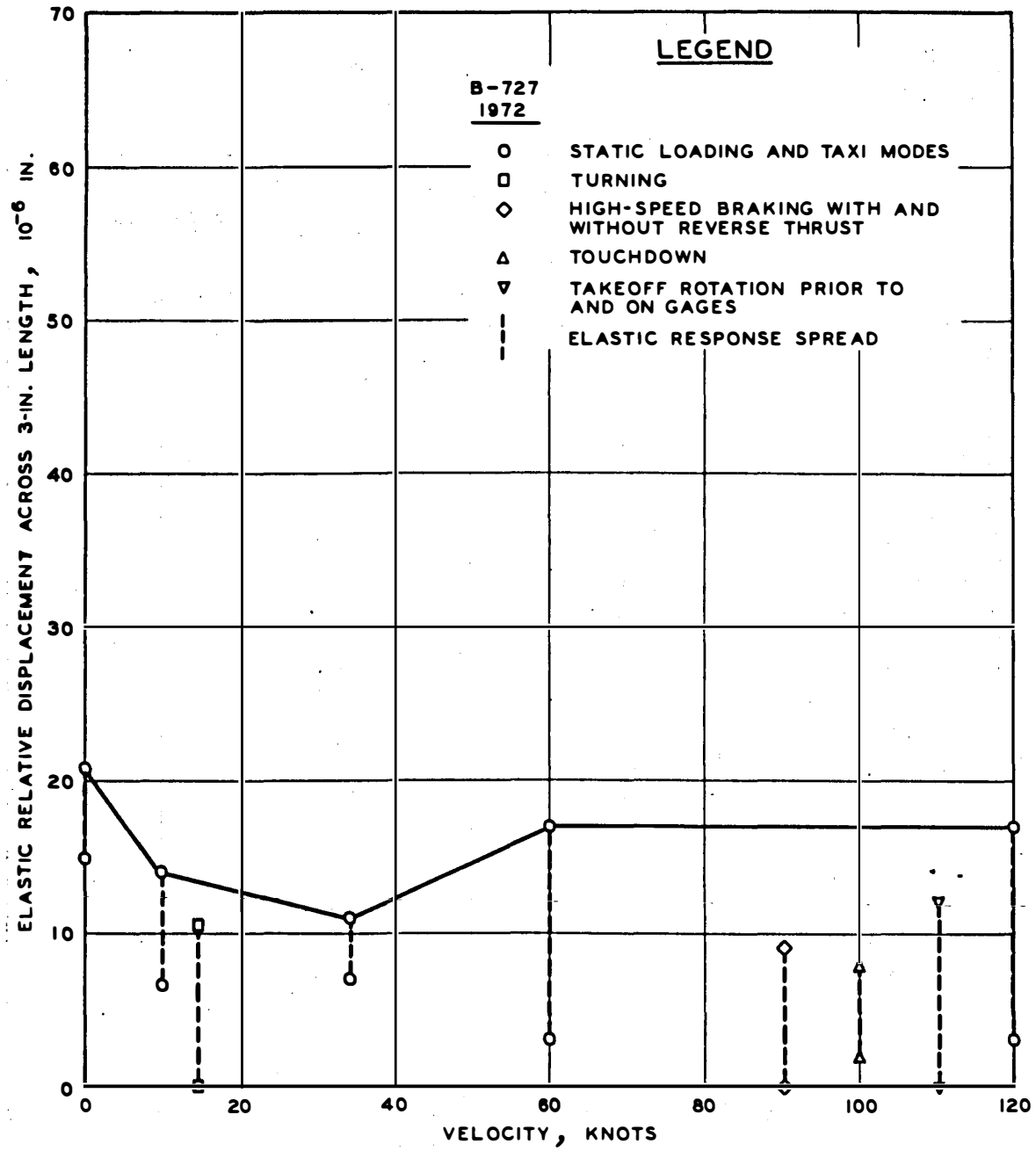

Figure 48. Maximum elastic horizontal (transverse) relative displacement across 3-in. length at 0-in. depth versus velocity, rigid pavement

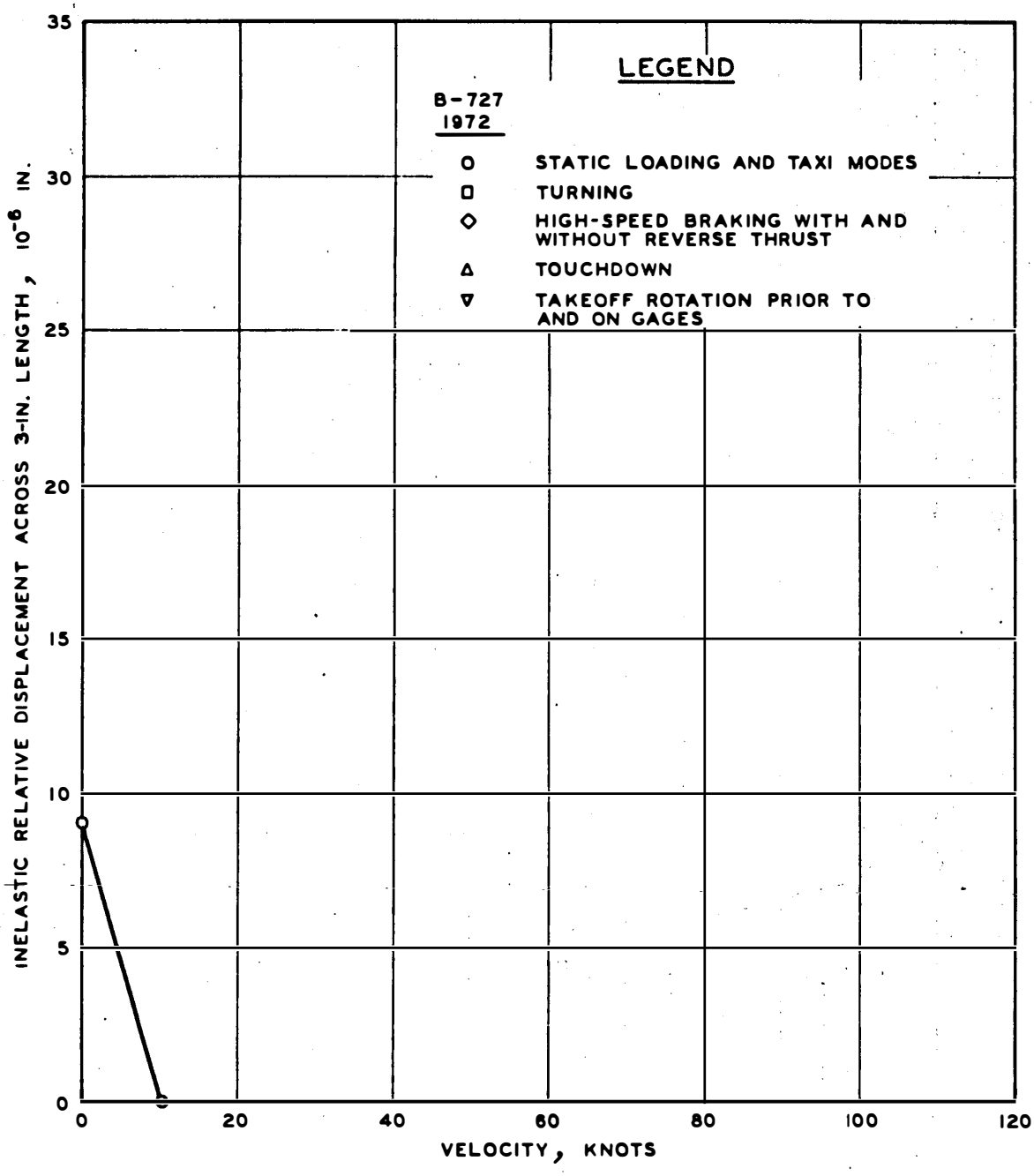

Figure 49. Maximum inelastic horizontal (transverse) relative displacement across 3-in. length at 0-in. depth versus velocity, rigid pavement

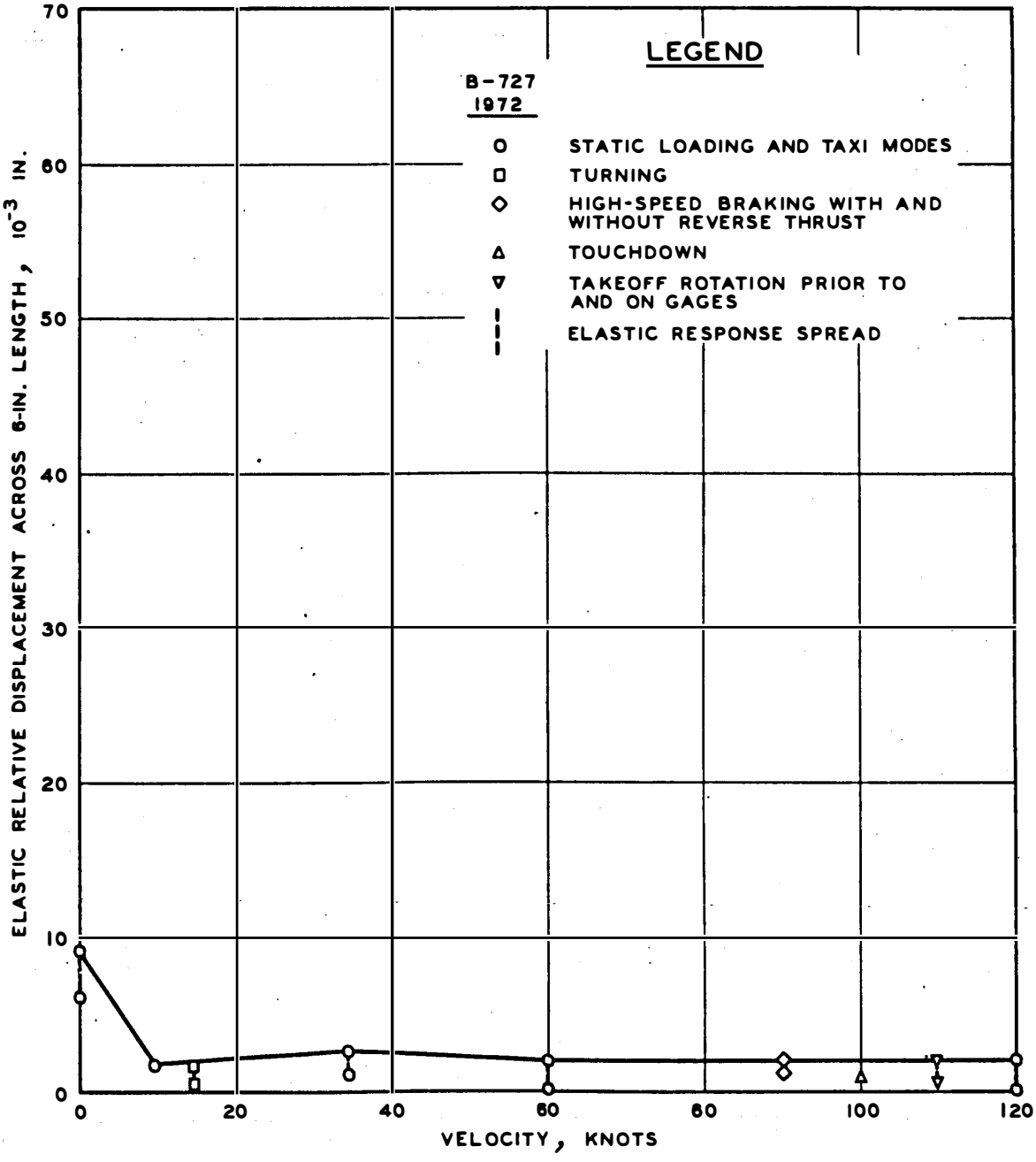

Figure 50. Maximum elastic horizontal (longitudinal) relative displacement across 6-in. length at 15-in. depth versus velocity, rigid pavement

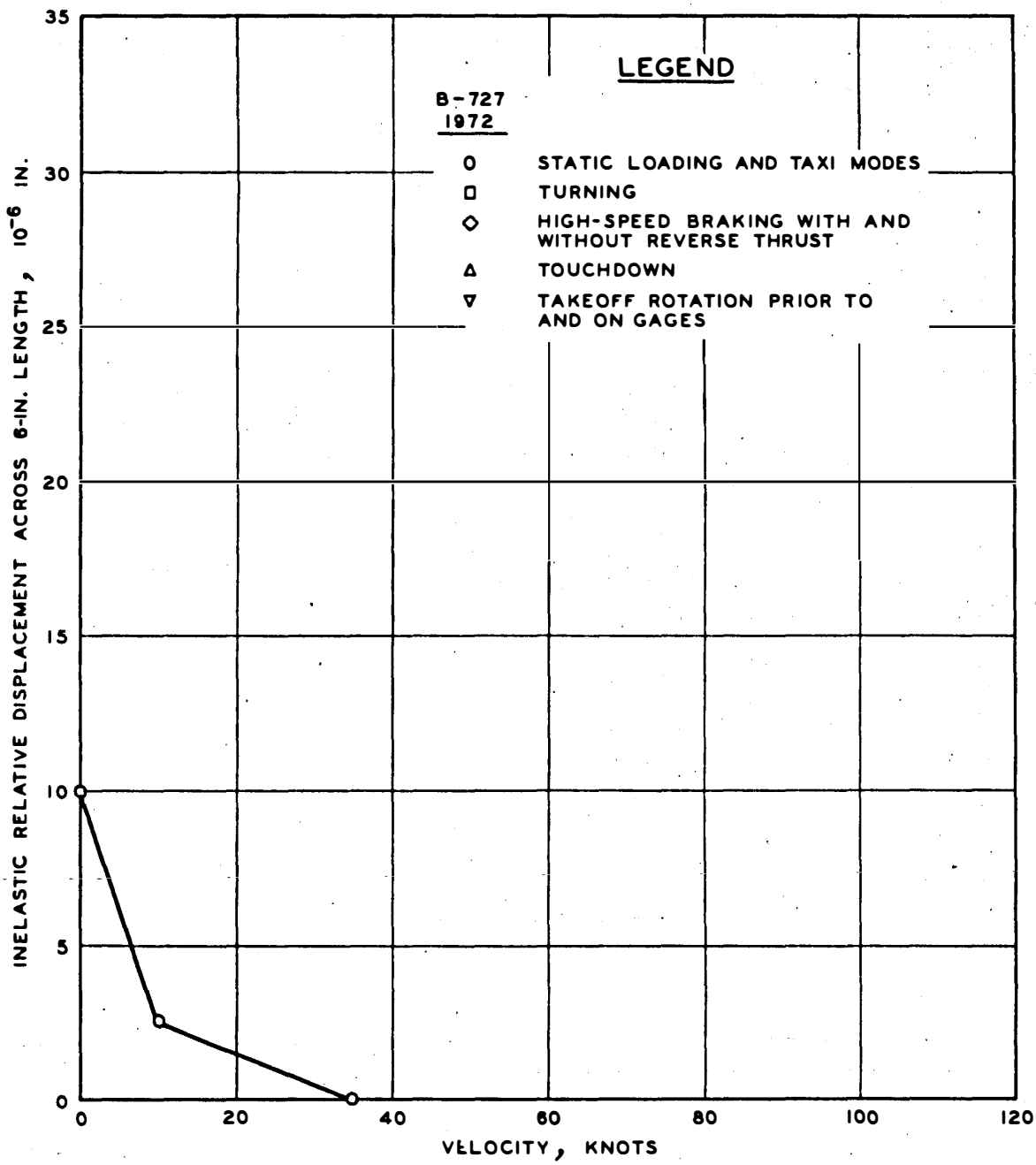

Figure 51. Maximum inelastic horizontal (longitudinal) relative displacement across 6-in. length at 15-in. depth versus velocity, rigid pavement

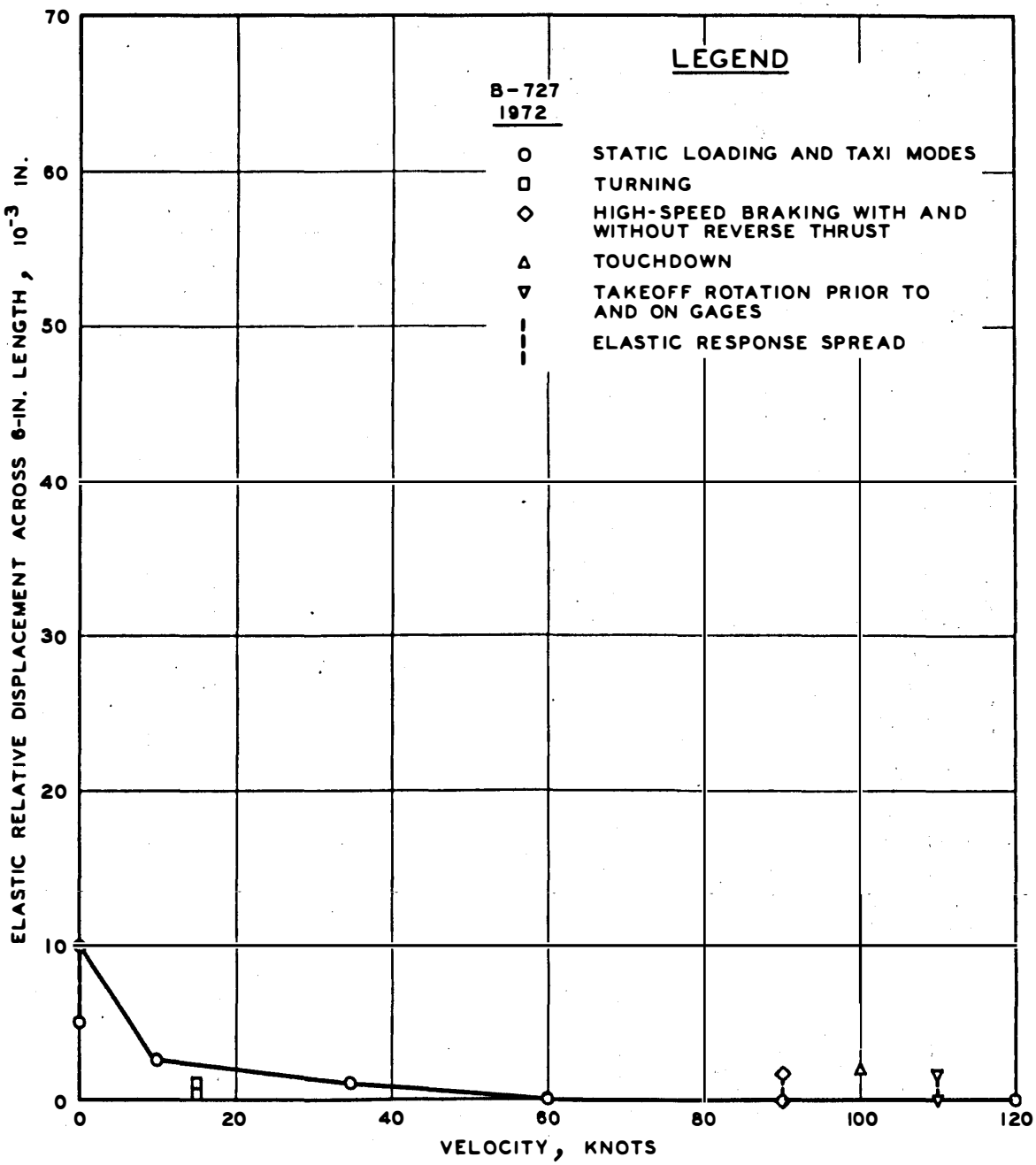

Figure 52. Maximum elastic horizontal (transverse) relative displacement across 6-in. length at 15-in. depth versus velocity, rigid pavement

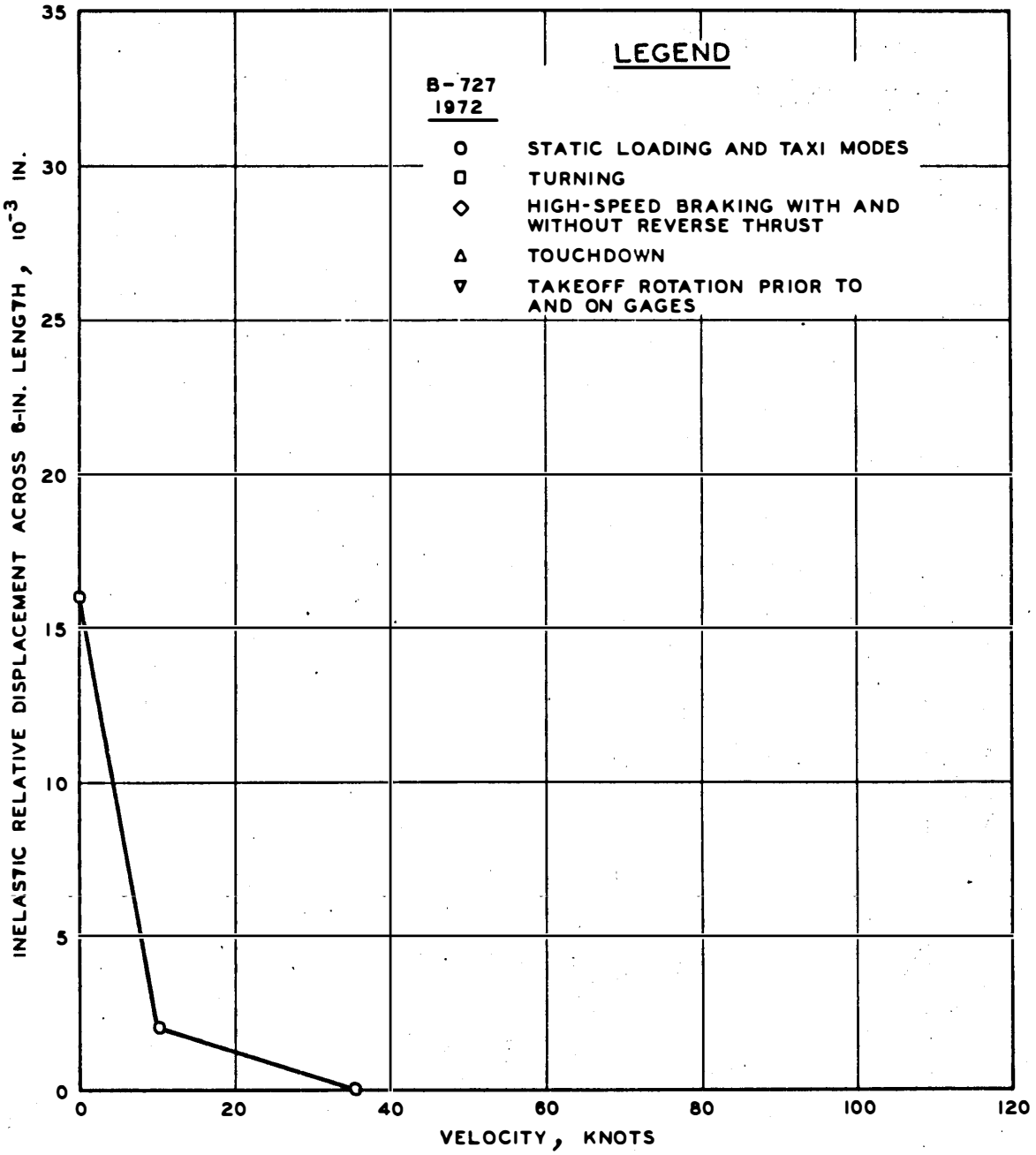

Figure 53. Maximum inelastic horizontal (transverse) relative displacement across 6-in. length at 15-in. depth versus velocity, rigid pavement

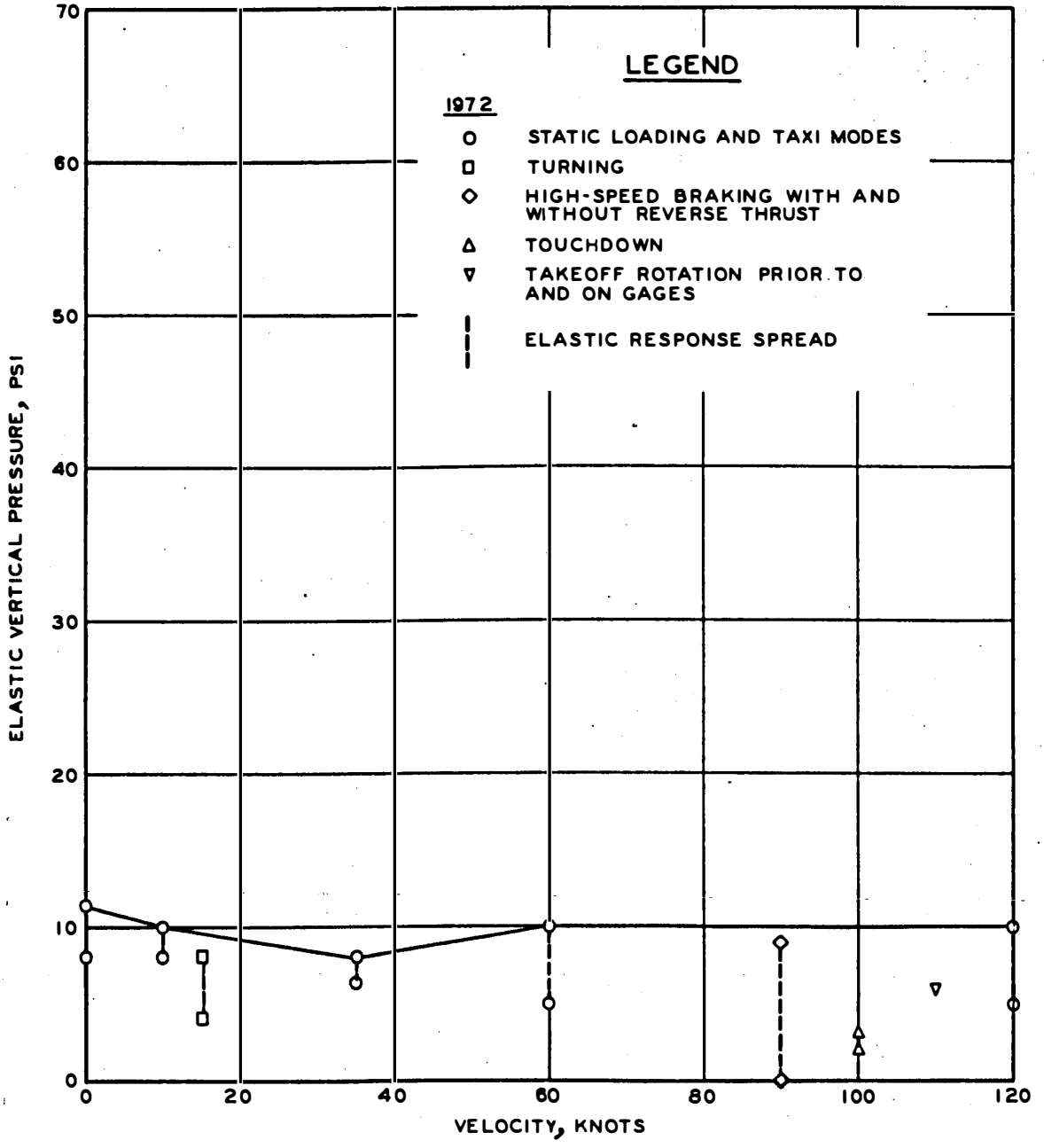

Figure 54. Maximum elastic vertical pressure at 7-in. depth versus velocity, rigid pavement, B-727

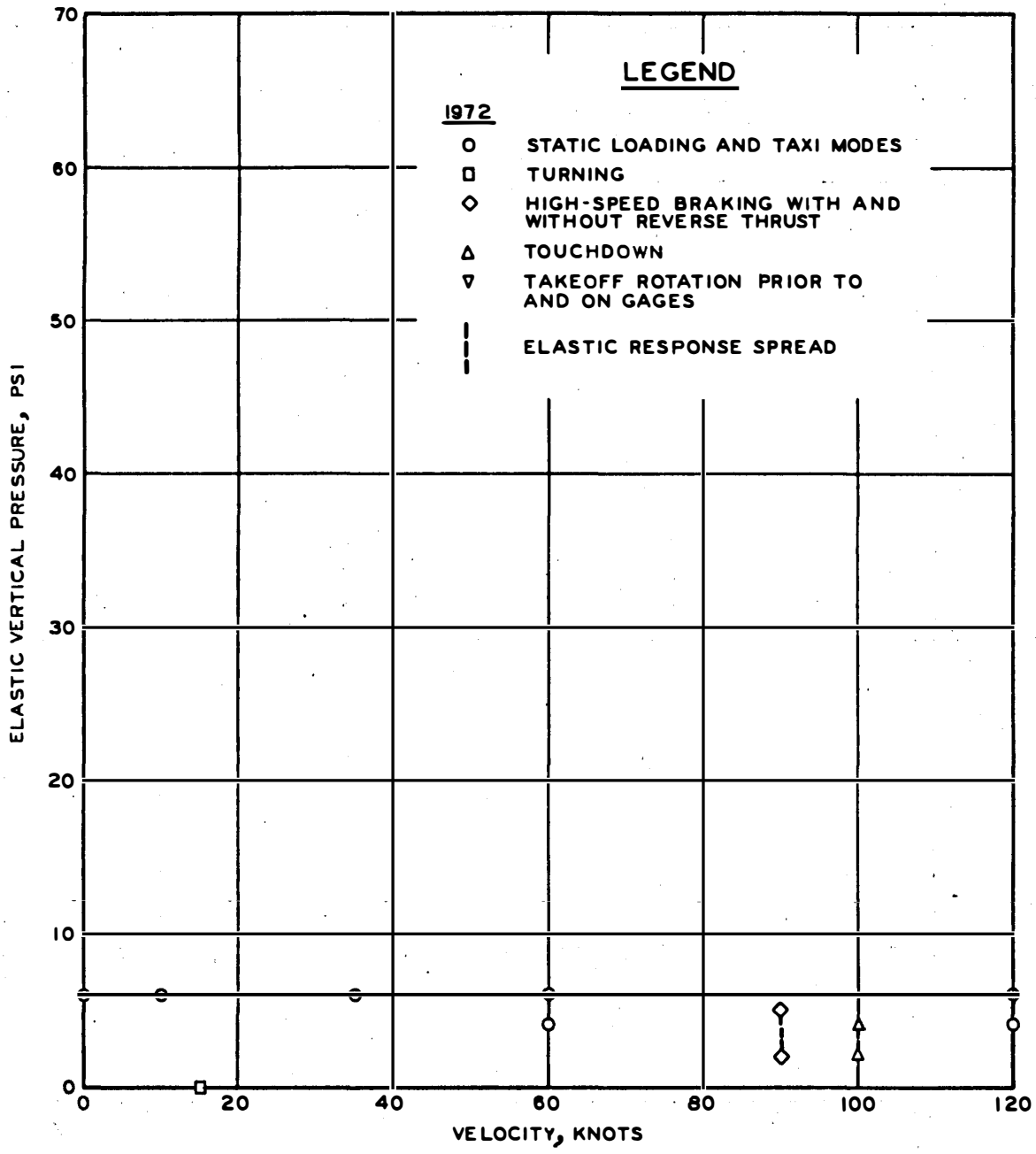

Figure 55. Maximum elastic vertical pressure at 15-in. depth versus velocity, rigid pavement, B-727

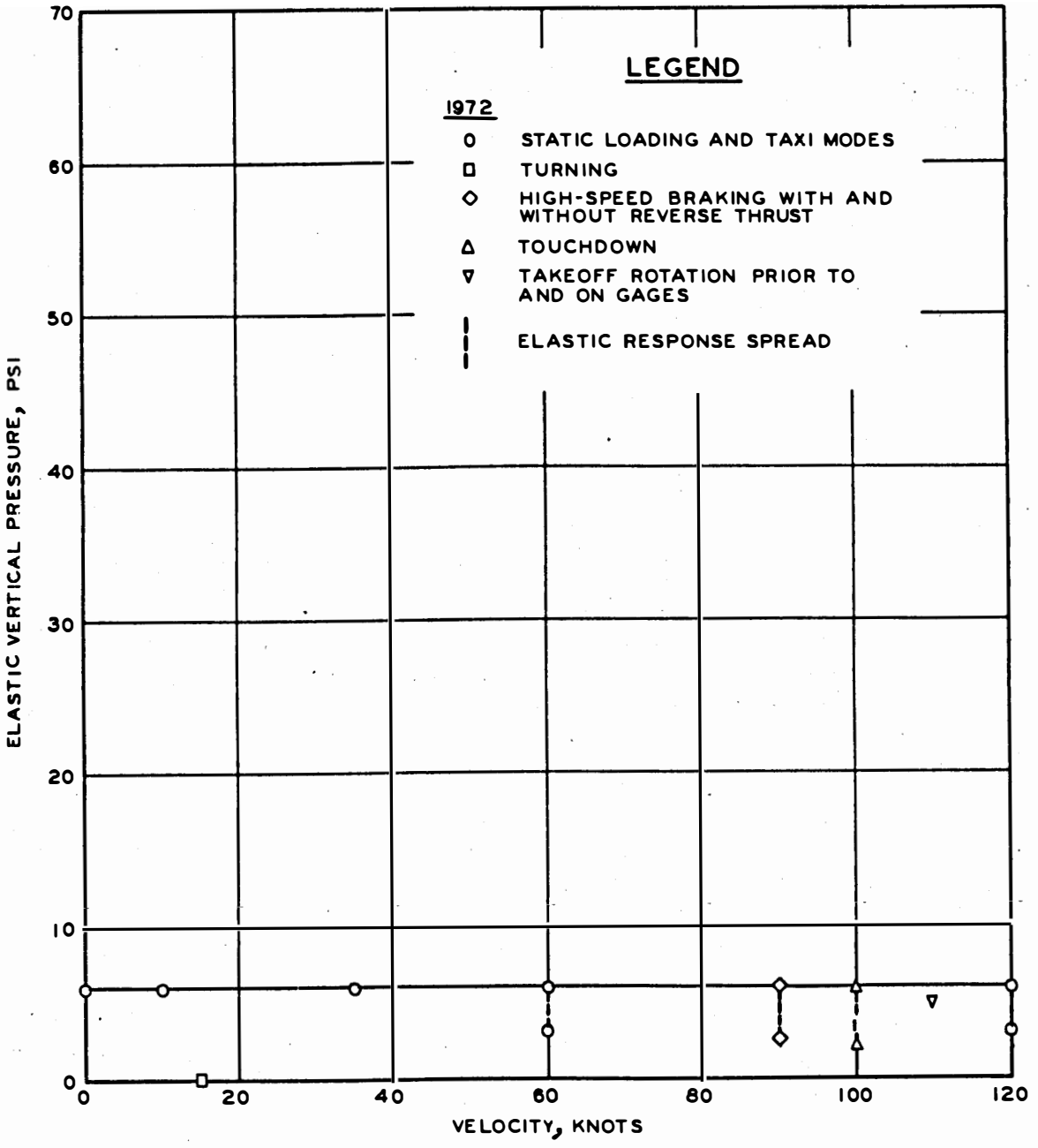

Figure 56. Maximum elastic vertical pressure at 24-in. depth versus velocity, rigid pavement, B-727

CONCLUSIONS AND RECOMMENDATIONS

CONCLUSIONS

Based on the measurements of the nonconditioned flexible and rigid pavement structure responses under aircraft static and dynamic load tests, the following conclusions are believed justified:

a. B-727 aircraft dynamic load tests in 1972 (cold weather) and 1974 (warm weather) on the flexible pavement structure and in 1972 on the rigid pavement structure at NAFEC showed that no basic aircraft ground operating mode induced pavement responses (elastic plus inelastic) greater than those occurring for static load conditions, even though the aircraft dynamic loads were as large as 1.2 times the static load. Elastic response alone generally indicates this also to be true. The pavement surfaces were relatively smooth in the test site areas.

b. However, extrapolation of the test results indicates that for stiff pavement structures, such as the rigid pavement and the flexible pavement in cold weather, unusual conditions of large dynamic loading that could result from rougher surfaces than at NAFEC (holes or bumps, vertical curves, etc.) could possibly cause aircraft dynamic loads greater than 1.2 times the static load and pavement responses larger than those that would occur under static loading. This behavior is possible because of the inelastic behavior being of low magnitude for the stiff pavements and the elastic response being essentially of a constant magnitude with changes in the rate of load application. The larger than static load response that could occur should be entirely elastic and should not be detrimental to the pavement structure except by contributing to an increase in elastic fatigue damage.

c. Based upon gradually reduced elastic response but primarily upon reduced inelastic response with high speeds, indications are that thickness can be reduced in the interior of runways.

d. Measured aircraft loads during turns showed that high horizontal loads are applied to the pavement surfaces. (Airports such as Baltimore Friendship International have experienced pavement distress in turn areas.[7])

e. Test results showed inelastic behavior to be highly dependent on temperature, aircraft speed, and load history (magnitude of load and lateral position of aircraft) for flexible pavements, and to be dependent on speed and load history for rigid pavements.

f. Inelastic displacements larger than the elastic displacements were measured within the velocity range of static load to low-speed taxi.

g. Test results showed elastic behavior to be almost constant for stiff pavement structures (rigid and low-temperature flexible pavements) and the probable viscoelastic effects to be more pronounced at high temperatures in bituminous materials.

h. The flexible pavement structure layer at a depth of 39 to 51 in. responded slightly (less than 10 percent of surface response) to the various modes of aircraft operation. The rigid pavement structure layer at a depth of 15 to 24 in. responded (about 30 percent of surface response) to the various modes of aircraft operation. These were the deepest layers monitored during dynamic load tests for both pavement structures.

i. The elastic and inelastic displacement behavioral phases directly associate the behavior of WES pavement test sections under simulated aircraft loads and wheel configurations and distributed (nonconditioning) traffic to actual pavement behavior under actual aircraft operations (NAFEC tests). This connection means that the investigation of dynamic load effects can probably be conducted on pavement structure test sections of limited size.

RECOMMENDATIONS

The required thickness of pavements subjected to parked or slow-moving aircraft should be based upon the static weight of the aircraft, as is the current practice. This is considered to include the parking aprons, taxiways other than high-speed exit areas, and runway ends. In high-speed exit areas, runway interiors, and other areas that are subject entirely to high-speed aircraft operations, the design should be based upon an analysis of the dynamic loading to the pavement and upon the pavement response to dynamic loading. In high-speed exit areas, high horizontal loads are applied to the pavement surface and should be considered in pavement design. Due to the large loads and thus the likelihood of excessive deterioration in turn areas, the pavement surface in exit areas of flexible pavement runways should be strengthened or be stronger than the main runway. In runway interiors, the NAFEC test data indicate that thickness reductions can be considered. In order to take

full advantage of the NAFEC test data in pavement design, more knowledge is needed concerning pavement failure mechanisms and deterioration growth functions and causes.

REFERENCES

1. Wignot, J. E. et al., "Aircraft Dynamic Wheel Load Effects on Airport Pavements; Final Report," Report No. FAA-RD-70-19, May 1970, Federal Aviation Administration, Washington, D. C.

2. Horn, W. J. and Ledbetter, R. H., "Pavement Response to Aircraft Dynamic Loads; Instrumentation Systems and Testing Program," Report No. FAA-RD-74-39, Vol I, Jun 1975, Federal Aviation Administration, Washington, D. C., and Technical Report S-75-11, Vol I, Jun 1975, U. S. Army Engineer Waterways Experiment Station, CE, Vicksburg, Miss.

3. Ledbetter, R. H., "Pavement Response to Aircraft Dynamic Loads; Presentation and Analysis of Data; Appendix B: Data," Report No. FAA-RD-74-39, Vol II, Sep 1975, Federal Aviation Administration, Washington, D. C., and Technical Report S-75-11, Vol II, Sep 1975, U. S. Army Engineer Waterways Experiment Station, CE, Vicksburg, Miss.

4. New Jersey State Highway Department, "Standard Specifications for Road and Bridge Construction," 1961, Trenton, N. J.

5. Federal Aviation Administration, "Standard Specifications for Construction of Airports," Advisory Circular AC 150/5370-1A, May 1968, Washington, D. C.

6. Ledbetter, R. H. et al., "Multiple-Wheel Heavy Gear Load Pavement Tests; Presentation and Initial Analysis of Stress-Strain-Deflection and Vibratory Measurements; Data and Analysis," Technical Report S-71-17, Vol IIIB, Nov 1971, U. S. Army Engineer Waterways Experiment Station, CE, Vicksburg, Miss.

7. Witczak, M. W., "A Comparison of Layered Theory Design Approaches to Observed Asphalt Airfield Pavement Performance," Jul 1973, Asphalt Institute, College Park, Md.